

6-9-2016

FPGA IMPLEMENTATION OF A REALTIME CYCLOSTATIONARY FEATURE DETECTOR FOR OFDM SIGNALS

Sean Hamlin

Follow this and additional works at: https://digitalrepository.unm.edu/ece_etds

Recommended Citation

Hamlin, Sean. "FPGA IMPLEMENTATION OF A REALTIME CYCLOSTATIONARY FEATURE DETECTOR FOR OFDM SIGNALS." (2016). https://digitalrepository.unm.edu/ece_etds/112

This Thesis is brought to you for free and open access by the Engineering ETDs at UNM Digital Repository. It has been accepted for inclusion in Electrical and Computer Engineering ETDs by an authorized administrator of UNM Digital Repository. For more information, please contact disc@unm.edu.

Sean Hamlin

Candidate

Electrical and Computer Engineering

Department

This thesis is approved, and it is acceptable in quality and form for publication:

Approved by the Thesis Committee:

Dr. Christos Christodoulou, Chairperson

Dr. Sudharman Jayaweera

Dr. Manel Martinez-Ramon

**FPGA IMPLEMENTATION OF A REALTIME
CYCLOSTATIONARY FEATURE DETECTOR
FOR OFDM SIGNALS**

by

SEAN HAMLIN

**BACHELOR OF SCIENCE-ELECTRICAL ENGINEERING
WICHITA STATE UNIVERSITY, 2010**

THESIS

Submitted in Partial Fulfillment of the
Requirements for the Degree of

**Master of Science
Electrical Engineering**

The University of New Mexico
Albuquerque, New Mexico

May, 2016

**FPGA IMPLEMENTATION OF A REALTIME
CYCLOSTATIONARY FEATURE DETECTOR
FOR OFDM SIGNALS**

by

Sean Hamlin

B.S. Electrical Engineering, Wichita State University, 2010

M.S. Electrical Engineering, University of New Mexico, 2016

ABSTRACT

The demand for wireless connectivity has prompted regulatory authorities in the United States to investigate spectrum sharing of the DSRC band with U-NII operators. However, DSRC operation has public safety implications, and moreover, time-critical requirements due to the vehicular nature of its application. The field of cognitive radio has identified several sensing techniques for the identification of licensed operators in a given band. This thesis explores cyclostationary detection techniques for primary users. A method will be identified for the detection of the 802.11p OFDM modulation used for DSRC communications. A test statistic will be given that is invariant to the signal noise covariance to allow simple and robust operation. Finally, the detection algorithm will be implemented in FPGA digital logic in order to demonstrate the methods ability to be employed in a commercial radio chipset with minimum resource requirements, yet still provide real-time detection.

TABLE OF CONTENTS

LIST OF FIGURES	v
LIST OF TABLES	vii
CHAPTER 1 INTRODUCTION TO COGNITIVE RADIO.....	1
1.1 Overview of Cognitive Radio	1
1.2 DSRC Spectrum Sharing.....	1
1.3 Overview of Feature Detection Techniques	3
1.3.1 Energy Detectors.....	4
1.3.2 Matched Filters	7
1.3.3 Cyclostationary Detection.....	7
CHAPTER 2 CYCLOSTATIONARY SIGNAL ANALYSIS	11
2.1 Introduction	11
2.2 Cyclic Autocorrelation Function.....	11
2.3 Spectral Correlation Function	13
2.4 Spectral Coherence Function	19
CHAPTER 3 OFDM FEATURE DETECTION.....	20
3.1 OFDM Overview	20
3.2 DSRC Modulation.....	22
3.3 802.11p Simulation Model	27
3.4 OFDM Features for Cyclostationary Detection	28
3.4.1 Preamble	30
3.4.2 Pilots	33
3.4.3 Cyclic Prefix	36
3.5 Detection of Cyclic Prefix with CAF	38
CHAPTER 4 DSRC DETECTION WITH CAF.....	41
4.1 Spatial Sign Cyclic Correlation Estimator.....	41
4.2 Dual-Lag SSCCE with Cyclic Phase Compensation	44
4.3 MATLAB Simulation.....	45
4.3.1 Probability of Detection vs. SNR.....	46
4.3.2 ROC at Fixed SNR.....	49
4.3.3 Histogram at Fixed SNR.....	50
CHAPTER 5 FPGA IMPLEMENTATION.....	51
5.1 FPGA Overview	51
5.2 SSCCE Algorithm Implementation.....	53
5.2.1 Spatial Sign Function.....	54
5.2.2 Lead/Lag Shift Register	55
5.2.3 Multipliers.....	56
5.2.4 Numerically Controlled Oscillator	57
5.2.5 Moving Average Filter	59
5.3 SSCCE Behavioral Simulation.....	60
5.4 SSCCE Resource Utilization	66
5.5 Conclusion.....	67
APPENDIX A MATLAB CODE.....	69
APPENDIX B HDL CODE	74
REFERENCES.....	100

LIST OF FIGURES

Figure 1.1 DSRC channel plan in the ITS band (from [5]).	2
Figure 1.2 Proposed new UNII-4 band (from [5]).	3
Figure 1.3 Example of a receiver operating characteristic (ROC) curve.	6
Figure 1.4 (a) Power spectral density of lowpass signal. (b) Power spectral density of AM signal. (c) Power spectral density of squared lowpass signal. (d) Power spectral density of squared AM signal.	10
Figure 2.1 Simplified block diagram of a spectrum analyzer for measuring the power spectral density at center frequency f (from [12]).	15
Figure 2.2 Block diagram of a spectral correlation analyzer for center frequency f and cyclic frequency α (from [12]).	16
Figure 2.3 Estimated spectral correlation density of an AM modulated signal with: (top) no additive noise, (middle) 5dB SNR, (bottom) -5dB SNR.	18
Figure 2.4 Contour of the estimated spectral correlation density of an AM modulated signal.	19
Figure 3.1 Simplified block diagram of an OFDM modulator and demodulator.	22
Figure 3.2 DSRC channel plan (from [18]).	23
Figure 3.3 PPDU frame format (from [21]).	25
Figure 3.4 Time-domain plot an 802.11p PPDU frame of 10 symbols encoded with 64-QAM.	28
Figure 3.5 Power spectral density of an 802.11p PPDU frame of 100 symbols encoded with 64-QAM.	29
Figure 3.6 Estimated spectral correlation density of an 802.11p PPDU frame.	31
Figure 3.7 Contour of the estimated spectral correlation density of an 802.11p PPDU frame.	32
Figure 3.8 Contour of the estimated spectral correlation density of an 802.11p PPDU frame modified by replacing the pilot subcarriers with nulls.	34
Figure 3.9 Contour of the estimated spectral correlation density of an 802.11p PPDU frame modified by randomizing the pilot subcarriers.	35
Figure 3.10 Estimated cyclic correlation density of an 802.11p PPDU frame.	37
Figure 3.11 Autocorrelation function of an 802.11p PPDU frame.	38
Figure 4.1 Probability of detection vs. SNR of an 802.11p signal corrupted by an AWGN fading channel using SSCCE method with sample size of 1000.	48
Figure 4.2 Probability of detection vs. SNR of an 802.11p signal without additional impairments using SSCCE method with sample size of 1000.	48

Figure 4.3 Receiver operating characteristic curve of the SSCCE method for an 802.11p signal.	49
Figure 4.4 Histogram of SSCCE test statistic for an 802.11p signal with -5dB SNR.	50
Figure 5.1 Flowchart of a typical FPGA design flow.	52
Figure 5.2 Block diagram of the FPGA implementation of the SSCCE algorithm.	53
Figure 5.3 Block diagram showing the implementation of the SSF using CORDIC routines.	55
Figure 5.4 Block diagram showing the implementation of the lead/lag shift register.	56
Figure 5.5 Block diagram showing the implementation of a NCO using CORDIC.	59
Figure 5.6 Screenshot of design simulation using Questa Sim.	62
Figure 5.7 SSCCE algorithm probability of detection vs. SNR results from MATLAB simulation.	63
Figure 5.8 SSCCE algorithm probability of detection vs. SNR from HDL implementation behavioral simulation.	64
Figure 5.9 Difference in probability of detection between MATLAB simulation and HDL implementation.	64
Figure 5.10 RMSD of the SSCCE test statistic between MATLAB simulation and HDL implementation.	65
Figure 5.11 Histogram of the first test statistic value to exceed the threshold for 5% P_{fa}	65

LIST OF TABLES

Table 1 OFDM PHY Modulation Parameters of 802.11p.....	24
Table 2 Subcarrier Modulation Parameters of 802.11p.....	26
Table 3 SSCCE Implementation Resource Utilization.....	66

CHAPTER 1

INTRODUCTION TO COGNITIVE RADIO

1.1 Overview of Cognitive Radio

The demand on spectrum access has exploded within the past decade. Wireless connectivity has seen rapid growth through 4G LTE, the ubiquity of Wi-Fi connection hotspots, and the advent of LTE-A. Along with the incumbent spectrum users for LMR, TV, radio, avionics and military communications, the ability to service all users will become increasingly difficult with the current allocation schema. With this growing strain on the wireless spectrum, interest in cognitive radio has transitioned from its inception in the late 1990's as a means to enhance the radio operator experience [1], to legislative mandate by which the growing spectrum crisis can be mitigated [2].

Several definitions exist for the term cognitive radio. However, when discussed in the context of spectrum sharing, perhaps the most germane description is that provided by a spectrum regulating authority. According to the Federal Communications Commission (FCC), cognitive radio is defined as an emerging technology of software defined radios that monitor, sense, detect, and autonomously adapt their channel access to suit the RF environment in which they are operating [3].

1.2 DSRC Spectrum Sharing

In 1999, the FCC licensed the 5.9 GHz band (5850-5925 MHz) for the purposes of Dedicated Short Range Communications (DSRC) as an Intelligent Transportation

Systems radio service [4]. The intended purpose of this licensed spectrum is enhanced transportation safety via Vehicle-to-Vehicle (V2V) and Vehicle-to-Infrastructure (V2I) communications. Potential uses of DSRC are to alert drivers of approaching emergency vehicles, blind spot, sudden braking, collision avoidance, adverse road conditions, as well as traffic condition updates. Figure 1.1 shows the approved DSRC channel frequency and power limit plan.

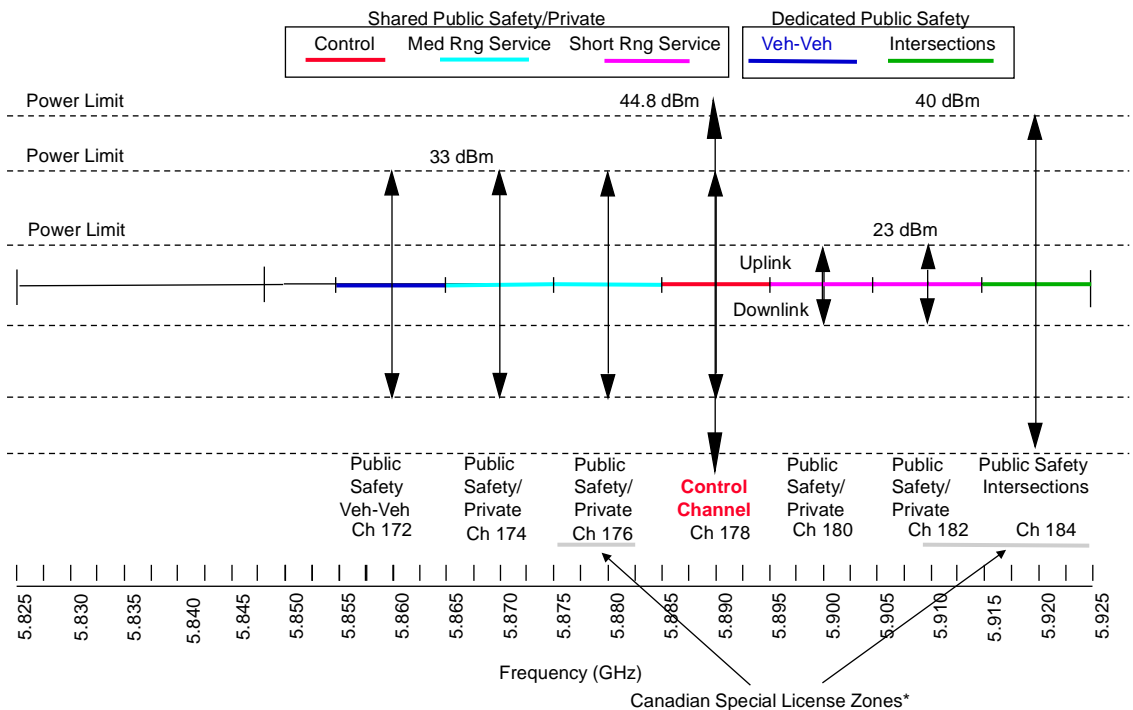


Figure 1.1 DSRC channel plan in the ITS band (from [5]).

Recently, the FCC and NTIA have been legislatively tasked with opening the 5850-5925 MHz frequency band to U-NII devices [6] as shown in Figure 1.2. Due to the public safety aspect of DSRC, any spectral reuse in this band by secondary users must be subject to the principal constraint of robust detection. Furthermore, due to the potentially high vehicular speed (and thus rapidly changing) mobile environment in which DSRC

transceivers operate, secondary users must quickly detect primary users and relinquish the spectrum. Additionally, given the nature of the currently identified secondary user devices (802.11ac devices) the spectral detection mechanism must be power efficient and consume minimum device resources in order to be commercially viable. Given these constraints, the spectral detection and classification engine will likely reside in the radio chipset of the secondary user device. This thesis will explore a new feature detection technique, focused on the application of spectral reuse in the dedicated DSRC band for 802.11p primary users.

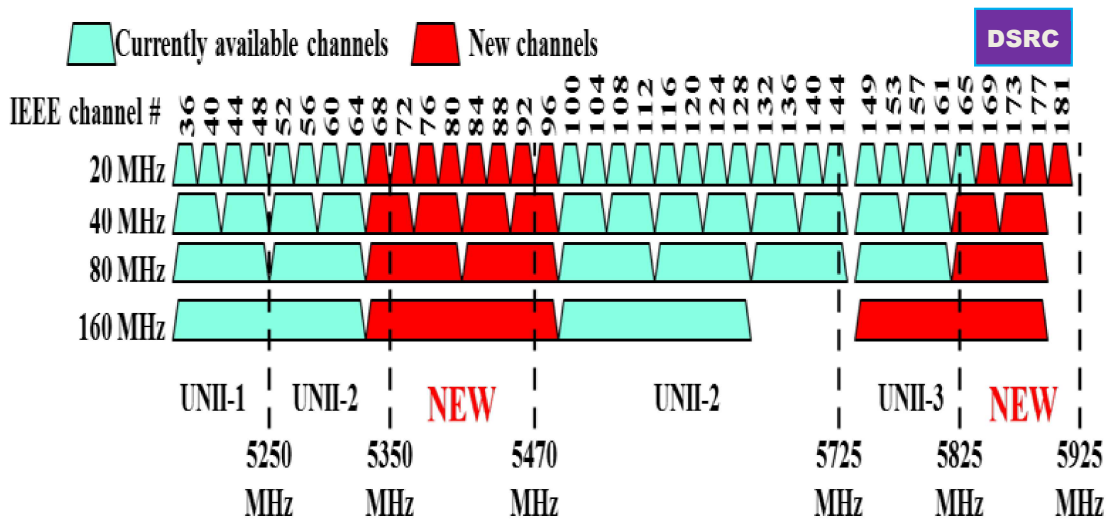


Figure 1.2 Proposed new UNII-4 band (from [5]).

1.3 Overview of Feature Detection Techniques

The scope of the term cognitive radio can include receiver side technologies for detecting spectrum holes, channel estimation, and capacity prediction as well as transmitter side technologies for transmitter power control and dynamic spectrum management [7]. Arguably the main focus of cognitive radio is to enable the sharing of

spectrum between licensed primary users and unlicensed secondary users. Towards this end, spectrum sensing and signal detection techniques comprise a large portion of the research in the field of cognitive radio [8].

In the field of cognitive radio, three primary signal detection techniques are prominent, each with performance and design tradeoffs. These are energy based detection, matched filter based detection, and cyclostationary based detection [8], [9].

1.3.1 Energy Detectors

Energy based detection is the simplest spectrum sensing technique. This approach does not require knowledge of the primary signal and has a low implementation complexity and computational cost. Energy based detectors simply compare the energy of a receiver output against a threshold value. The threshold value is calculated according to the level of noise in the received signal. In their simplest form, energy detectors calculate a test statistic from N received samples as follows:

$$T(y) = \frac{1}{N} \sum_{n=0}^{N-1} |y[n]|^2 \quad (1)$$

where the received signal is assumed to have the form:

$$y[n] = s[n] + w[n] \quad (2)$$

with $s[n]$ being the primary signal to be detected and $w[n]$ is additive white Gaussian noise. The goal of spectrum sensing algorithms is to form a decision as to the presence of

the primary signal. Therefore, the null hypothesis, that the primary signal is not present, and its alternative are formulated as:

$$\begin{aligned}\mathcal{H}_0 & : y[n] = w[n], \\ \mathcal{H}_1 & : y[n] = s[n] + w[n].\end{aligned}\tag{3}$$

A threshold value, λ , is determined for the test statistic, above which the null hypothesis is rejected. The performance of the energy detector to correctly detect the presence of the primary signal (i.e. its sensitivity) is given as:

$$P_D = Prob\{T(y) > \lambda | \mathcal{H}_1\}\tag{4}$$

Similarly, the performance of the detectors false alarm rate, that is the probability of asserting the presence of a primary signal when it is not present (i.e. its specificity), is given as:

$$P_{FA} = Prob\{T(y) > \lambda | \mathcal{H}_0\}\tag{5}$$

A receiver operating characteristic (ROC) curve is obtained by plotting the probability of detection versus the probability of false alarm, an example of which is shown in Figure 1.3. Naturally it is desired to maximize the probability of detection while minimizing the probability of false alarm. The desired balance between probability of detection and probability of false alarm is controlled by the threshold value λ . In order to determine the value of λ , it is observed that the noise component $w[n]$ is assumed to be normally distributed with zero-mean and variance σ_w^2 . The distribution of the test statistic (1) is then given as:

$$T(y)|\mathcal{H}_0 \sim \mathcal{N}\left(\sigma_w^2, \frac{2}{N}\sigma_w^4\right) \quad (6)$$

Using (6), (5) can then be rewritten as

$$P_{FA} = Q\left(\frac{\lambda - \sigma_w^2}{\sqrt{\frac{2}{N}\sigma_w^2}}\right) \quad (7)$$

where $Q(\cdot)$ is the Gaussian complementary cumulative density function [10]. For a given false alarm rate, the threshold value λ can be determined from (7). Typical values for P_{FA} are 1% and 5%.

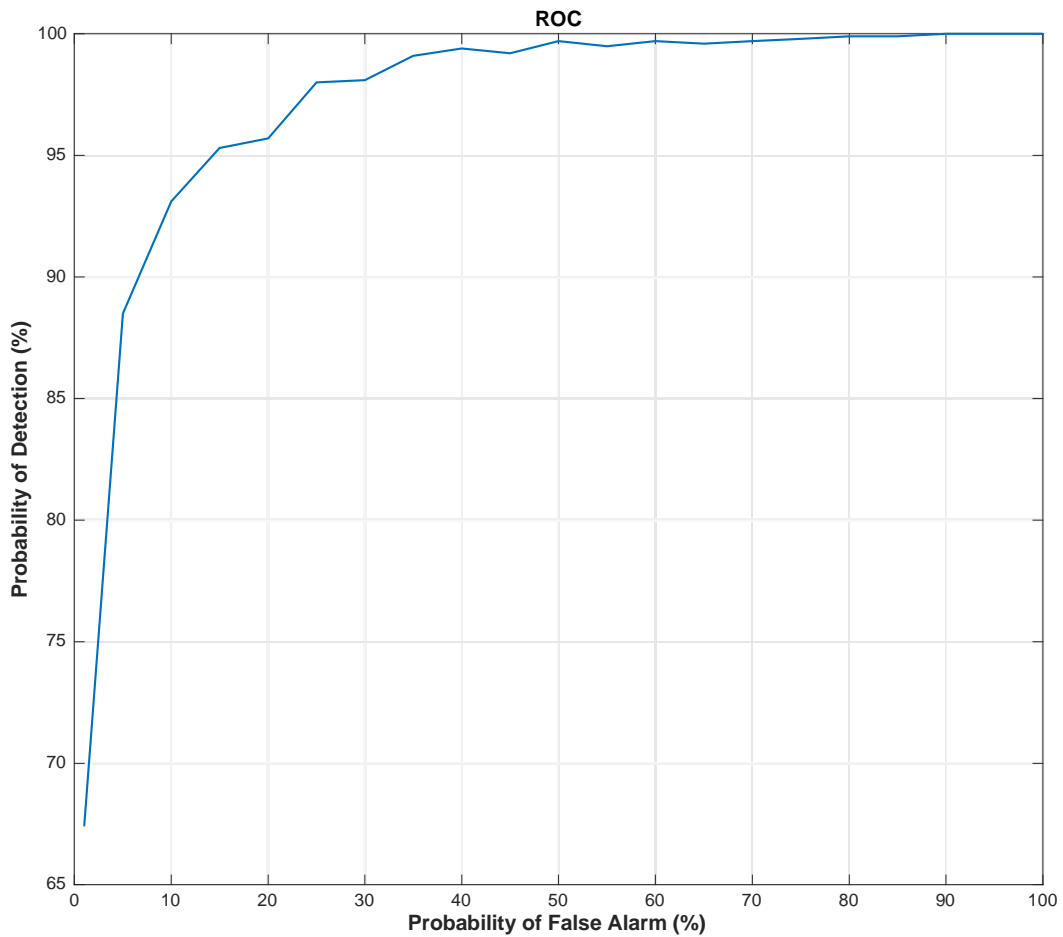


Figure 1.3 Example of a receiver operating characteristic (ROC) curve.

As can be seen from the above derivation, the presence of a signal is determined by the energy detector with no apriori information about the primary signal. However, there is also no distinction between a primary signal and interference or other secondary signals. Furthermore, as can be seen from (7), knowledge of the noise power is required to determine the optimal threshold value. It may also be observed that by averaging more samples, an arbitrarily low signal-to-noise ratio could still allow for positive signal detection. However, as shown in [10] any slight uncertainty in the knowledge of the noise variance drastically affects the performance of the detection scheme below a certain SNR, regardless of the number of samples averaged.

1.3.2 Matched Filters

Matched filters provide the optimal detection method for a known signal type. These filters are created by correlating a known signal with the received signal, and are optimal in the sense that they maximize the signal to noise ratio of the filter output. Unfortunately, this method requires complete knowledge of the primary signal, and demodulation of the same, in order to implement. For all but the most simple of modulation types, this method entails a high-computational complexity.

1.3.3 Cyclostationary Detection

Cyclostationary processes are those whose statistical parameters vary periodically as a function of time [11]. A common example is meteorological data, which has strong periodicities according to the season. Many communications modulation and coding schemes exhibit cyclostationarity as well.

Periodicity in signals can typically be found by visual inspection of either their time series data or through spectral analysis. For example, a signal corrupted by noise, $x(t) = A \cos(2\pi\alpha t + \theta) + w(t)$, when subject to the linear transformation with the Fourier kernel will produce spectral lines at $f = \pm\alpha$. In such case, regardless of the noise component, the signal is said to contain first-order periodicity in frequency α [12]. However, a time-series may contain other types of periodicities that do not produce spectral lines. These signals are said to possess wide-sense cyclostationarity of order- n if and only if there exists a non-linear time-invariant transformation of the time-series such that the transformed time-series produces spectral lines [12]. Therefore, a signal contains second-order periodicity (i.e. $n=2$) if its time-series undergoes a quadratic time-invariant transformation

$$y(t) = \int_{-\infty}^{\infty} \int_{-\infty}^{\infty} k(u, v) x(t - u) x(t - v) du dv \quad (8)$$

such that $y(t)$ exhibits first-order periodicity in frequency α [13]. Some possible quadratic nonlinear time invariant transformation functions could be the squaring operation on the time-series or the multiplication of the time-series with a time lagged version of itself.

The following example adapted from [12] illustrates the above discussion. Consider a random bit sequence lowpass signal, $a(t)$, with bandwidth $B = 0.1$, that does not produce spectral lines as illustrated by the estimated power spectral density $S_a(f)$ shown in Figure 1.4(a). Next, assume $a(t)$ is modulated with a carrier at frequency $f_c = 0.2$ to produce the AM signal

$$x(t) = a(t) \cos(2\pi f_c t). \quad (9)$$

The resulting power spectral density $S_x(f)$ of the modulated signal is then

$$S_x(f) = \frac{1}{4} [S_a(f + f_c) + S_a(f - f_c)], \quad (10)$$

whose estimate is shown in Figure 1.4(b). Observe that the power spectral density of the modulated signal still does not contain any spectral lines. In order to test the modulated signal for second-order periodicity, we use a squaring function as a quadratic time-invariant transformation:

$$\begin{aligned} y(t) &= x^2(t) = a^2(t) + \cos^2(2\pi f_c t) \\ &= \frac{1}{2} [b(t) + b(t) \cos(4\pi f_c t)] \end{aligned} \quad (11)$$

where

$$b(t) = a^2(t) \quad (12)$$

The squaring operation forces $b(t)$ to be completely non-negative, boosting the DC component, doubling the bandwidth of $a(t)$ and leading to the spectral line at $f = 0$ shown Figure 1.4(c). The power spectral density of (11) is

$$S_y(f) = \frac{1}{4} \left[S_b(f) + \frac{1}{4} S_b(f + 2f_c) + \frac{1}{4} S_b(f - 2f_c) \right], \quad (13)$$

which is estimated in Figure 1.4(d). The quadratic transformation has therefore produced first-order periodicity by revealing spectral lines at $f = 0$ and $f = \pm 2f_c$. The next chapter will explore cyclostationary methods in more depth.

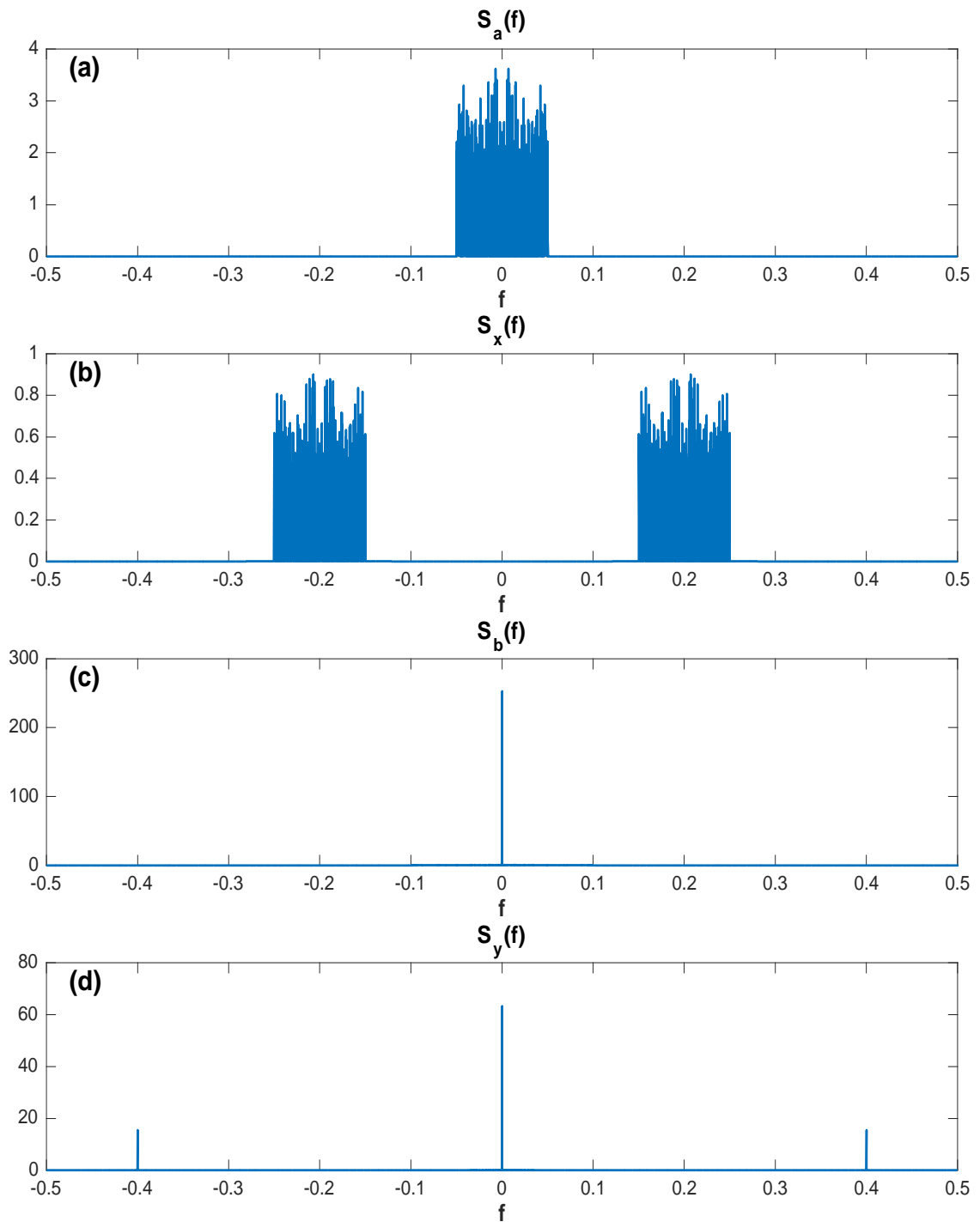


Figure 1.4 (a) Power spectral density of lowpass signal. (b) Power spectral density of AM signal. (c) Power spectral density of squared lowpass signal. (d) Power spectral density of squared AM signal.

CHAPTER 2

CYCLOSTATIONARY SIGNAL ANALYSIS

2.1 Introduction

The previous chapter introduced the concept of cyclostationary time-series. For signals of second-order periodicity, it was shown that a quadratic time-invariant transformation could be used to create a time-series that exhibited first-order periodicity. A simple example of such a transformation was given as the squaring operation. However, the squaring operation is really an example of a more generalized quadratic transformation as shown examination of (8). Specifically, any operation that measures second-order moment (variance) is required. Two second-order measures are the autocorrelation function in the time domain and the power spectrum transform in the frequency domain. Therefore, the definition of wide-sense cyclostationary time-series can be restated as one whose first-order measure (expectation value) and second-order measure (autocorrelation function) are periodic with some period T_0 [11].

2.2 Cyclic Autocorrelation Function

From the definition of wide-sense cyclostationary time-series it is implied that for all t, τ :

$$E[x(t + T_0)] = E[x(t)] \quad (14)$$

$$R_x(t + T_0, \tau) = R_x(t, \tau) \quad (15)$$

where the autocorrelation function is defined as

$$R_x(t, \tau) \triangleq E[x^*(t + \tau)x(t)]. \quad (16)$$

Because the autocorrelation function (16) is wide-sense stationary, (15) can be simplified to only be a function of τ :

$$R_x(t, \tau) = R_x(\tau). \quad (17)$$

In order to show if a time-series exhibits second-order periodicity, it is then necessary to see if the time-series that has undergone transformation via the autocorrelation function generates spectral lines. The most intuitive test of first-order periodicity at a frequency α would be to determine the Fourier coefficient of the autocorrelation function at that frequency [13]:

$$R_x^\alpha(\tau) \triangleq \lim_{T \rightarrow \infty} \frac{1}{T} \int_{-T/2}^{T/2} x\left(t + \frac{\tau}{2}\right) x^*\left(t - \frac{\tau}{2}\right) e^{-j2\pi\alpha t} dt. \quad (18)$$

The above expression is referred to as the Cyclic Autocorrelation Function (CAF). Using the CAF, $x(t)$ can be said to exhibit second-order cyclostationarity if and only if for some nonzero value of α , $R_x^\alpha(\tau) \neq 0$, i.e. it contains a sine-wave component. The frequency parameter α is referred to as the cycle or cyclic frequency and implies that a time-series with cyclostationary periodicity of T_0 has a nonzero CAF at cyclic frequency $\alpha = 1/T_0$. Note, that for $\alpha = 0$ the CAF is the usual continuous-time autocorrelation function.

2.3 Spectral Correlation Function

As in any signal analysis, transformation into the frequency domain can reveal details about the signal of interest that might be obscured or not easily detected by time-domain examination. Cyclostationary signal analysis is no exception. If the CAF is considered a time-domain transform of the time-series, then the question naturally arises as to determining the frequency domain equivalent. Not surprisingly, the answer appears by simply taking the Fourier transform of (18), yielding

$$S_x^\alpha(f) \triangleq \int_{-\infty}^{\infty} R_x^\alpha(\tau) e^{-j2\pi f\tau} d\tau, \quad (19)$$

which is referred to as the Spectral Correlation Function (SCF). The autocorrelation function and the power spectral density are related from the Wiener-Khinchin theorem, a relationship that also applies between the CAF and the SCF as

$$S_x^\alpha(f) = \mathcal{F}\{R_x^\alpha(\tau)\}. \quad (20)$$

For this reason, (20) is sometimes referred to as the cyclic Wiener relation [12], [13].

As a consequence of the Wiener-Khinchin theorem, for wide sense stationary signals the power spectral density function can be obtained without explicitly calculating the autocorrelation function:

$$S_x(f) = \int_{-\infty}^{\infty} R_x(\tau) e^{-j2\pi f\tau} d\tau = E[|X(f)|^2]. \quad (21)$$

The power spectrum density can then be estimated from time-smoothing of the finite-time signal $x_T(t)$ as follows

$$S_x(f) = \lim_{T \rightarrow \infty} S_{x_T}(f) = \lim_{T \rightarrow \infty} E[|X_T(f)|^2]. \quad (22)$$

$X_T(f)$ can be estimated from the short-time Fourier transform

$$X_T(t, f) = \frac{1}{\sqrt{T}} \int_{t-T/2}^{t+T/2} x(u) e^{-j2\pi f u} du. \quad (23)$$

The finite-time estimate of the power spectrum density is then

$$S_{x_T}(t, f)_{\Delta t} = \frac{1}{\Delta t} \int_{-\Delta t/2}^{\Delta t/2} \frac{1}{T} X_T(t+u, f) X_T^*(t+u, f) du, \quad (24)$$

from which the power spectrum density is calculated according to the limits

$$S_x(f) = \lim_{T \rightarrow \infty} \lim_{\Delta t \rightarrow \infty} S_{x_T}(t, f)_{\Delta t}. \quad (25)$$

Graphically, (24) can be realized as the familiar spectrum analyzer, shown in Figure 2.1, whose output yields the power spectrum density as the filter bandwidth $B = 1/T \rightarrow 0$ and the observation time $\Delta t \rightarrow \infty$

$$S_x(f) = \lim_{B \rightarrow 0} \frac{1}{B} \left\langle \left| h_{BPF}(t) * x(t) \right|^2 \right\rangle. \quad (26)$$

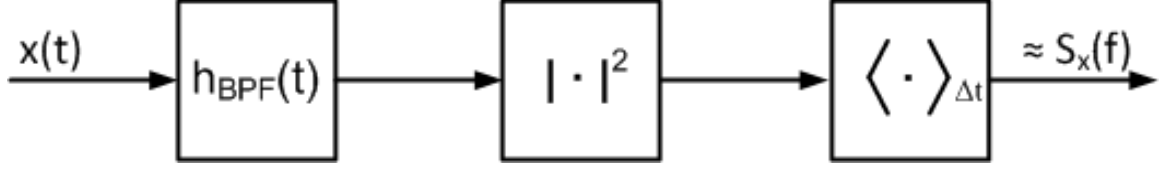


Figure 2.1 Simplified block diagram of a spectrum analyzer for measuring the power spectral density at center frequency f (from [12]).

Likewise, the spectral correlation function can be estimated from frequency-shifting and time-smoothing the finite-time signal [13]. First, the complex exponential term in (18) can be factored into the time-series as a frequency shift operation, represented as

$$\begin{aligned} u(t) &= x(t)e^{-j\pi\alpha t}, \\ v(t) &= x(t)e^{j\pi\alpha t}, \end{aligned} \quad (27)$$

and having corresponding short-time Fourier transforms

$$\begin{aligned} \frac{1}{\sqrt{T}}U_T(t, f) &= \frac{1}{\sqrt{T}}X_T\left(t, f + \frac{\alpha}{2}\right), \\ \frac{1}{\sqrt{T}}V_T(t, f) &= \frac{1}{\sqrt{T}}X_T\left(t, f - \frac{\alpha}{2}\right). \end{aligned} \quad (28)$$

Then, analogous to (22)

$$S_x^\alpha(f) = \lim_{T \rightarrow \infty} S_{uv_T}^\alpha(f) = \lim_{T \rightarrow \infty} E[U_T(f)V_T^*(f)]. \quad (29)$$

From which the finite-time estimate of the spectral correlation function is calculated

$$S_{x_T}^\alpha(t, f)_{\Delta t} = \frac{1}{\Delta t} \int_{-\Delta t/2}^{\Delta t/2} \frac{1}{T} U_T(t+u, f) V_T^*(t+u, f) du. \quad (30)$$

And finally yielding the spectral correlation function in the limits

$$S_x^\alpha(f) = \lim_{T \rightarrow \infty} \lim_{\Delta t \rightarrow \infty} S_{x_T}^\alpha(t, f)_{\Delta t}. \quad (31)$$

Similar to the spectrum analyzer, a spectral correlation analyzer, illustrated in

Figure 2.2, provides the spectral correlation function output as the filter bandwidth

$B = 1/T \rightarrow 0$ and the observation time $\Delta t \rightarrow \infty$ [12]

$$S_x^\alpha(f) = \lim_{B \rightarrow 0} \frac{1}{B} \left\langle \left[h_{BPF}(t) * u(t) \right] \left[h_{BPF}(t) * v(t) \right]^* \right\rangle. \quad (32)$$

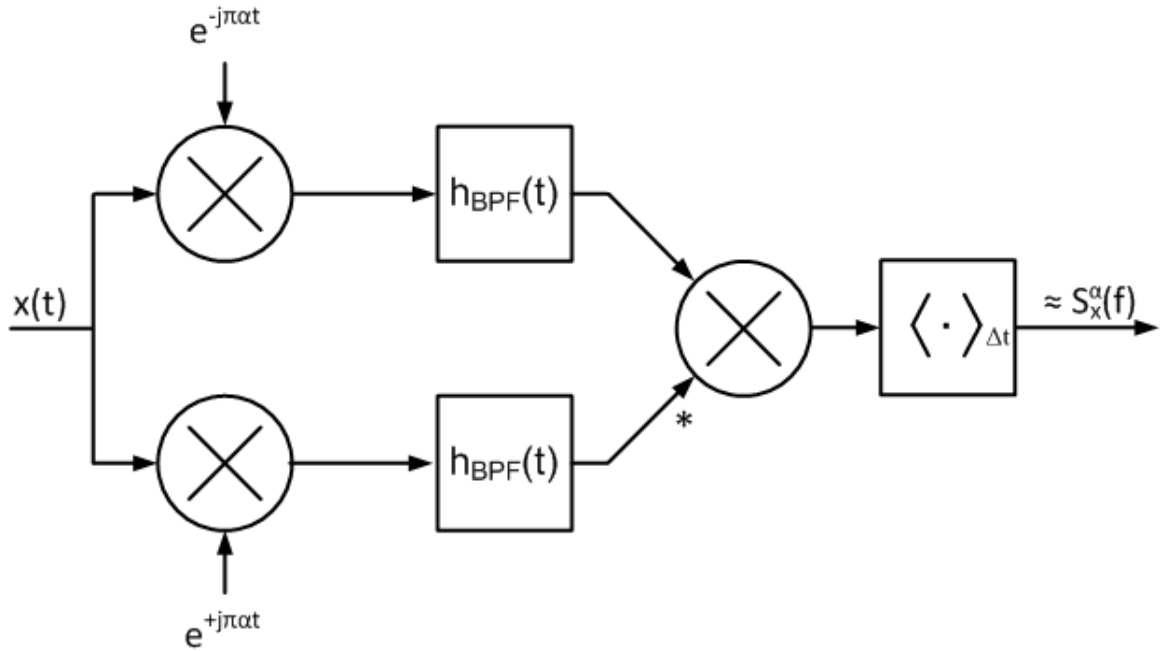


Figure 2.2 Block diagram of a spectral correlation analyzer for center frequency f and cyclic frequency α (from [12]).

Because the SCF allows visualization of a time-series in the bi-frequency plane (cyclic frequency vs. spectral frequency), the cyclostationary parameters of multiple incident signals can be examined simultaneously. Communications signals exhibit cyclostationarity due to symbol rate, sampling rate, multiplexing, modulation, and coding operations [11]. These cyclostationary effects manifest themselves in the SCF such that many modulation types will present unique signatures in the bi-frequency plane, which can aid in their identification. Additionally, because the SCF is a correlation of the spectral components of the time-series, and white noise is uncorrelated, the SCF is insensitive to the effects of additive white noise for cyclic frequencies other than zero [14]. Figure 2.3 shows an estimated spectral correlation density of the AM signal (9) examined previously in Section 1.3.3 along with the same signal corrupted by various amounts of noise. Note, in the bottom plot, even though the signal is buried in the noise floor, the cyclic peaks are still clearly visible. The contour plot of the estimated spectral correlation density for the no additive noise case is shown in Figure 2.4. Observe using Figure 2.3 and Figure 2.4 that for cyclic frequency $\alpha = 0$ the SCF matches the PSD shown in Figure 1.4(b) and that cyclic frequency peaks match those shown in Figure 1.4(d).

One of the drawbacks of the SCF is its computational complexity, which is significantly higher than ordinary spectral analysis. It is the large number of correlation factors that must be computed that drives the computational expense [15]. Several methods have been developed to approximate the SCF via averaging in time or frequency, but even these methods require the parallel computation of several FFTs and complex multiplications.

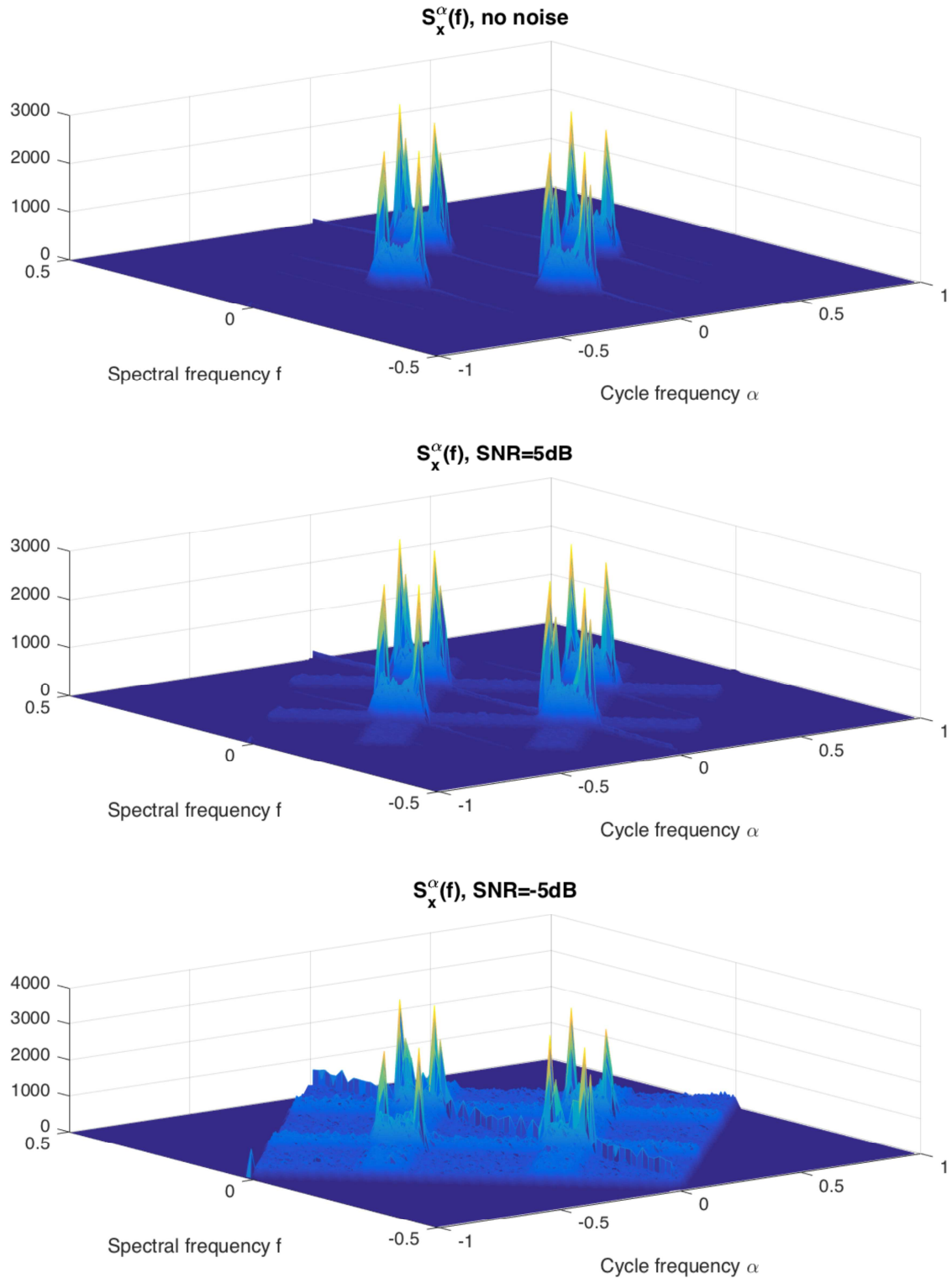


Figure 2.3 Estimated spectral correlation density of an AM modulated signal with: (top) no additive noise, (middle) 5dB SNR, (bottom) -5dB SNR.

2.4 Spectral Coherence Function

Lastly, the SCF can be normalized to produce a proper coherence value, referred to as the spectral coherence function (abbreviated SOF) with a magnitude in the range [0,1], given as [14]

$$C_x^\alpha(f) = \frac{S_x^\alpha(f)}{[S_x^0(f + \frac{\alpha}{2})S_x^\alpha(f - \frac{\alpha}{2})^*]^{1/2}}. \quad (33)$$

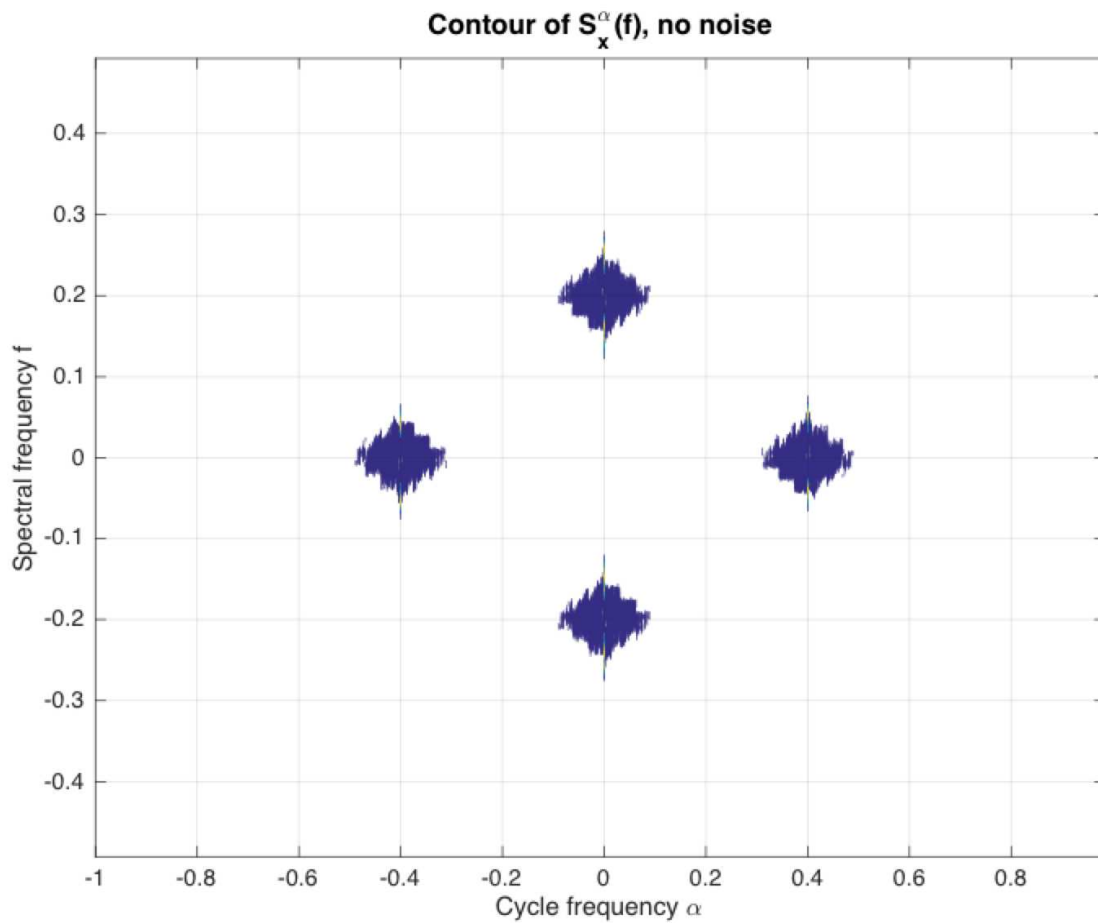


Figure 2.4 Contour of the estimated spectral correlation density of an AM modulated signal.

CHAPTER 3

OFDM FEATURE DETECTION

3.1 OFDM Overview

Orthogonal frequency-division multiplexing (OFDM) is a digital modulation scheme that is ideally suited for the transmission of data in multipath fading environments. As data rates continue to increase, the symbol time of single-carrier modulation methods becomes less than the channel impulse response time and which can result in severe intersymbol interference (ISI) from multipath propagation. OFDM instead utilizes multiple carriers to transmit the same aggregate data rate but at a lower per carrier symbol rate, conceptually analogous to parallelizing a data bus to achieve the same bandwidth as a much faster serial bus. The subcarriers are spaced orthogonally in frequency according to the inverse of the data symbol time T_{FFT}

$$\Delta f = \frac{1}{T_{FFT}}. \quad (34)$$

In this way, OFDM can achieve high-spectral efficiency by maintaining optimal spacing between subcarriers. The subcarriers themselves can be modulated with any suitable quadrature amplitude modulation encoding scheme.

The longer symbol times in OFDM modulation techniques make mitigation of multipath propagation easier by the insertion of a sub-symbol time guard interval. This guard interval is referred to as a cyclic prefix and consists of a portion of the end of the OFDM symbol appended to the front of the symbol, the duration of which is chosen to be longer than the channel impulse response. Typical lengths for the guard interval are $\frac{1}{8}$ to

$\frac{1}{4}$ of the symbol time. By copying the end of the symbol to its beginning and assuming the channel impulse response is shorter than or equal to the length of the guard interval, the linear convolution of the transmitted symbol with the channel response can be modeled as a circular convolution. By assuming a flat fading model per subcarrier, receiver equalization is then simplified to a one-tap equalizer for each subcarrier.

The concept of OFDM modulation has been known for some time, but only recently has been exploited on a commercial basis with the advent of low-cost, high-performance digital signal processors and application specific integrated circuits. OFDM modulators and demodulators are efficiently implemented with the use of the Fast Fourier Transform (FFT). In the case of the modulator, the inverse-FFT converts the parallel set of mapped complex baseband data, which are conceptually in the frequency domain and separated by the bin spacing of the IFFT, into a serial stream of time domain data. This transformation of the baseband data from frequency domain to time domain has the effect of modulating the baseband samples by their respective subcarriers. Not all of the subcarriers may necessarily be used for modulating data. Depending on the modulation type, some subcarriers may be assigned a pilot signal to assist the receiver in equalization and other subcarriers may be null. Afterwards the cyclic prefix is appended to the symbol before transmission. Note, due to the optimal spacing of the subcarriers, the bandwidth of the OFDM transmission is related to the number of subcarriers, N_{FFT} and the subcarrier spacing:

$$BW = N_{FFT} \cdot \Delta f \quad (35)$$

An OFDM demodulator operates in reverse to the modulator. First, the cyclic prefix is removed to obtain a symbol frame corresponding to the expected number of subcarriers, which is then fed to an FFT. The FFT output bins represent the demodulated data of each of the subcarriers. The output bins are equalized, de-mapped, and serialized to provide the output data. Figure 3.1 presents a simplified block diagram of an OFDM modulator and demodulator.

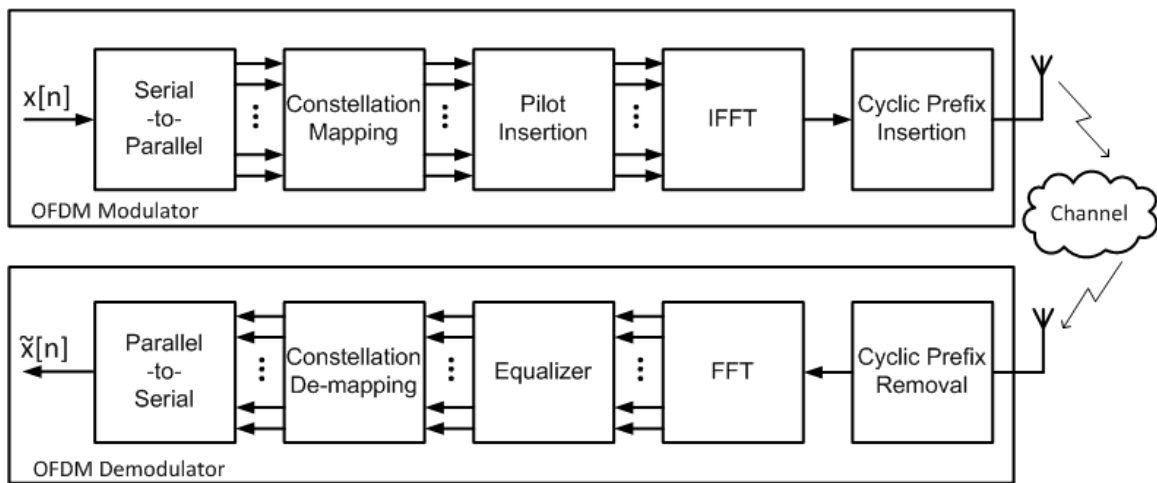


Figure 3.1 Simplified block diagram of an OFDM modulator and demodulator.

3.2 DSRC Modulation

Dedicated Short Range Communications (DSRC) is properly defined by ASTM Standard E2213-03 and is identified as the 5.9 GHz band allocated for Intelligent Transportation Systems (ITS) communications. The DSRC band consists of seven 10 MHz-wide channels starting at 5.855 GHz, shown in Figure 3.2 (a 5 MHz guard band separates DSRC from the lower adjacent band) [16]. ASTM E2213-03 utilizes IEEE-802.11p amendment (referred to as Wireless Access in Vehicular Environments—

WAVE) for the definition of the medium access control (MAC) and physical layer (PHY) aspects of DSRC [17]. Likewise, IEEE amendment 802.11p derives from 802.11a, which is commonly known as the Wireless LAN standard employing OFDM modulation in the 5 GHz band.

The spectral efficiency, high-bandwidth, and resilience to multipath fading make OFDM a well-suited modulation for use in the highly mobile wireless vehicular environment. WAVE defines several enhancements to the MAC and PHY aspects of 802.11a in order to increase its suitability for vehicle-to-vehicle and vehicle-to-infrastructure communications. The PHY modifications entail increasing the OFDM symbol duration by a factor of two. This reduces the subcarrier spacing by half, resulting in an occupied bandwidth of 10 MHz vs. 20 MHz for 802.11a. Table 1 lists the OFDM PHY modulation parameters for 802.11p [18].

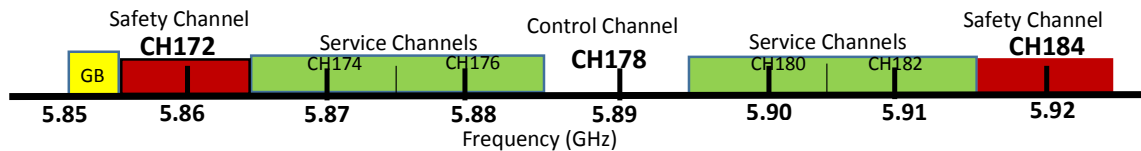


Figure 3.2 DSRC channel plan (from [18]).

The PHY layer in 802.11p is responsible for the movement of data between the MAC layer and the physical transmission medium. This is done in two sub layers. The first sub layer is the Physical Layer Convergence Protocol (PLCP), which communicates with the MAC by organizing the MAC Packet Data Units (MPDU) into the necessary OFDM frame format known as the PPDU (Protocol Packet Data Unit) [18], [19]. The

second sub layer is the Physical Medium Dependent (PMD). The PMD places the PPDU on the physical medium (RF in the case of DSRC applications).

Table 1 OFDM PHY Modulation Parameters of 802.11p

Parameters	Notation	802.11p
Total number of subcarriers	N_{FFT}	64
Total number of used subcarriers	N_{ST}	52
Data subcarriers	N_{SD}	48
Pilot subcarriers	N_{SP}	4 (subcarriers $\pm 7, \pm 21$)
Null subcarriers	Null	12 (IFFT bins 0, [27:37])
Subcarrier frequency spacing	Δf	0.15625 MHz ($1/T_{\text{FFT}}$)
Symbol duration	T_{SYM}	8 μs ($T_{\text{GI}}+T_{\text{FFT}}$)
Guard interval duration	T_{GI}	1.6 μs ($1/4 T_{\text{FFT}}$)
FFT duration	T_{FFT}	6.4 μs
Chip duration	T_{c}	100 ns
Preamble duration	T_{PREM}	32 μs ($10T_{\text{STS}} + 2T_{\text{GI}} + 2T_{\text{LTS}}$)
Short training symbol duration	T_{STS}	1.6 μs
Long training symbol duration	T_{LTS}	6.4 μs

A PPDU frame consists of three main elements. The first element in the frame is the preamble, which also marks the frame's beginning. The preamble is comprised of ten short training sequences (STS) and two long training sequences (LTS) separated by a double length guard interval. The STS consists of 12 subcarriers (subcarriers $\pm 4, \pm 8, \pm 12, \pm 16, \pm 20$, and ± 24), which are used by the receiver for signal detection, automatic gain control, diversity detection, and coarse frequency offset using the known pattern

$$\begin{aligned}
 STS = [& 1 + j, -1 - j, 1 + j, -1 - j, -1 + j, \\
 & -1 - j, -1 - j, 1 + j, 1 + j, 1 + j, 1 + j].
 \end{aligned} \tag{36}$$

The STS symbols have a shorter duration of 1.6 μs , resulting in total short training sequence duration of 16 μs . Afterwards, the LTS is transmitted, consisting of two long

training symbols. Each long training symbol consists of all ± 26 used subcarriers, which allow for channel estimation and fine frequency offset correction using the known pattern

$$LTS = [-1, 1, 1, -1, 1, -1, 1, 1, 1, 1, 1, -1, -1, 1, -1, 1, 1, 1, 1, 0, 1, -1, -1, 1, 1, -1, 1, -1, 1, -1, -1, -1, -1, -1, 1, 1, -1, -1, 1, -1, 1, -1, 1, 1, 1, 1]. \quad (37)$$

The LTS symbols have a duration of $6.4 \mu\text{s}$, which when combined with the double length guard interval results in a total long training sequence length of $16 \mu\text{s}$ and a total preamble length of $32 \mu\text{s}$.

The second field element in a PPDU frame is the signal field (SIG) consisting of a single OFDM symbol. The SIG field consists of header information that details the coding rate, modulation scheme, and packet length of the following data field in the PPDU. The SIG field is always encoded at $\frac{1}{2}$ rate with BPSK modulation, resulting in 24 bits. The first four bits encode the modulation rate and scheme and are referred to as the RATE subfield. The next bits are a null bit followed by twelve bits referred to as the LENGTH subfield, which describes the number of bytes in the PPDU data field. The remaining bits in the SIG field are parity and null [18], [20], [21].

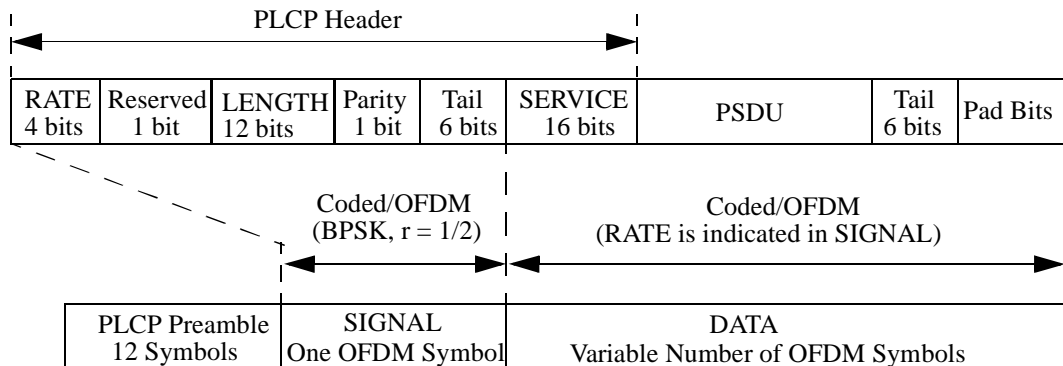


Figure 3.3 PPDU frame format (from [21]).

The final element in the PPDU frame is the data field. The data field uses a convolutional code for forward error correction at either $\frac{1}{2}$ or $\frac{3}{4}$ coding rate [18]. Additionally, the modulation scheme can be either BPSK, QPSK, 16-QAM, or 64-QAM. The coding rate and modulation scheme are chosen by the higher-level protocol according to the error rate of the transmission channel [21]. The parameters and data rates for the various modulation schemes are listed in Table 2. The rate and modulation scheme apply to all bytes of the data field in the PPDU frame, which may contain a maximum of 4096 bytes. The four pilot subcarriers (± 7 and ± 21) in each OFDM symbol are always encoded as BPSK and are modulated with a pseudo-random binary sequence to prevent the generation of spectral lines [20], [21]. The PPDU frame format is illustrated in Figure 3.3

Table 2 Subcarrier Modulation Parameters of 802.11p

Modulation Type	Coding rate	Coded bits per subcarrier	Data bits per symbol (N_{DBPS})	Data rate (Mbps)
BPSK	$\frac{1}{2}$	1	24	3
BPSK	$\frac{3}{4}$	1	36	4.5
QPSK	$\frac{1}{2}$	2	48	6
QPSK	$\frac{3}{4}$	2	72	9
16-QAM	$\frac{1}{2}$	4	96	12
16-QAM	$\frac{3}{4}$	4	144	18
64-QAM	$\frac{1}{2}$	6	192	24
64-QAM	$\frac{3}{4}$	6	216	27

3.3 802.11p Simulation Model

In order to test the cyclostationary features of an 802.11p signal, a simulation model that generates the complex baseband modulation was developed. The physical layer of 802.11p is identical to that of 802.11a, but with the timing parameters doubled. Therefore, the MATLAB model developed for 802.11a in [19] was modified and reused to produce 802.11p compliant waveforms.

The baseband data is generated with the function `WiFi_BasebandMod.m`, which is included in Appendix A. The function is parameterized by Q the number of symbols to generate (variable), m the number of bits per chip (1, 2, 4, or 6), bk the actual binary packet data (a sequence of random integers in the set $[0\ 1]$ of length $m*Q*48$), and *Frame* the number of OFDM symbols per PPDU frame (variable up to the maximum depending on bits per symbol). With the supplied parameters, the baseband simulation model first modulates the data according to the appropriate M-ary QAM object, then the preamble sequence consisting of 10 STS and 2 LTS symbols with guard intervals is created. Afterwards, the SIG symbol is generated, indicating the number of symbols and their encoding rate. The pseudo-random pilot subcarrier vector is created, and along with the data, guard bands, and DC null, the time-domain vector is generated with an inverse FFT. The cyclic prefix is created from the output of the inverse FFT for every symbol and the combined samples are then serialized to provide the baseband signal output. An example time-domain plot of a signal with 10 symbols encoded with $m=6$ is shown in Figure 3.4. An example power spectral density of a signal with 100 symbols encoded with $m=6$ is shown in Figure 3.5.

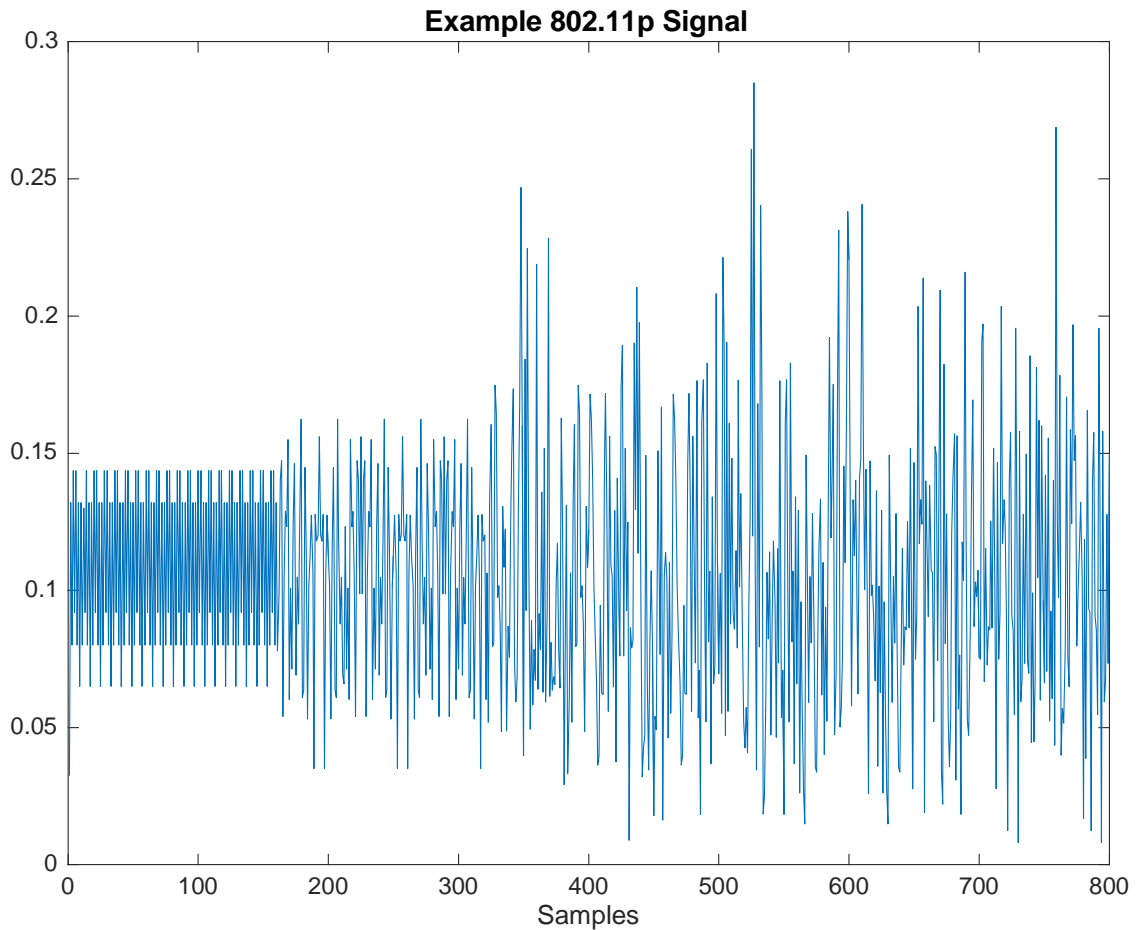


Figure 3.4 Time-domain plot an 802.11p PPDU frame of 10 symbols encoded with 64-QAM.

3.4 OFDM Features for Cyclostationary Detection

In Section 1.3 various signal detection methods were reviewed. Cyclostationary signal analysis was revealed to provide several benefits over alternative techniques such as energy detection and matched filtering approaches. Specifically, cyclostationary analysis provides reduced sensitivity to noise and the ability to obtain signal parametric signatures related to modulation type and carrier frequencies. Additionally, cyclostationary techniques do not require frequency or phase synchronization with the

signal of interest, unlike coherent approaches such as matched filtering [22]. The main drawback of cyclostationary techniques that rely upon the calculation of the SCF is the computational expense. The algorithms developed in [15] for the estimation of (30) relate the cyclic frequency resolution to be inversely proportional to the observation time

$$\Delta\alpha = 1/\Delta t. \quad (38)$$

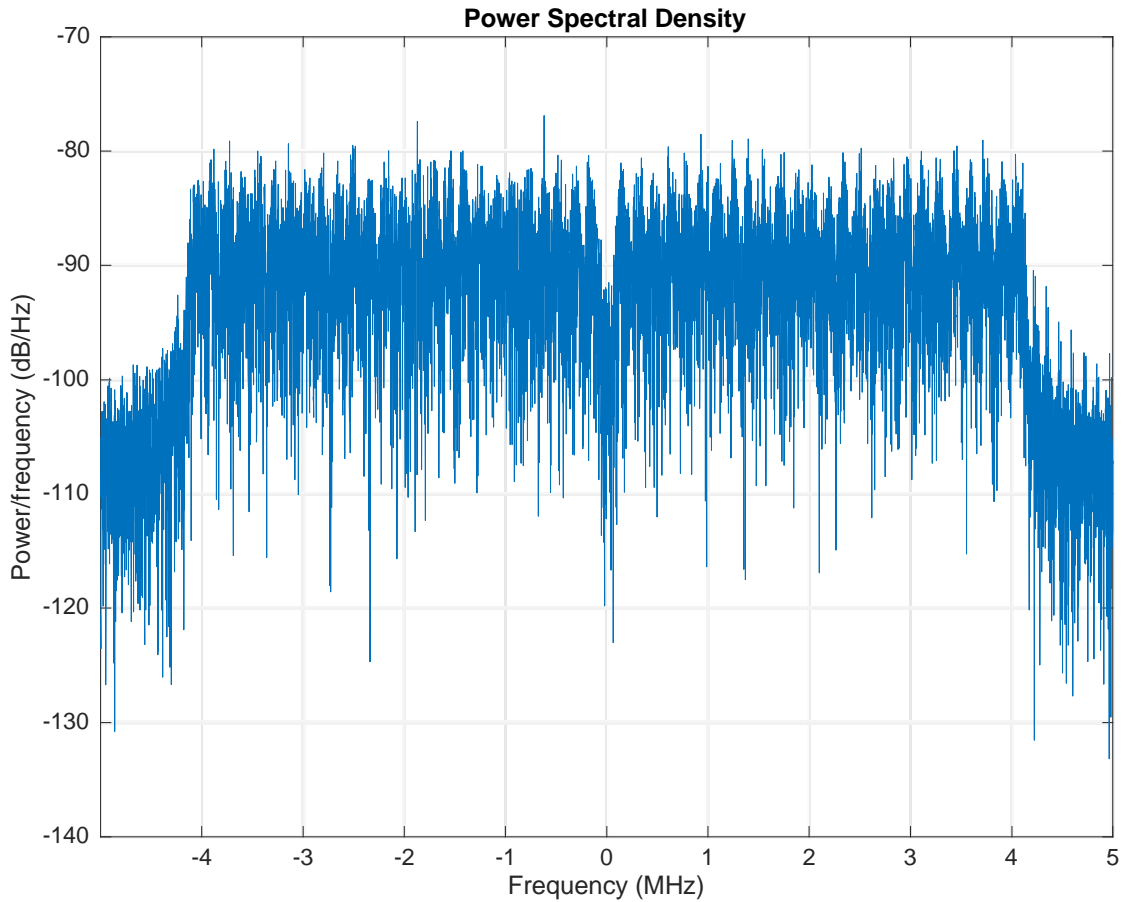


Figure 3.5 Power spectral density of an 802.11p PPDU frame of 100 symbols encoded with 64-QAM.

The reliability of the SCF approximations to adequately resolve spectral and cyclic frequency elements of the signal of interest can thus impose a heavy computational burden as well as slow down the detection time by requiring longer observation periods. However, if the signal of interest is known apriori, then the SCF can reveal cyclic signatures that could be utilized in the detection of the signal. Consequently, provided the cyclic signatures are unique, the computation of the SCF may be avoided in favor of the computationally inexpensive calculation of the CAF that corresponds to specific lag values and cyclic frequencies of the related signatures. Therefore, using the model described in the previous section, the SCF is generated for an example 802.11p frame, shown in Figure 3.6. The related contour is shown in Figure 3.7.

3.4.1 Preamble

Perhaps the most obvious signal signature of an 802.11p frame that is useful for detection is the PPDU preamble consisting of short and long training sequences. These sequences are located at known subcarriers with known amplitude and phase, as given in (36) and (37). In fact, one of the intended functions of the preamble sequences is identification by a corresponding 802.11p device for clear channel assessment prior to transmission as well as incoming signal detection. However, the main drawback of the preamble sequence is its relatively infrequent occurrence. The preamble sequence occurs only at the beginning of a PPDU frame transmission. The number of symbols, N_{SYM} , in a PPDU frame is given by [21]

$$N_{SYM} = [(16 + 8 \cdot LENGTH + 6)/N_{DBPS}]. \quad (39)$$

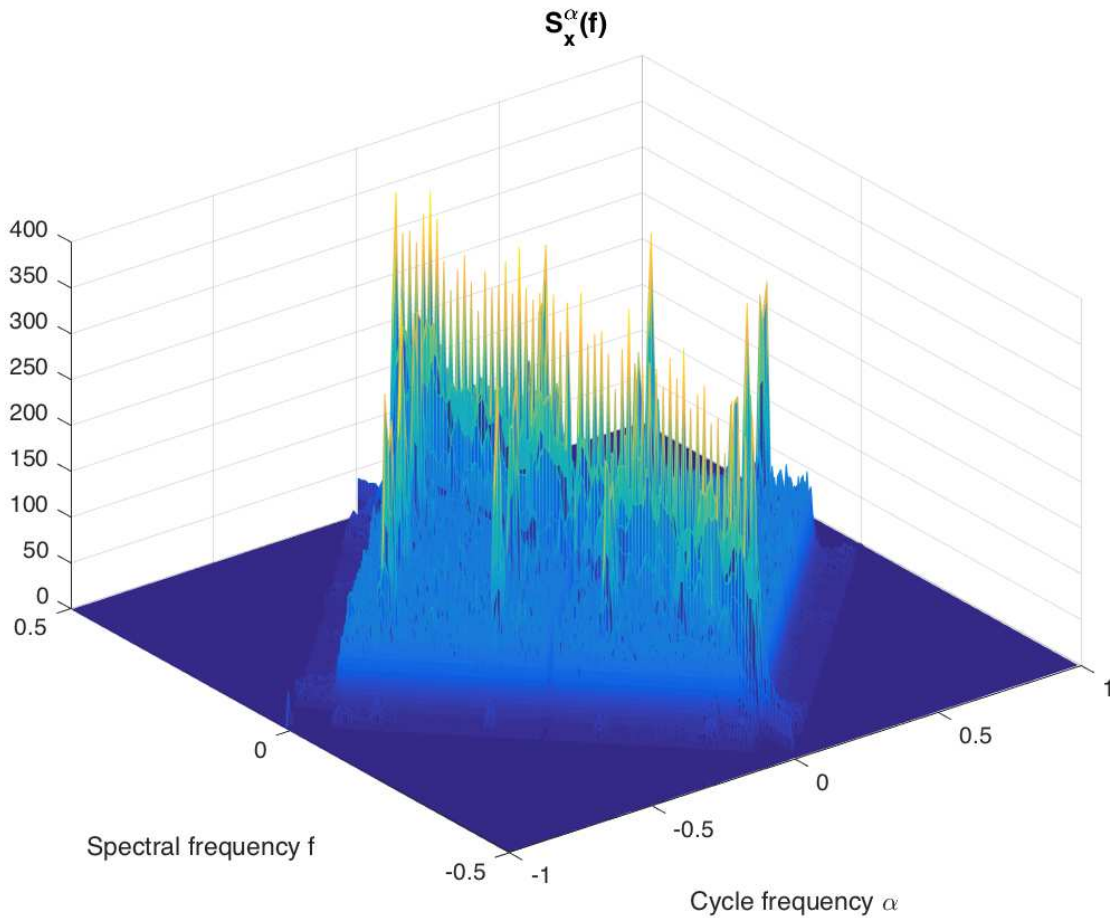


Figure 3.6 Estimated spectral correlation density of an 802.11p PPDU frame.

Because the byte length of a PPDU frame may be up to 4095 bytes according to the 12-bit LENGTH subfield, the probability of detection of an 802.11p transmitter using only the 12 symbols of the preamble sequence is less than 1% in the worst case scenario where the modulation type is $\frac{1}{2}$ rate BPSK with a data bits per symbol, N_{DBPS} , of 24. Such a detection mechanism by a secondary user would be susceptible to assuming an unoccupied channel when in fact a primary user may indeed be transmitting. Extended sensing time prior to transmission would be required in order to mitigate the possibility of

interfering with an 802.11p frame in progress. However, this leads to an inefficient reuse of the spectral resource by the secondary user. As a result, this method is not considered as a reliable mechanism for the detection of highly mobile and time critical 802.11p transmissions.

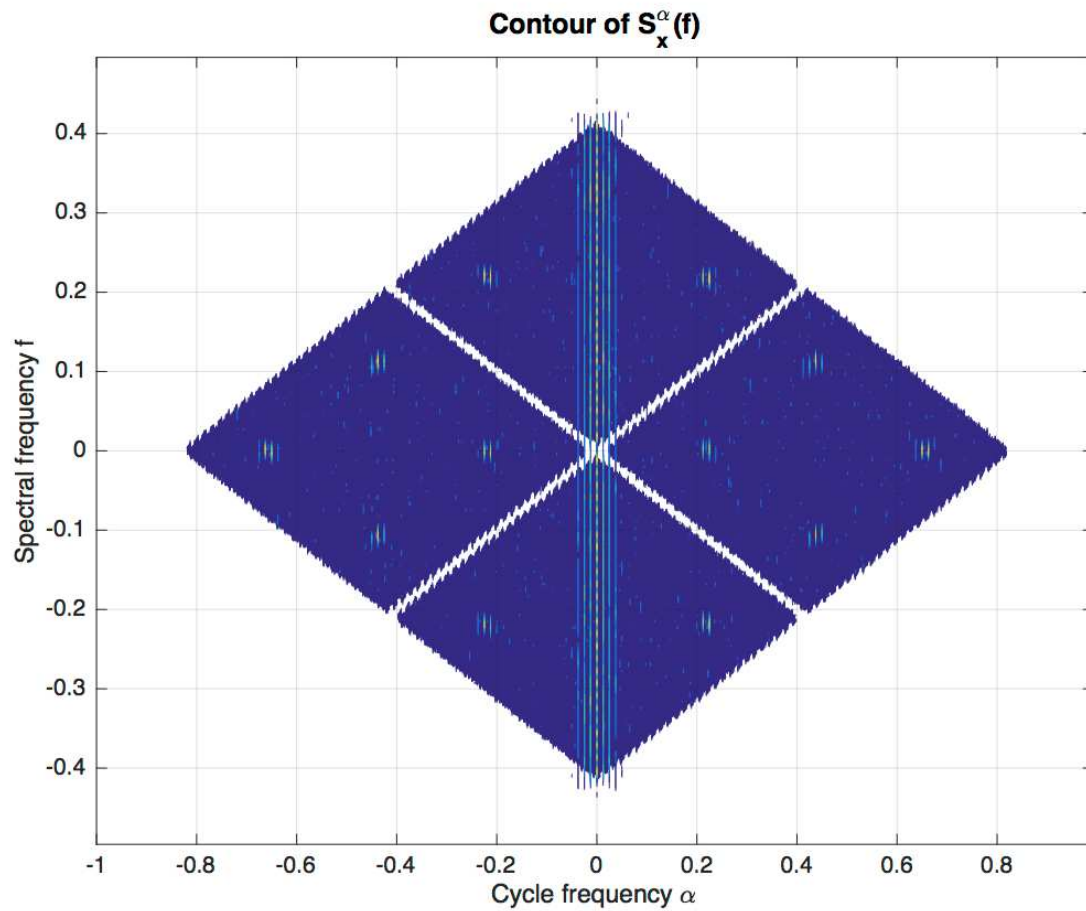


Figure 3.7 Contour of the estimated spectral correlation density of an 802.11p PPDU frame.

3.4.2 Pilots

Each OFDM symbol dedicates four subcarriers for use as pilot signals. These signals are utilized by an 802.11p receiver in order to provide robustness against frequency offsets and phase noise [21]. They are received coherently with the rest of the symbol and used by the receiver for frequency correction and equalization. The pilot subcarriers are modulated by a pseudo-random binary sequence to prevent the generation of spectral lines. However, each subcarrier is modulated by the same value in the pseudo-random binary sequence, creating the opportunity for cyclic detection. Moreover, the pseudo-random sequence is only 127 elements long, after which the sequence repeats [21]. For PPDU frames that exceed 127 OFDM symbols, this repetition should also provide a means for cyclic detection. Indeed, careful examination of Figure 3.7 reveals the presence of cyclic features that correspond to the pilot symbols located at subcarriers $\pm 7, \pm 21$. These cyclic features can be more clearly revealed by modifying the model to replace the pilot subcarriers with null subcarriers. This exposes the pilot subcarriers in a similar pattern to the null subcarrier located at DC and is shown in Figure 3.8. Between Figure 3.7 and Figure 3.8, it can be observed that spectral lines are produced at the cyclic intersections of the pilot subcarriers, which are given by the coordinates

$$\begin{aligned} \alpha &= \pm(SC_x - SC_y) \cdot \Delta f \\ f &= \pm(SC_x + SC_y) \cdot \Delta f / 2 \end{aligned} \quad (40)$$

where

$$SC_x, SC_y = \{\pm 7, \pm 21 | SC_x \neq SC_y\}. \quad (41)$$

These intersections represent the correlation of the identical pilot subcarriers in a symbol at the various cyclic and spectral frequencies listed in (40), as well as the correlation from the contribution of the pilot subcarriers to the symbol's cyclic prefix. To illustrate this point, the simulation model is modified again to provide random modulation values for each pilot subcarrier, which eliminates their cyclic features in the SCD as shown in Figure 3.9.

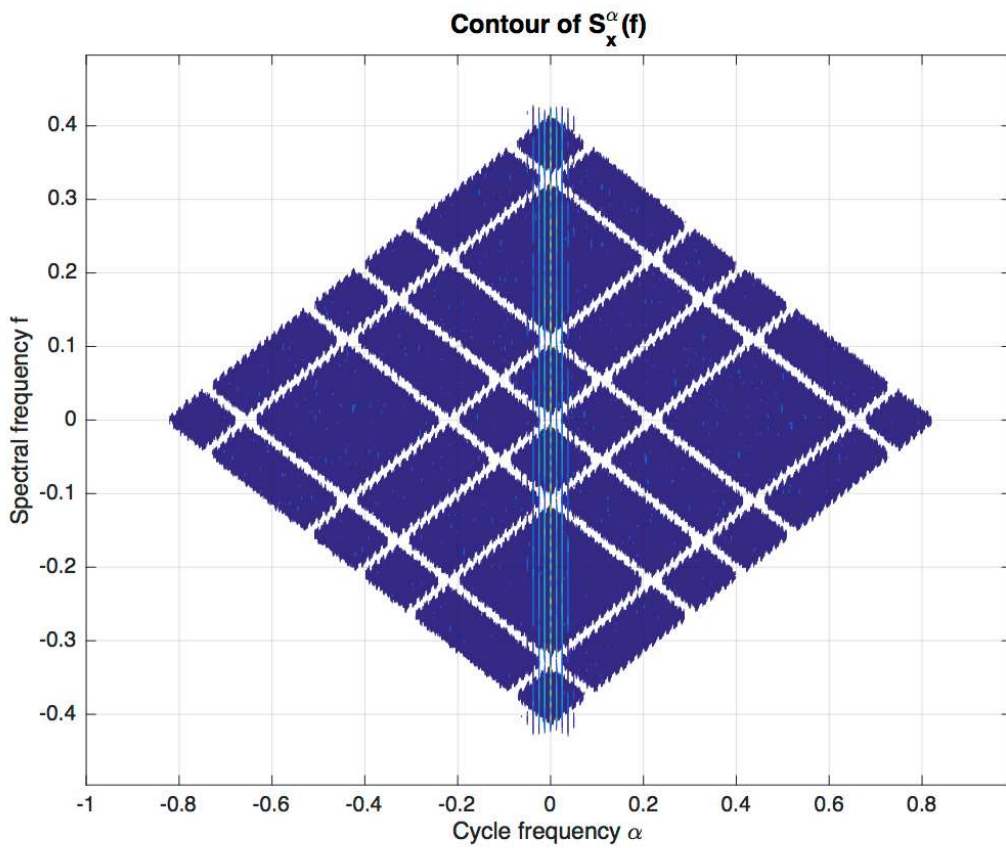


Figure 3.8 Contour of the estimated spectral correlation density of an 802.11p PPDU frame modified by replacing the pilot subcarriers with nulls.

Clearly the pilot subcarriers could be utilized as a means of detection of a primary 802.11p signal due to their cyclostationary signature. However, the pilots are spread over a relatively wide bandwidth, which is subject to dispersion. In fact, the pilots are intended to be used by an 802.11p receiver in order to provide channel estimation and frequency equalization. In poor channel conditions the pilots will begin to become uncorrelated, thus weakening their cyclic features. Additionally, the cyclic features produced by the pilots exist at relatively narrow spectral frequencies and occur at multiple cyclic frequencies, which complicates their detection. Therefore, the pilot subcarriers are deemed as a possible, but not desired, element to use for primary signal detection.

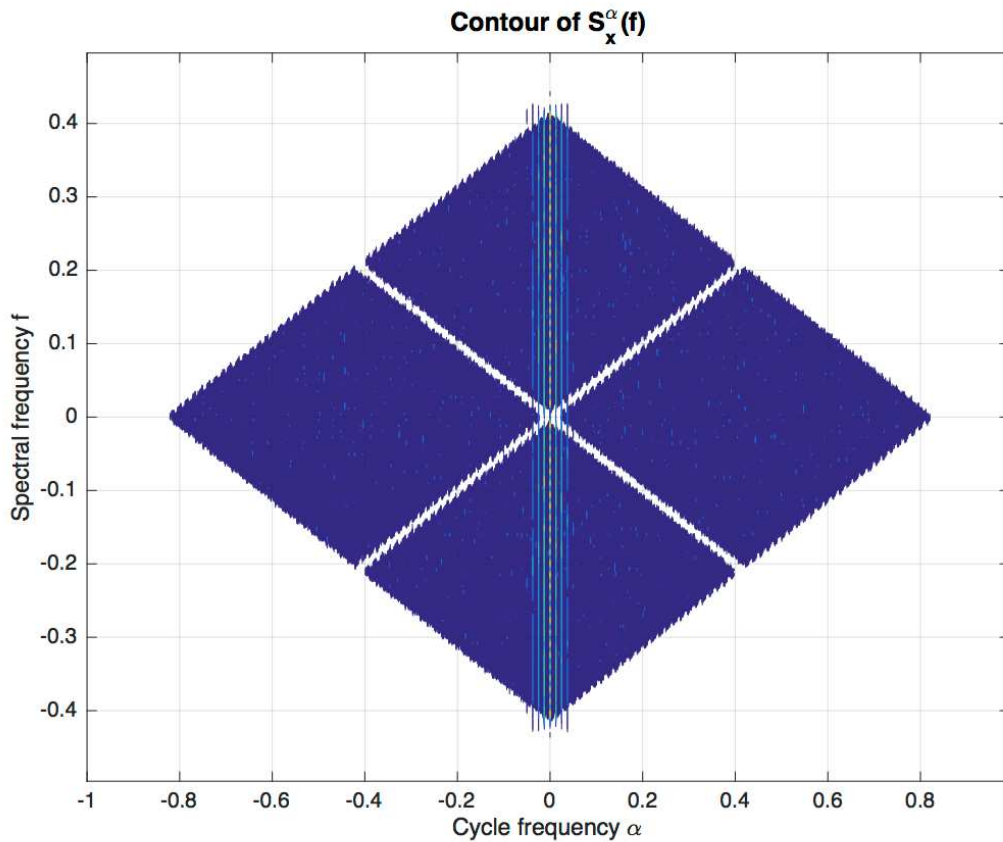


Figure 3.9 Contour of the estimated spectral correlation density of an 802.11p PPDU frame modified by randomizing the pilot subcarriers.

3.4.3 Cyclic Prefix

A cyclic prefix is utilized in OFDM systems, including 802.11p, in order to combat the effects of multipath fading. In 802.11p the cyclic prefix consists of the last 16 samples of the time-domain symbol being replicated at the front of the symbol. This predictable repetition should generate spectral lines in a cyclostationary analysis, and in fact they are revealed in the contour shown in Figure 3.7 as the multiple spectral lines close to $\alpha = 0$. Figure 3.10 shows the cycle frequency cross-section of Figure 3.6 to more clearly display these spectral lines.

The source of these spectral lines can be determined analytically. Consider that the complex envelop of an OFDM symbol with subcarriers modulated with QAM sequences can be represented by [23]

$$x(t) = \sum_k \sum_{n=0}^{N_{FFT}-1} \gamma_{n,l} e^{j2\pi n t / T_{FFT}} q(t - kT_{SYM}) \quad (42)$$

where $\gamma_{n,l}$ is an independent and identically distributed message sequence representing the symbol QAM data, $q(t)$ is a square shaping pulse with duration $T_{SYM} = T_{FFT} + T_{GI}$, and N_{FFT} is the number of subcarriers. The spectral correlation function of the complex envelope of $x(t)$ is then given as [23]

$$S_x^\alpha(f) = \begin{cases} \frac{\delta_\gamma^2}{T_{SYM}} \sum_{n=0}^{N_{FFT}-1} Q\left(f - \frac{n}{T_{FFT}} + \frac{\alpha}{2}\right) \cdot Q^*\left(f - \frac{n}{T_{FFT}} - \frac{\alpha}{2}\right), & \alpha = \frac{l}{T_{SYM}} \\ 0, & \alpha \neq \frac{l}{T_{SYM}} \end{cases} \quad (43)$$

where

$$Q(f) = \frac{\sin(\pi f T_{SYM})}{\pi f}. \quad (44)$$

It can be seen that the SCF exhibits periodicity with cyclic frequencies at multiples of the symbol rate. In the case of 802.11p, $T_{SYM} = 80 \cdot T_C$, and from Figure 3.10 periodicity from the cyclic prefix is easily discernable up to values of $l = 3$. Additionally, correlation from the cyclic prefix can be observed at the pilot subcarriers, but due to the limited spectral bandwidth of these correlations, periodicity can only be observed for $l = 1$.

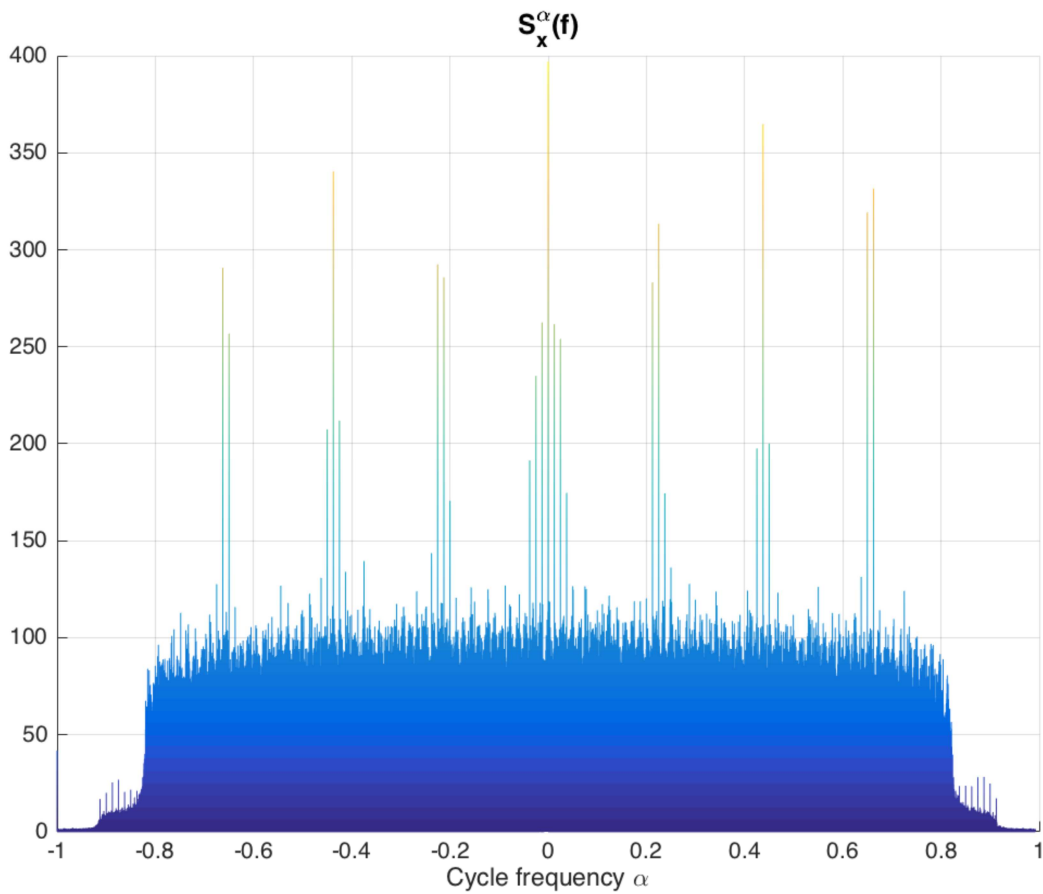


Figure 3.10 Estimated cyclic correlation density of an 802.11p PPDU frame.

3.5 Detection of Cyclic Prefix with CAF

Correlation due to the cyclic prefix provides an excellent means of detection of an 802.11p signal. The cyclostationary signature only exists for an OFDM signal possessing the same number of subcarriers, bandwidth, symbol rate, and cyclic prefix length.

Additionally, because the spectral bandwidth of the correlation from the cyclic prefix spans the entire bandwidth of the signal, implementation of a detection mechanism can be easily accomplished with an autocorrelation function. By computing the autocorrelation function with lags equal to $\pm N_{FFT}$, the repetition in the OFDM symbol caused by the cyclic prefix can easily be seen as shown in Figure 3.11.

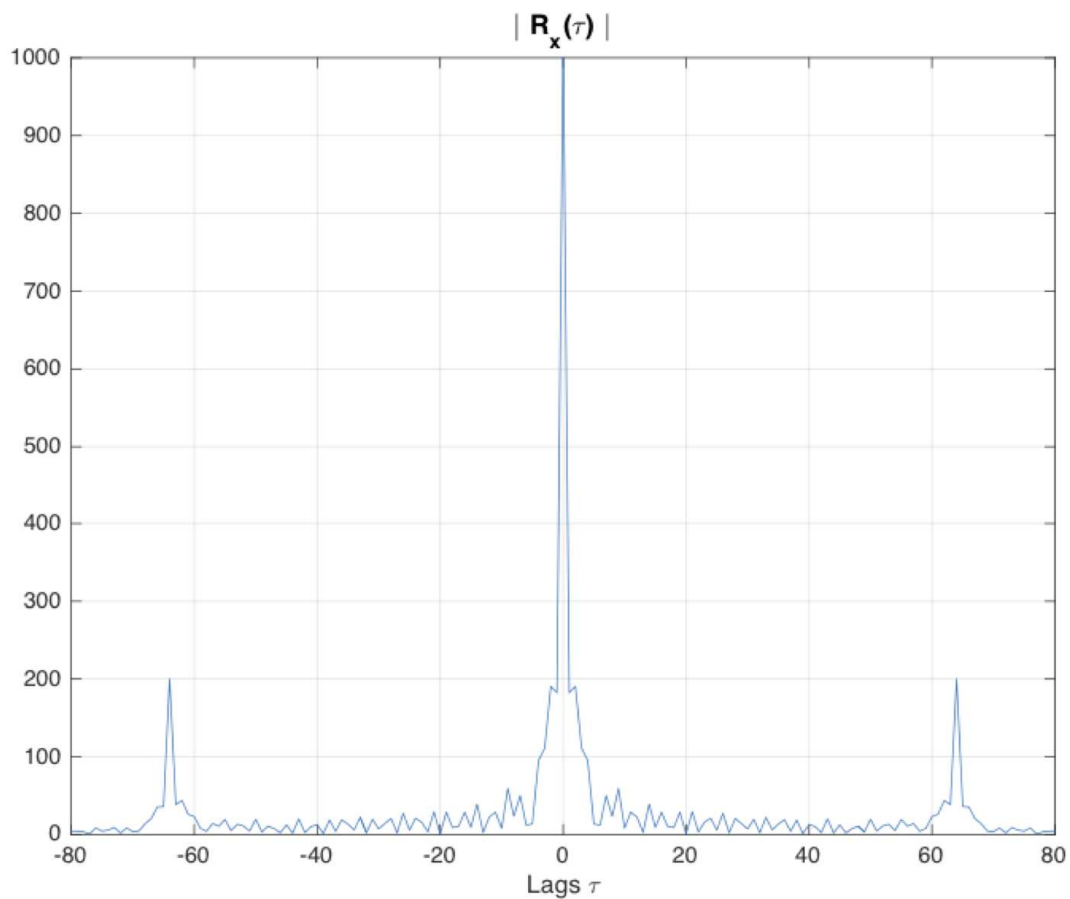


Figure 3.11 Autocorrelation function of an 802.11p PPDU frame.

The cyclic autocorrelation function (CAF) described by (18) can then be applied, assuming a signal at the baseband sampling rate, for fixed lag values $\tau = \pm N_{FFT}$ at cyclic frequencies corresponding to the total symbol sample length $\alpha = 1/(N_{FFT} + N_{GI})$, where N_{GI} indicates the number of baseband samples in the guard interval. The discrete estimation of the CAF over N samples is given by

$$\hat{R}_x^\alpha(\tau) = \sum_{n=0}^{N-1} x[n]x^*[n + \tau]e^{-j2\pi\alpha n} \quad (45)$$

which is the sum of the CAF and an error term $\varepsilon_x^\alpha(\tau)$

$$\hat{R}_x^\alpha(\tau) = R_x^\alpha(\tau) + \varepsilon_x^\alpha(\tau). \quad (46)$$

It is desired to form a test to determine the presence of the primary signal based on the computation of the CAF, therefore a test hypothesis is formulated similar to (3)

$$\begin{aligned} \mathcal{H}_0 & : \mathbf{r}_x = \boldsymbol{\varepsilon}_x \\ \mathcal{H}_1 & : \mathbf{r}_x = \hat{\mathbf{r}}_x + \boldsymbol{\varepsilon}_x, \end{aligned} \quad (47)$$

where

$$\hat{\mathbf{r}}_x = \begin{bmatrix} \text{Re}\{\hat{R}_x^\alpha(\tau_1)\}, \dots, \text{Re}\{\hat{R}_x^\alpha(\tau_k)\}, \\ \text{Im}\{\hat{R}_x^\alpha(\tau_1)\}, \dots, \text{Im}\{\hat{R}_x^\alpha(\tau_k)\} \end{bmatrix} \quad (48)$$

and

$$\boldsymbol{\varepsilon}_x = \begin{bmatrix} \text{Re}\{\varepsilon_x^\alpha(\tau_1)\}, \dots, \text{Re}\{\varepsilon_x^\alpha(\tau_k)\}, \\ \text{Im}\{\varepsilon_x^\alpha(\tau_1)\}, \dots, \text{Im}\{\varepsilon_x^\alpha(\tau_k)\} \end{bmatrix}. \quad (49)$$

For the scenario where $k = 2$, if the samples $x[n]$ that are well separated in time are approximately independent [24], then it can be shown that the error vector has a multivariate normal distribution with zero mean and noise covariance matrix $\mathbf{\Sigma}$, i.e.

$$\lim_{N \rightarrow \infty} \sqrt{N} \mathbf{\epsilon}_x \sim \mathcal{N}(\mathbf{0}, \mathbf{\Sigma}). \quad (50)$$

The test statistic is then defined as

$$T(\hat{\mathbf{r}}_x) = N \cdot \mathbf{r}_x \mathbf{\Sigma}^{-1} \mathbf{r}_x^T, \quad (51)$$

which under the null hypothesis is chi-square distributed with $2k$ degrees of freedom

$$T(\hat{\mathbf{r}}_x) | \mathcal{H}_0 \sim \chi_{2k}^2. \quad (52)$$

A threshold value can be set in order to provide a constant false alarm rate

$$P_{FA} = Prob\{T(\hat{\mathbf{r}}_x) > \lambda | \mathcal{H}_0\}, \quad (53)$$

which the distribution given by (52) allows to be calculated as

$$\lambda = F_{\chi_{2k}^2}^{-1}(1 - P_{FA}), \quad (54)$$

where $F_{\chi_{2k}^2}^{-1}$ is the inverse cumulative distribution function of χ_{2k}^2 [24].

Similar to the example energy based detector example given in Section 1.3.1, in order to implement a test for cyclostationarity using the CAF the covariance matrix must be estimated from the received signal and its inversion calculated [25]. In Chapter 4, a technique that eliminates the need to estimate and invert the covariance matrix will be introduced.

CHAPTER 4

DSRC DETECTION WITH CAF

4.1 Spatial Sign Cyclic Correlation Estimator

The previous chapter reviewed various OFDM signal features for potential use in a cyclostationary detection scheme. The cyclic prefix was found to introduce strong cyclostationary effects making it an ideal candidate for the detection of 802.11p primary users. Moreover, the CAF provides a computationally efficient means by which to calculate the cyclostationary properties of the cyclic prefix. Unfortunately, the detection method requires estimation and inversion of the signal noise covariance matrix. In real applications the noise statistics may not be known completely, in which case an SNR wall develops in the detection scheme as discussed in Section 1.3.1. Additionally, any statistics estimation is subject to frequent change due to the mobile environment in which 802.11p exists. It is therefore desired to develop a detection mechanism that does not require computation of the noise statistics.

One such method proposed in [26] utilizes the spatial sign function (SSF) in order to avoid estimation of the noise probability density function. The SSF for a complex input signal $x[n]$ is given as

$$S(x[n]) = \begin{cases} \frac{x[n]}{|x[n]|} & x[n] \neq 0 \\ 0 & x[n] = 0 \end{cases} \quad (55)$$

The SSF is a nonlinear operation that normalizes the input signal to exist on the unit circle in the complex plane, with the key assumption that the data possesses zero mean.

If the mean is not zero, it should be estimated and removed. The spatial sign cyclic correlation estimator (SSCCE) is then given as

$$\hat{R}_s^\alpha(\tau) = \frac{1}{N} \sum_{n=0}^{N-1} S(x[n])S(x^*[n+\tau])e^{-j2\pi\alpha n}, \quad \forall \tau \neq 0 \quad (56)$$

In [26] it is shown that the nonlinearity of the SSF does not affect the periodicity of the autocorrelation function for circularly symmetric complex Gaussian processes (an accurate model for OFDM systems).

As before, a test statistic is defined to reject the null hypothesis that the received signal does not contain the primary signals. In order to compute the test statistic, it is first necessary to determine the distribution of the SSCCE for an i.i.d. circular noise process with zero mean, $w[n]$. The mean of the SSCCE for $w[n]$ is thus [26]

$$\begin{aligned} E[\hat{R}_s^\alpha(\tau)] &= \frac{1}{N} \sum_{n=0}^{N-1} E[S(w[n])S(w^*[n+\tau])e^{-j2\pi\alpha n}] \\ &= \frac{1}{N} \sum_{n=0}^{N-1} E[S(w[n])E[S(w^*[n+\tau])]e^{-j2\pi\alpha n} = 0, \quad \forall \alpha \end{aligned} \quad (57)$$

The covariance of the SSCCE for $w[n]$ is given by

$$\begin{aligned} \Sigma_{\hat{R}_s^\alpha(\tau)} &= E[\hat{R}_s^\alpha(\tau)\hat{R}_s^{\alpha*}(\tau)] \\ &= E\left[\left(\frac{1}{N} \sum_{n=0}^{N-1} S(w[n])S(w^*[n+\tau])e^{-j2\pi\alpha n}\right) \left(\frac{1}{N} \sum_{n=0}^{N-1} S(w[n])S(w^*[n+\tau])e^{-j2\pi\alpha n}\right)^*\right] \\ &= \frac{1}{N^2} \sum_{n=0}^{N-1} E[|S(w[n])|^2|S(w[n+\tau])|^2]. \end{aligned} \quad (58)$$

The normalization property of the SSF ensures that

$$E[|S(w[n])|^2 |S(w[n + \tau])|^2] = 1 \quad (59)$$

Therefore the covariance of the noise process after normalization from the SSF is

$$\mathbf{\Sigma}_{\hat{R}_S^\alpha(\tau)} = \frac{1}{N} \mathbf{I}. \quad (60)$$

A test hypothesis is again formulated

$$\begin{aligned} \mathcal{H}_0 & : x[n] = w[n] \\ \mathcal{H}_1 & : x[n] = s[n] + w[n], \end{aligned} \quad (61)$$

where $s[n]$ is the primary signal of interest. A vector of the calculated SSCCE functions for various lag values is given as

$$\hat{\mathbf{r}}_s = [\hat{R}_S^\alpha(\tau_1), \dots, \hat{R}_S^\alpha(\tau_k)]. \quad (62)$$

From (60) it follows that $\hat{\mathbf{r}}_s$ is complex normal distributed

$$\lim_{N \rightarrow \infty} \hat{\mathbf{r}}_s | \mathcal{H}_0 \sim \mathcal{CN} \left(\mathbf{0}, \frac{1}{N} \mathbf{I} \right). \quad (63)$$

Then the test statistic can be given as [26]

$$T(\hat{\mathbf{r}}_s) = N \cdot \|\hat{\mathbf{r}}_s\|^2, \quad (64)$$

which under the null hypothesis is chi-square distributed with k complex degrees of freedom

$$T(\hat{\mathbf{r}}_s) | \mathcal{H}_o \sim \chi_k^2. \quad (65)$$

The threshold is then calculated according to the desired false alarm rate

$$\lambda = F_\gamma^{-1}(1 - P_{FA}), \quad (66)$$

where F_γ^{-1} is the inverse gamma cumulative distribution function with scale factor of one and shape factor k [25].

4.2 Dual-Lag SSCCE with Cyclic Phase Compensation

As discussed in Section 3.4.3, the cyclic prefix induces strong cyclostationary features that can be detected with the CAF. As illustrated in Figure 3.11, correlation occurs at lags $\pm N_{FFT}$, which is 64 in the case of 802.11p and clearly visible in Figure 3.10 for cyclic frequencies $\alpha = l/(N_{FFT} + N_{GI})$, $l = 0, \pm 1, \pm 2, \pm 3$. The detection scheme proposed is to calculate the SSCCE at dual lags $\tau = \pm 64$ and $\alpha = 1/80$. The test statistic from (64) is then

$$T(\hat{\mathbf{r}}_s) = N \cdot |\hat{R}_s^\alpha(\tau_1)|^2 + N \cdot |\hat{R}_s^\alpha(\tau_2)|^2. \quad (67)$$

In [27] it is shown that for a dual-lag ($k = 2$) with cyclic frequency $\alpha =$

$1/(N_{FFT} + N_{GI})$, a cyclic phase compensation can be introduced in order to align the

SSCCE values of the two lags in time. The two SSCCE computations are complex valued and have an instantaneous phase difference

$$\emptyset = \arg(\hat{R}_s^\alpha(\tau_1)) + \arg(\hat{R}_s^\alpha(\tau_2)). \quad (68)$$

For an 802.11p primary signal that exhibits correlation at the lag values from the cyclic prefix, the phase difference \emptyset is a constant value based on τ and α [27]

$$\emptyset = 2\pi\tau_1\alpha. \quad (69)$$

The constant phase difference correction is applied to the second SSCCE calculation

$$\hat{R}_s^{\alpha^\emptyset}(\tau_2) = \frac{1}{N} \sum_{n=0}^{N-1} S(x[n])S(x^*[n + \tau_2])e^{-j2\pi\alpha n + \emptyset}. \quad (70)$$

Because the two SSCCEs are now coherent the test statistic can be summed simply as

$$T(\hat{\mathbf{r}}_s^c) = \frac{N}{2} \cdot \left| \hat{R}_s^\alpha(\tau_1) + \hat{R}_s^{\alpha^\emptyset}(\tau_2) \right|^2, \quad (71)$$

which lowers the degrees of freedom to $k = 1$ as well as reduces the implementation complexity. The threshold value is computed the same as (66) but with scale and shape factors of one.

4.3 MATLAB Simulation

The previous section detailed a cyclostationary detection method based on the CAF that avoids the necessity of estimating the noise covariance by normalizing the

signal via the SSF. In order to test the performance and suitability of this method for hardware implementation, a MATLAB simulation was developed. The 802.11p baseband simulation model described in Section 3.3 was used to generate various size PPDU frames. The baseband data was subjected to several impairments to simulate real world channel effects. First, multipath fading was simulated via a Rayleigh model with Doppler shift corresponding to a mobile unit velocity of 130kph. Additionally, the baseband data was shifted 30kHz in order to model a local oscillator offset of 5ppm, which is representative of the maximum typical offset error [28]. Finally, measured additive white Gaussian noise was added to the baseband signal to further simulate the channel. The SSCCE algorithm with cyclic phase compensation, (70), was coded as a MATLAB function, `sscce_pc.m`, and is included in Appendix A. The function is parameterized by x the baseband input signal, α the cyclic frequency, ϕ the cyclic phase compensation (vector valued), and lag the desired lags for the autocorrelation (also vector valued). The signal test statistic is calculated from the SSCCE function for $\tau = \pm 64$ and $\alpha = 1/80$, which is returned along with the calculated SSCCE values. The threshold value is set according to (66) for a standard false alarm probability of 5%.

4.3.1 Probability of Detection vs. SNR

Because the detection scheme operates by correlating N samples, the probability of detection will increase with larger input signal length. However, to simulate realistic scenarios, typical message lengths should be used. The DSRC describes over 150 data elements that can be included in a DSRC message [29]. The data elements describe such information as vehicle acceleration, speed, heading, anti-lock brake status, wiper status,

etc. From these elements, eight high-priority safety messages have been defined. Since these messages are the ones for which detection is paramount, the simulated 802.11p frame should be representative of a typical safety message length. After encoding and protocol encapsulation of the per message data elements, a high-priority safety message may be comprised of approximately 856 to 1408 bits at the PHY PSDU [29]. Depending on the subcarrier modulation scheme, according to (39) the corresponding number of symbols for the smallest safety message encoded at the highest data rate of 27 Mbps is 33 symbols, which represents the worst case signal detection scenario.

Simulations were performed in order to test reliability and performance of the SSCCE detector in varied noise environments. A baseband 802.11p signal 33 symbols in length was generated with the impairments described in the previous section along with measured amounts of AWGN. The SSCCE output test statistic was compared against the threshold value computed for 5% false alarm rate and plotted versus signal SNR, as shown in Figure 4.1. The test was run with a sample size of 1000. As expected, the detection rate trends towards 5% as the noise level increases. Also, observe that despite the relatively few samples used for the correlation (2640 baseband samples), the probability of detection is effectively 100% for any SNR greater than 5dB. The same simulation repeated but without multipath fading or LO offset impairments is shown in Figure 4.2, which indicates approximately 5dB improvement over the previous scenario.

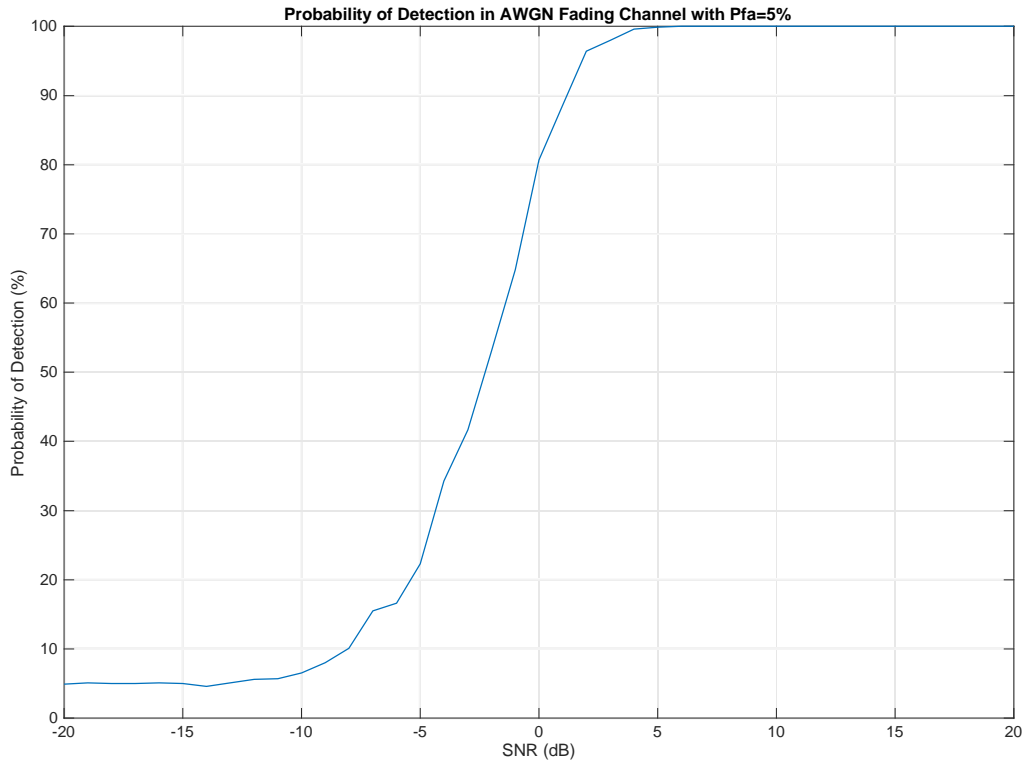


Figure 4.1 Probability of detection vs. SNR of an 802.11p signal corrupted by an AWGN fading channel using SSCCE method with sample size of 1000.

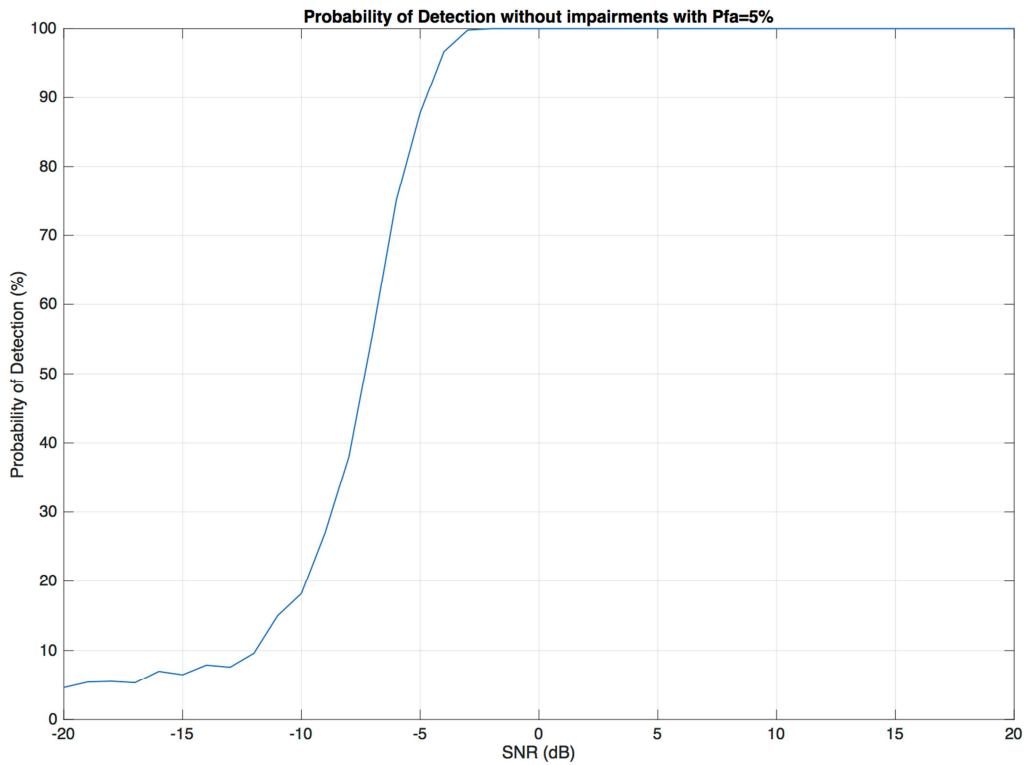


Figure 4.2 Probability of detection vs. SNR of an 802.11p signal without additional impairments using SSCCE method with sample size of 1000.

4.3.2 ROC at Fixed SNR

The receiver operating characteristic curve was evaluated using the same signal length as the previous section and without fading or LO impairments. The specificity vs. sensitivity is shown in Figure 4.3 when the signal is corrupted by AWGN such that the SNR is -5dB.

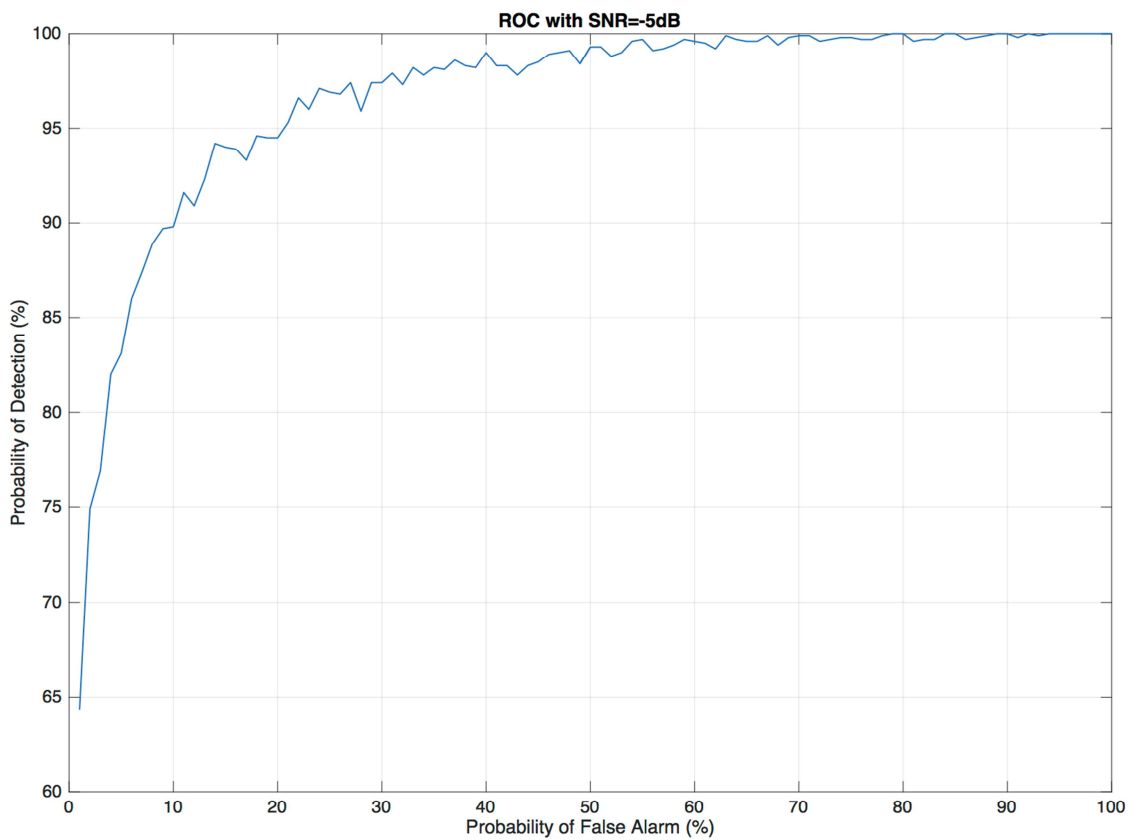


Figure 4.3 Receiver operating characteristic curve of the SSCCE method for an 802.11p signal.

4.3.3 Histogram at Fixed SNR

Finally, the histogram of the test statistic at SNR of -5dB is shown in Figure 4.4 for a sample size of 1000, indicating the test statistic is well modeled by the chi-squared probability density function.

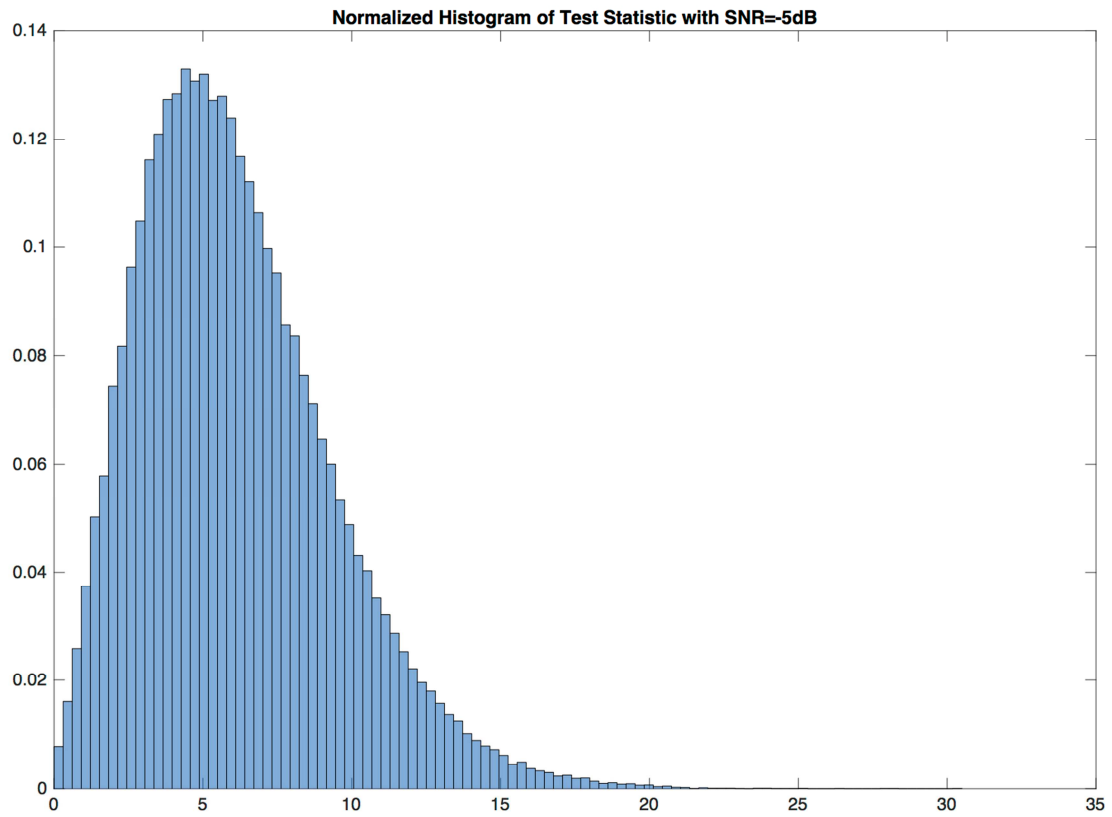


Figure 4.4 Histogram of SSCCE test statistic for an 802.11p signal with -5dB SNR.

CHAPTER 5

FPGA IMPLEMENTATION

5.1 FPGA Overview

As discussed in Section 1.2, spectrum sharing in the DSRC band has several unique challenges. First, the detection methodology must be robust. Several detection schemes have been discussed in the previous chapters. Of those discussed, a cyclostationary method for the detection of the OFDM symbol's cyclic prefix appears to be the most promising for robustness against noise and probability of detection. Secondly, the detection method must provide rapid discovery of primary users. The SSCCE approach reviewed in Chapter 4 was shown to provide detection of 802.11p signals within a fixed number of baseband samples corresponding to a shortest case DSRC safety message. Furthermore, the SSCCE method is not computationally taxing, which addresses the final constraints for a DSRC spectrum-sharing device, namely that it be power and resource efficient. It is expected that a detection engine for 802.11p signals would be implemented in a radio chipset to achieve real-time and power efficient operation. This chapter will review a field programmable gate array (FPGA) implementation of the SSCCE algorithm discussed in Chapter 4.

FPGAs are programmable digital logic devices that contain various logic gates (NOT, OR, AND, XOR, etc.) along with flip-flops and configurable routing interconnects. The logic elements can be programmed after manufacture to implement arbitrary and complex digital logic functionality. A hardware description language (HDL) is used to define the design functionality, typically either Verilog or VHDL.

Figure 5.1 provides a graphical overview of the typical FPGA design flow. One of the use cases for FPGAs is for the creation of fast, deterministic, and efficient digital implementations of algorithms. The resulting FPGA designs may be complete low-volume product solutions or may serve as validation test beds before committing to expensive and time-consuming ASIC (Application Specific Integrated Circuit) design. Therefore, in order to evaluate the functionality, logic resource requirements, and estimated power consumption of the SSCCE algorithm this chapter will detail an FPGA design implementation of the test statistic calculation.

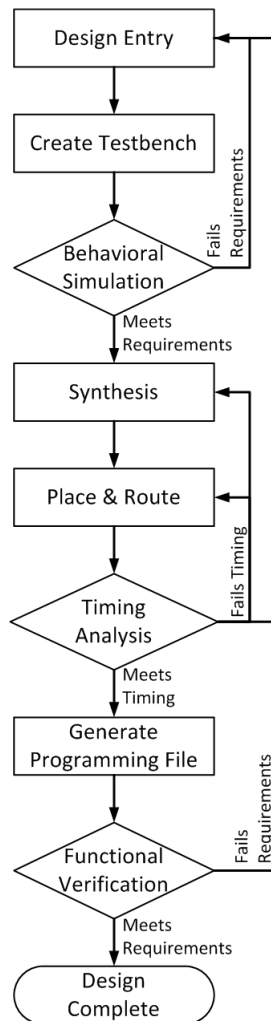


Figure 5.1 Flowchart of a typical FPGA design flow.

5.2 SSCCE Algorithm Implementation

The SSCCE algorithm was broken into several design elements to simplify development into smaller, more easily verified blocks, which also increases design reusability. The design was coded in VHDL, whereas the behavioral testbench was coded in SystemVerilog. All design blocks were coded in pure HDL in order to make use of synthesis inference as opposed to using vendor intellectual property design cores that limit portability. The design was divided into the following blocks: SSF, lead/lag shift register, complex multiplier for the correlation coefficient, numerically controlled oscillator and complex multiplier for the cyclic down conversion of the correlation coefficients, moving average, real multiplier, and adders, all as indicated in Figure 5.2. The top-level design file is given in Appendix B as `sscce.vhd`.

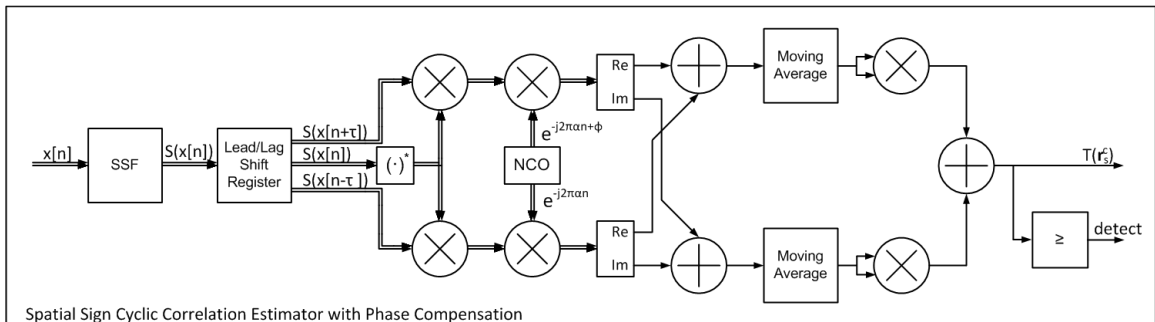


Figure 5.2 Block diagram of the FPGA implementation of the SSCCE algorithm.

5.2.1 Spatial Sign Function

The SSF computes the unit vector of the input signal. Normally, this involves the calculation

$$S(x[n]) = \sqrt{\operatorname{Re}(x[n])^2 + \operatorname{Im}(x[n])^2}. \quad (72)$$

However, this method is expensive in digital logic due to the multiplication required for the two square terms and especially the square-root function. One method to avoid both operations is to obtain the phase angle of the Cartesian input signal and then convert the angle to Cartesian coordinates assuming a normalized magnitude

$$\theta = \tan\left(\frac{\operatorname{Im}(x)}{\operatorname{Re}(x)}\right) \quad (73)$$

$$S(x) = \cos(\theta) + j \sin(\theta).$$

The transcendental functions required in (73) would appear to be more troublesome than the square-root function in (72), however very efficient methods exist for their calculation in digital hardware. The Coordinate Rotational Digital Computer (CORDIC) algorithm calculates trigonometric functions iteratively using only additions and bit shift operations [30].

Two general modes of the algorithm exist. The vectoring mode accepts a Cartesian input signal and through a series of additions and shifts rotates the vector to lie on the real axis. The rotation angle that was required to rotate the vector onto the real axis is the resulting phase angle and the real component of the rotated vector is proportional to the vector magnitude. The other mode of operation is known as the

rotation mode and alternately accepts a polar input, which through a similar set of shifts and additions transforms the input to Cartesian coordinates [31]. The SSF can therefore be efficiently implemented in digital logic without multiplication or square-root operations by using a pair of CORDIC routines as depicted in Figure 5.3.

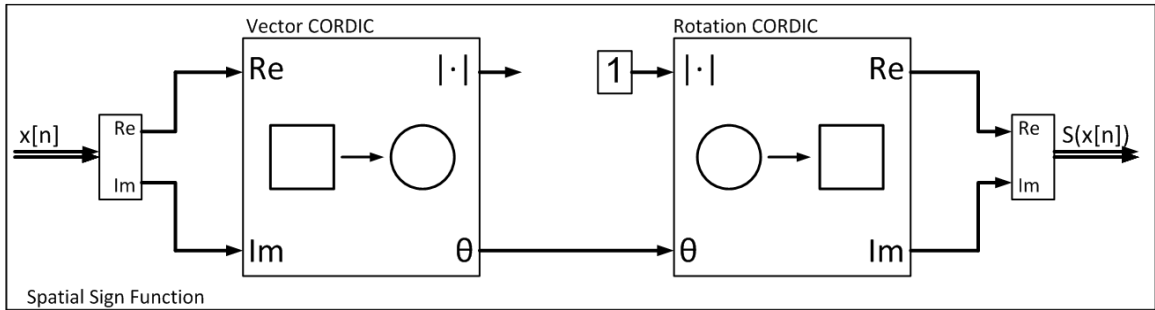


Figure 5.3 Block diagram showing the implementation of the SSF using CORDIC routines.

The SSF implementation is given in Appendix B as the entity `SSF.vhd` along with the two CORDIC entities, `vector_cordic.vhd` and `rotation_cordic.vhd`. The design is parameterized by generics for the input and output data widths and the number of iterations used in the CORDIC routines. Lowering either parameter reduces the logic resources required for implementation but also increases the error in the SSF computation. All parameter values are set to 18 for this design implementation.

5.2.2 Lead/Lag Shift Register

In order to calculate the autocorrelation function of the input signal for $\tau = \pm 64$ a lead/lag shift register is implemented by the file `lead_lag_shift_reg.vhd`, located in Appendix B. Obviously, causality must be preserved, so the lead component of the shift register output is simply the zero-lag input signal. Likewise, the zero-lag output

component is actually the input signal lagged by 64 samples and similarly the lag output component is the input signal lagged by 128 samples, as shown in Figure 5.4. The design is implemented by inferring device block RAM resources, which are typically abundant in FPGAs [32]. This avoids a more resource and power intensive implementation using flip-flop based shift registers. The lead/lag outputs feed into complex multipliers, which produce the autocorrelation coefficients through multiplication of the lead and lag components by the conjugate of the zero-lag component. The block is parameterized by generics for the input and output data width and the lead/lag sample amount, which are set to 18, 18, and 64, respectively, for this design.

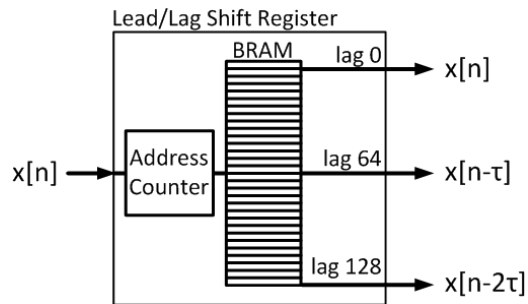


Figure 5.4 Block diagram showing the implementation of the lead/lag shift register.

5.2.3 Multipliers

The SSCCE design requires multipliers for the calculation of the autocorrelation coefficients, the cyclic down conversion products, and the squaring operation of the SSCCE outputs in order to generate the test statistic. Fortunately, most modern FPGAs contain embedded multipliers. Additionally, to maintain design code portability, these elements can be inferred directly from HDL code by most newer synthesis engines. The

autocorrelation and cyclic down conversion operations have complex inputs and therefore require complex multipliers. The complex multiplier design actually consists of four individual multiplication operations along with addition and subtraction of the four products to provide the complex output. The design implementation is provided in Appendix B as `complex_mult.vhd`. Likewise, the squaring operation used in the formation of the test statistic has purely real or purely imaginary inputs and so only requires a real multiplication, which is also given in Appendix B as `real_mult.vhd`. Binary multiplications create an output bit width of twice the input bit width. However, it is often desired to maintain a constant bus width between processing elements. Therefore, the above designs are parameterized by a generic that scales the output by a desired factor-of-two to help maintain numerical precision of the multiplication output when its length is reduced to the input width. This scaling factor needs to be accounted for in the final output. When the multiplier output signal length is reduced, the least significant bits can be rounded off or simply truncated. Rounding reduces error but increases device resource utilization. This design uses a data width of 18 bits for all multipliers, which matches the typical multiplier width common to most FPGA manufacturers. Through empirical testing, rounding was not shown to improve the accuracy of the test statistic and so was disabled to reduce resource requirements.

5.2.4 Numerically Controlled Oscillator

The calculation of the cyclic down conversion of the autocorrelation coefficients requires a multiplication by a pair of complex exponentials that are offset by a constant phase shift. There are several common methods to generate a complex exponential in

programmable logic with tradeoffs in device logic utilization, coding complexity, and spectral purity of the generated output signal. In this case, however, because the required output signal frequency is relatively low compared to the baseband sample rate, the rotation CORDIC provides a simple, low complexity, and minimal logic resource implementation. A numerically controlled oscillator (NCO) can be produced by the polar-to-Cartesian mapping operation of the CORDIC by simply providing a phase accumulator input to the CORDIC block as illustrated in Figure 5.5. The output frequency, F_{out} , of the NCO is set according to the sample rate F_s , the rate of the phase accumulator input θ_{inc} , and the bit width of the phase accumulator W according to

$$F_{out} = \frac{F_s \cdot \theta_{inc}}{2^W}. \quad (74)$$

The starting phase offset θ_{out} can be set by initializing the phase accumulator value θ_{init}

$$\theta_{out} = \frac{360 \cdot \theta_{init}}{2^W}. \quad (75)$$

The implementation of the NCO for the SSCCE algorithm is given in Appendix B as `fixed_nco.vhd`. This design provides a fixed NCO output frequency that is set by generics for the frequency output, phase offset, and phase accumulator bit width. Additionally, the number of iterations used in the rotation CORDIC is controlled by a generic setting. Two NCOs are used, one for each complex exponential output. The settings used in this implementation are calculated for $\alpha = 1/80$ and $\phi = 64/80$ and $\phi = 0$, respectively for frequency output and phase offset. Phase accumulator width was set to 32 bits for both NCOs.

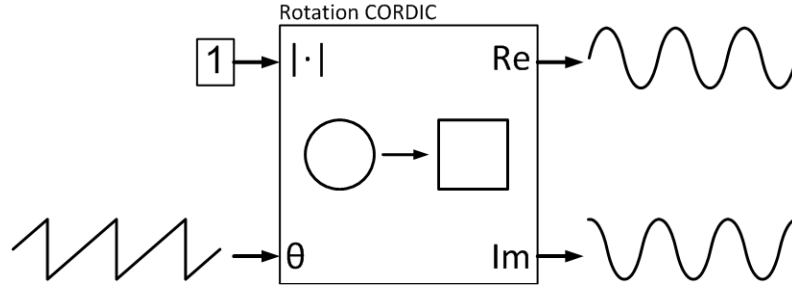


Figure 5.5 Block diagram showing the implementation of a NCO using CORDIC.

5.2.5 Moving Average Filter

The SSCCE calculation in (70) requires the computation of the average over N samples of the cyclic down conversion products. The implementation of an arithmetic mean in digital logic is particularly straightforward if the value of N can be restricted to powers-of-two. This restriction allows simple right shifts by the quantity $\lceil \log_2 N \rceil$ in order to perform the division operation. Unfortunately, the calculation of the SSCCE test statistic output requires the collection of all N samples before a decision can be made based on the threshold value. Depending on the value of N , in particularly high SNR scenarios, the test statistic may exceed the threshold well before all N samples have been collected. In such case, the decision could be made sooner if visibility to the test statistic value was available on a sequential, sample-by-sample basis. To provide this enhancement of the detection algorithm the simple average is replaced with a moving average calculation. A recursive moving average calculation is given as

$$y[n] = \frac{1}{N} \sum_{m=0}^{N-1} x[n+m] = y[n-1] + \frac{x[n] - x[n-N]}{N}, \quad (76)$$

which is easily implemented in digital logic (again with the caveat that N is restricted to powers-of-two), but requires additional block RAM resources that are otherwise not necessary in a simple arithmetic mean. However, the ability to provide immediate detection of a primary user before the collection of all N samples is considered a favorable tradeoff against increased logic utilization. The moving average design implementation is located in Appendix B as `moving_average.vhd`. The design is parameterized by a generic to set the maximum number of samples in the calculation. The size of the moving average can be adjusted during runtime up to the maximum value specified. The design implementation for the SSCCE sets the maximum number of samples to 2048. Binary addition grows the summand by one bit for every addition operation performed. Similar to the multiplier implementations, it is often desirable to maintain the output signal width to match the input signal width with an implied scaling applied to the output signal following truncation. A generic parameter is available to maintain bit precision of the output by shifting the output by a power-of-two. Through empirical examination of the output signal, the scaling parameter of four was determined to provide enhanced bit precision while preventing numerical overflow. This scales the output by an additional factor of 16. The design was implemented such that the sample memory infers device block RAM resources for efficient implementation [32].

5.3 SSCCE Behavioral Simulation

Following design implementation in HDL the next step is to verify the coded operation meets design expectations. This is typically done using a design behavioral simulation. There are a variety of methodologies in practice to perform behavioral

simulation, but the general model is to create a separate entity referred to as a testbench, which feeds stimulus to the design under test (DUT) and captures the resulting response. The response is compared against the expected results for a given stimulus to detect design errors. Often it is desirable to test using some form of constrained random stimulus in order to attempt to test various corner cases in the design implementation. The testbench and DUT are simulated using an HDL simulator that allows per cycle analysis and debug of the various design elements.

For this design, Mentor Graphics® Questa Sim was used along with a testbench written in SystemVerilog. A screenshot of the simulator with several of the `ssce.vhd` signals plotted is shown in Figure 5.6. The test methodology of the SSCCE design implementation is as follows. First, the MATLAB functions used for the generation of the 802.11p baseband signal were reused, including the multipath fading and LO frequency offset impairments. Sixteen thousand random baseband signals were generated with SNR values ranging between -20dB to +10dB. Because the implementation of the SSCCE function is restricted to average over powers-of-two, the signal length was reduced from 2640 (as used in Chapter 4 as a shortest-case DSRC safety message) to 2048 baseband samples. Each stimulus signal was saved individually in a file as a set of integer values less than the full-scale data width used in the `ssce.vhd` design (18 bits). The stimulus files were opened by the testbench simulation and the baseband signal used as input to the `ssce.vhd` DUT. The test statistic output signal of the DUT was likewise captured as a response file for every stimulus file.

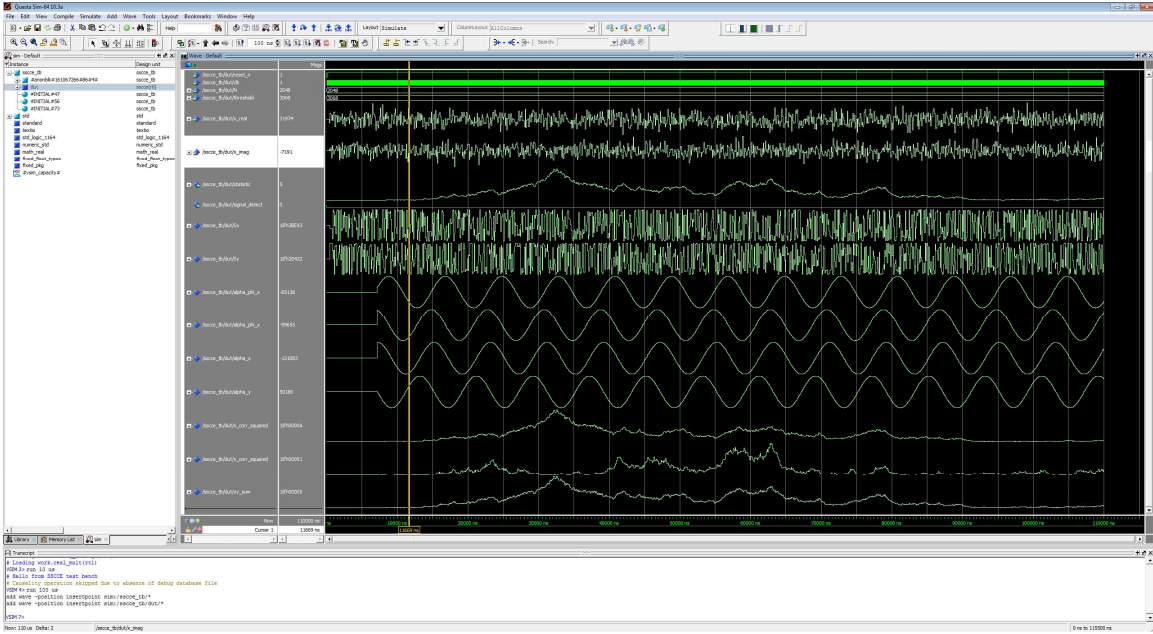


Figure 5.6 Screenshot of design simulation using Questa Sim.

After the completion of the simulation the stimulus and response files were imported into MATLAB. The stimulus files were analyzed using the `sscce_pc.m` used in Chapter 4 and the output test statistic used as the expected result for a given stimulus. Because the number of samples used in the calculation is 2048, the performance is slightly reduced compared to the results using 2640 samples shown in Chapter 4. The expected results are shown in Figure 5.7. Likewise, the probability of detection versus SNR is shown for the response files generated from the SSCCE implementation testbench and are shown in Figure 5.8. As can be seen, the two curves show excellent correlation. The differences in the probability of detection between the floating point precision MATLAB simulation and the 18 bit fixed point HDL implementation are shown in Figure 5.9. Additionally, the root mean square deviation between the MATLAB simulation and the HDL implementation is given in Figure 5.10. The RMSD values follow a similar curve as that of the probability of detection curve, with absolute error

that increases along with the increasing strength of the correlation. These effects are likely caused from the finite precision of the HDL implementation, especially the limited angular resolution from the SSF. Finally, a histogram of the first output test statistic sample that exceeded the threshold for $P_{fa} = 5\%$ in a signal with SNR = 6dB is given in Figure 5.11. While a sample distribution is not immediately evident, it is clear that a significant number of the 802.11p signals could be detected well before the completion of the 2048 sample averaging duration used in the SSCCE implementation, leading to an obvious improvement in primary user detection time.

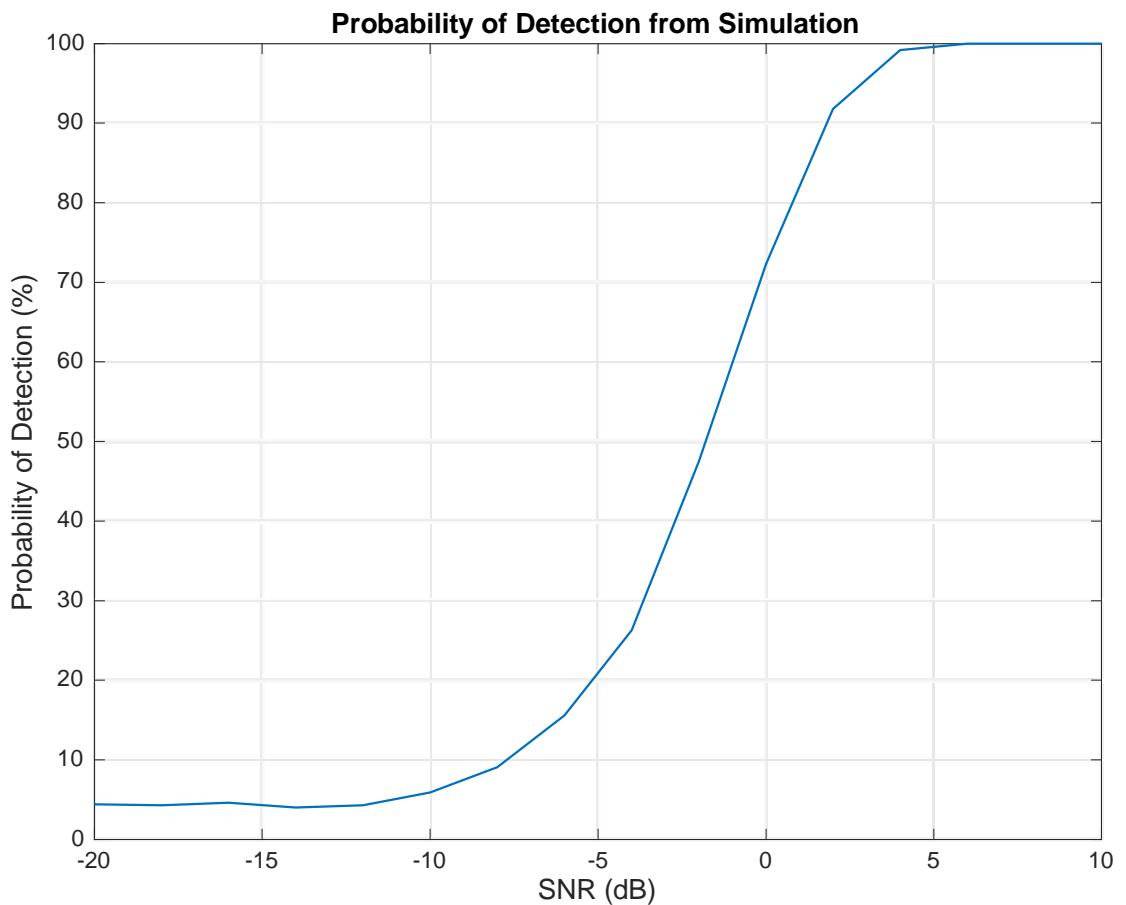


Figure 5.7 SSCCE algorithm probability of detection vs. SNR results from MATLAB simulation.

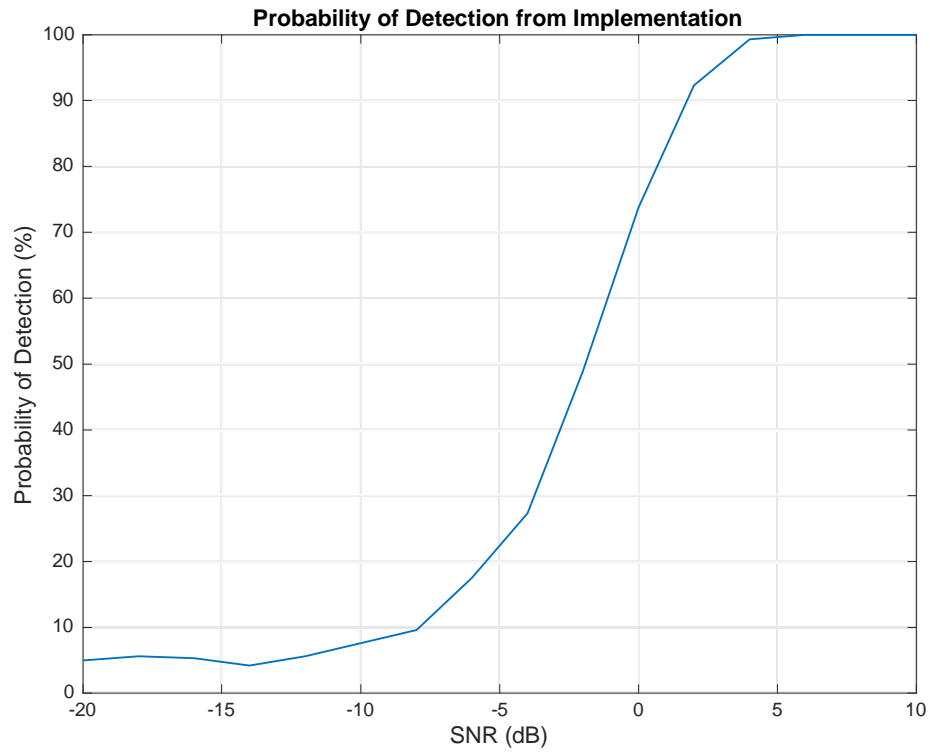


Figure 5.8 SSCE algorithm probability of detection vs. SNR from HDL implementation behavioral simulation.

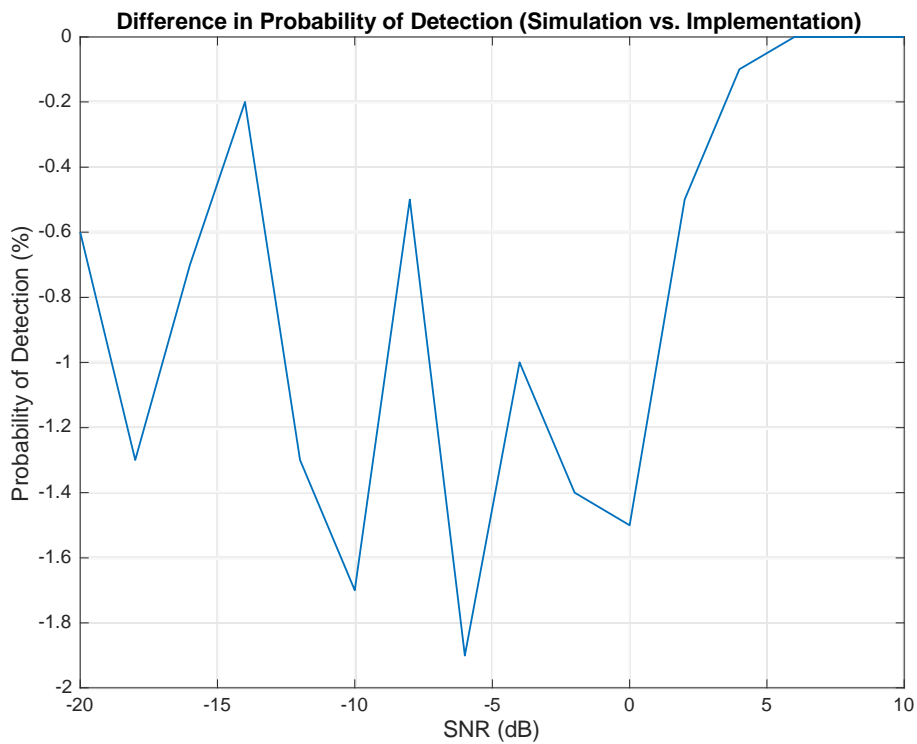


Figure 5.9 Difference in probability of detection between MATLAB simulation and HDL implementation.

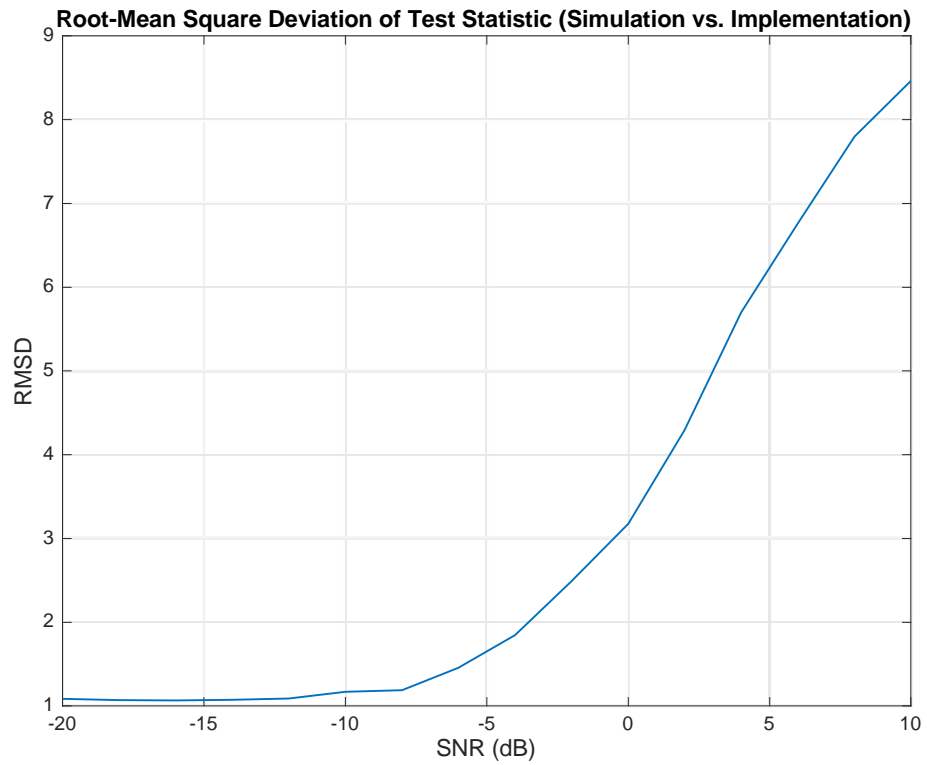


Figure 5.10 RMSD of the SSCCE test statistic between MATLAB simulation and HDL implementation.

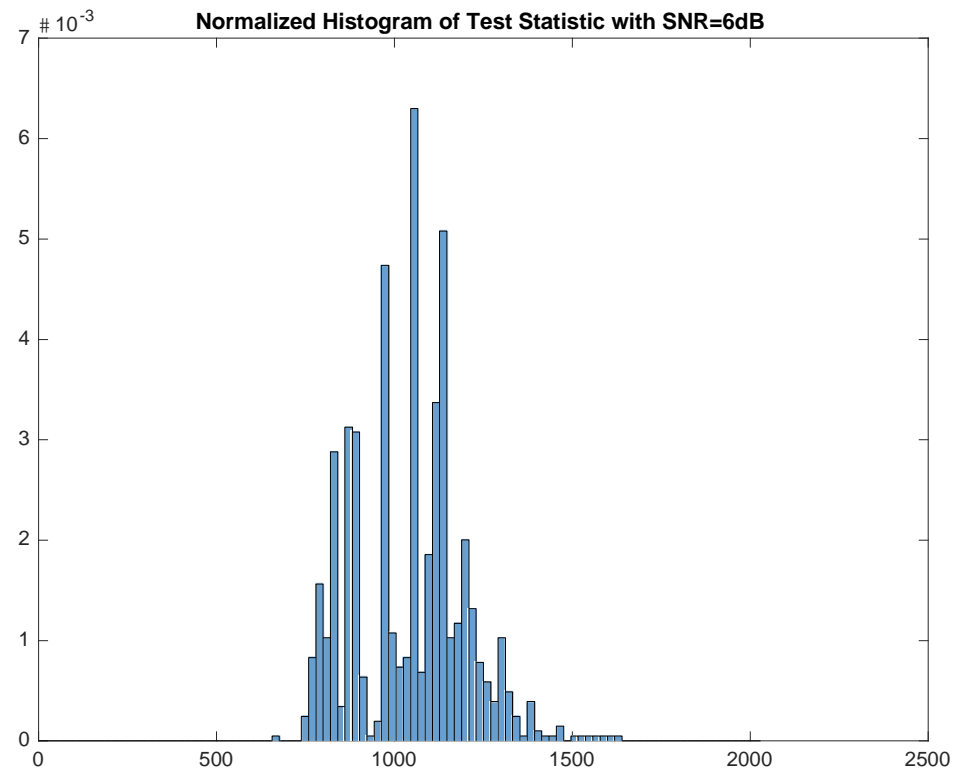


Figure 5.11 Histogram of the first test statistic value to exceed the threshold for 5% P_{fa} .

5.4 SSCCE Resource Utilization

Once expected results are obtained from behavioral simulation, the following steps are to synthesize, place, and route the HDL design. In order to estimate the necessary design resources and power consumption of the SSCCE design, Altera® Quartus II software was used. A Cyclone V family device was targeted for implementation because it represents a modern 28nm, low-power process device architecture. The results per design block are presented in Table 3. Overall, the resource utilization is relatively low. The block RAM utilization is the largest resource requirement by far, which is driven primarily by the moving average blocks.

Table 3 SSCCE Implementation Resource Utilization

Design Block	Logic Elements	Flip-Flops	Block RAM Bits	Multipliers	Dynamic Power Dissipation
SSF	2059	2033	0	0	54mW
Lead/Lag Shift Register	29	57	4608	0	3mW
Complex Multiplier	0	545	0	8	55mW
NCO	2043	2118	0	0	112mW
Moving Average	199	130	118784	0	18mW
Real Multiplier	0	72	0	2	25mW
Misc.	157	53	0	0	61mW
Total	4458	5008	123392	10	328mW

5.5 Conclusion

As the demands on the wireless spectrum continue to increase, regulatory authorities will seek out ways to achieve sharing and reuse of licensed bands. The techniques being explored in the area of cognitive radio hold promise to help address this issue. One of the recently proposed areas for spectrum sharing is the DSRC band at 5.9 GHz. The reuse scenario in this band has specific constraints due to the nature of DSRC communications. Devices wishing to make unlicensed use of the 5.9 GHz band will require robust and rapid detection of primary users in order to avoid disruption to the intended operation of DSRC. This thesis explored various cognitive radio detection methods, including cyclostationary analysis, which was shown to perform well in the presence of noise. A baseband signal model for 802.11p modulation used by DSRC was created to explore various features for cyclostationary detection. Several OFDM modulation features of 802.11p useful for signal identification were discussed. This thesis investigated a detection method based on the OFDM symbol cyclic prefix. The cyclic autocorrelation function was introduced as a low computational complexity method to detect the cyclic prefix. To avoid computation of the signal noise statistics, the spatial sign function was introduced. The spatial sign cyclic correlation estimator was then developed in MATLAB and tested with the 802.11p baseband model, showing encouraging results in the presence of signal impairments for a short duration signal. To allow real-time execution of the detection algorithm, a digital hardware implementation was explored by implementing the SSCCE function in HDL. Behavioral simulations showed good match between the fixed-point hardware implementation and the floating

point MATLAB model. Afterwards, resource utilization of the algorithm was estimated by synthesizing and fitting the design to a FPGA device.

The SSCCE algorithm explored in this thesis appears to be a promising method for OFDM signal identification, with particular applicability towards spectral reuse in the DSRC band. The algorithm provides excellent identification of primary users in the presence of noise and impairments yet has a low computational complexity that provides for straightforward implementation in digital logic, allowing for low latency, real-time execution. Further investigation in this area is warranted. A potential area of additional research includes deployment of the HDL implementation with a RF receiver capable of operation in the DSRC band in order to test for real world signal environment effects and performance. Also, the algorithm presented in this thesis operated assuming a baseband sampling rate. Further research should be performed to identify the effects of sampling beyond the baseband rate, including non-integer multiples of the baseband rate.

APPENDIX A

MATLAB CODE

```

%% 802.11p Baseband Data Generator and Modulator
% Adapted from Steven Schnur [19]
%
function [x]=WiFi_BasebandMod(Q,m,bk,Frame);
if nargin~=4
    error('Wrong number of arguments')
end
L=64;           % Number of subcarriers
Ndata=48;      % Number of data subcarriers
CP=16;        % Cyclic prefix length
G=1;          % Gain of CP

% Choose subcarrier modulation type
switch m
    case 6
        % Generates 64-QAM modulation object
        c=sqrt(42); % Normalization Value of 64-QAM symbol
        object = modem.genqammod('Constellation', [ (-7-7j)/c,(7-7j)/c,...
            (-1-7j)/c, (1-7j)/c, (-5-7j)/c, (5-7j)/c, (-3-7j)/c, (3-7j)/c, ...
            (-7+7j)/c, (+7+7j)/c, (-1+7j)/c,(1+7j)/c, (-5+7j)/c, (5+7j)/c,...
            (-3+7j)/c, (3+7j)/c, (-7-1j)/c, (7-1j)/c, (-1-1j)/c,(1-1j)/c,...
            (-5-1j)/c, (5-1j)/c, (-3-1j)/c, (3-1j)/c (-7+1j)/c,(7+1j)/c,...
            (-1+1j)/c,(1+1j)/c, (-5+1j)/c, (5+1j)/c, (-3+1j)/c, (3+1j)/c,...
            (-7-5j)/c, (+7-5j)/c, (-1-5j)/c (1-5j)/c, (-5-5j)/c, (5-5j)/c,...
            (-3-5j)/c, (3-5j)/c, (-7+5j)/c, (7+5j)/c, (-1+5j)/c, (1+5j)/c,...
            (-5+5j)/c, (5+5j)/c, (-3+5j)/c, (3+5j)/c, (-7-3j)/c, (7-3j)/c,...
            (-1-3j)/c, (1-3j)/c, (-5-3j)/c, (5-3j)/c, (-3-3j)/c, (3-3j)/c,...
            (-7+3j)/c, (7+3j)/c, (-1+3j)/c, (1+3j)/c, (-5+3j)/c, (5+3j)/c,...
            (-3+3j)/c, (+3+3j)/c ], ...
            'InputType', 'Bit');
    case 4
        % Generates 16-QAM modulation object
        c=sqrt(10); % Normalization value of 16-QAM symbol
        object = modem.genqammod('Constellation', [ (-3-3j)/c, ...
            (3-3j)/c, (-1-3j)/c, (1-3j)/c, (-3+3j)/c, (3+3j)/c, ...
            (-1+3j)/c, (1+3j)/c, (-3-1j)/c, (3-1j)/c, (-1-1j)/c, ...
            (1-1j)/c, (-3+1j)/c, (3+1j)/c,(-1+1j)/c, (1+1j)/c ], ...
            'InputType', 'Bit');
    case 2
        % Generates QPSK modulation object
        c=sqrt(2);
        object = modem.genqammod('Constellation', [ (-1-1j)/c, ...
            (1-1j)/c, (-1+1j)/c, (1+1j)/c ], ...
            'InputType', 'Bit');
    case 1
        % Generates BPSK modulation object
        object = modem.genqammod('Constellation', [ -1, 1 ], ...
            'InputType', 'Bit');
    otherwise
        % do nothing
end

% Dummy vectors and index to load preamble
temp=bk;
index=mod([-3:Q],Frame) & mod([-2:Q+1],Frame)...
    & mod([-1:Q+2],Frame) & mod([0:Q+3],Frame);

% Pilot subcarrier sequence generator
Pilot_SC=[ 1,1,1,1, -1,-1,-1,1, -1,-1,-1,-1, 1,1,-1,1, -1,-1,1,1,...
    -1,1,1,-1, 1,1,1,1, 1,1,-1,1, 1,1,-1,1, 1,-1,-1,1, 1,1,-1,1, ...
    -1,-1,-1,1, -1,1,-1,-1, 1,-1,-1,1, 1,1,1,1, -1,-1,1,1,...
    -1,-1,1,-1, 1,-1,1,1, -1,-1,-1,1, 1,-1,-1,-1, -1,1,-1,-1, ...
    1,-1,1,1, 1,1,-1,1, -1,1,-1,1, -1,-1,-1,-1, -1,1,-1,1, 1,-1,1, ...
    -1,1,1,1,-1, -1,1,-1,-1, -1,1,1,1, -1,-1,-1,-1, -1,-1,-1 ];

% Form overall tx data vector
for k=1:Q
    if ((index(1,k)==0)&(index(1,k+3)==0))

```

```

[short1,short2]=WiFi_short_preamble;
xl=short1;
else if ((index(1,k)==0)&(index(1,k+2)==0) & (index(1,k+3)==1))
[short1,short2]=WiFi_short_preamble;
xl=short2;
else if ((index(1,k)==0)&(index(1,k+1)==0)&(index(1,k+2)==1))
[long1,long2]=WiFi_long_preamble;
xl=long1;
else if ((index(1,k)==0)&(index(1,k+1)==1))
[long1,long2]=WiFi_long_preamble;
xl=long2;
bkp=wextend('addcol','zpd',temp,Ndata*m*4,'r');
bkp=circshift(bkp,[0,Ndata*m*4]);
temp=bkp;
else if (index(1,k)==1)
xl=0;
a=bkp(1,Ndata*m*(k-1)+1:m*Ndata*k);
xt=0;

% Loop to form OFDM symbol
for w=1:Ndata % loop through vector
aa=a(1,(m)*(w-1)+1:m*w); % fetch bits for m-symbol
mk=aa(1,1:m); % load storage vector
Xp=modulate(object,mk'); % modulates the data to IQ
X1(w,1)=Xp; % stack the symbols
end

% Load vector X with Guard SC=0, DC=0, Pilot SC, Data
X(1,1)=0; % DC null
X(2:7,1)=X1(25:30,1); % data
X(8,1)=Pilot_SC(1,2)*G*1; % positive pilot (7)
X(9:21,1)=X1(31:43,1); % data
X(22,1)=Pilot_SC(1,2)*G*-1; % positive pilot (21)
X(23:27,1)=X1(44:48,1); % data
X(28:32,1)=0; % lower guard
X(33:38,1)=0; % upper guard
X(39:43,1)=X1(1:5,1); % data
X(44,1)=Pilot_SC(1,2)*G*1; % negative pilot (-7)
X(45:57,1)=X1(6:18,1); % data
X(58,1)=Pilot_SC(1,2)*G*1; % negative pilot (-21)
X(59:64,1)=X1(19:24,1); % data

% Pseudo-randomize pilot seq IAW Wifi standard
Pilot_SC=circshift(Pilot_SC,[0,-1]);
end

% Generate time signal
xt=ifft(X,L); % L-size IFFT to convert IQ data to time
g(1:CP,1)=xt((L-CP+1):L,1); % CP data from end of symbol
x1(1:CP,1)=g; % place CP at front of symbol
x1(CP+1:L+CP,1)=xt; % load rest of symbol into vector
end
end
end
% Fill the tx vector w/ CP appended
x(((k-1)*(L+CP)+1):k*(L+CP),1)=x1;
end
end

```

```

%% WiFi Short Preamble Time Samples
% Adapted from Steven Schnur [19]
%

function [short1,short2]=WiFi_short_preamble;
short1=[0.023+0.023j;-0.132+0.002j;-0.013-0.079j;0.143-0.013j;...
0.092+0.000j;0.143-0.013j;-0.013-0.079j;-0.132+0.002j;...
0.046+0.046j;0.002-0.132j;-0.079-0.013j;-0.013+0.143j;...
0.000+0.092j;-0.013+0.143j;-0.079-0.013j;0.002-0.132j;...
0.046+0.046j;-0.132+0.002j;-0.013-0.079j;0.143-0.013j;...
0.092+0.000j;0.143-0.013j;-0.013-0.079j;-0.132+0.002j;...
0.046+0.046j;0.002-0.132j;-0.079-0.013j;-0.013+0.143j;...
0.000+0.092j;-0.013+0.143j;-0.079-0.013j;0.002-0.132j;...
0.046+0.046j;-0.132+0.002j;-0.013-0.079j;0.143-0.013j;...
0.092+0.000j;0.143-0.013j;-0.013-0.079j;-0.132+0.002j;...
0.046+0.046j;0.002-0.132j;-0.079-0.013j;-0.013+0.143j;...
0.000+0.092j;0.013+0.143j;-0.079-0.013j;0.002-0.132j;...
0.046+0.046j;-0.132+0.002j;-0.013-0.079j;0.143-0.013j;...
0.092+0.000j;0.143-0.013j;-0.013-0.079j;-0.132+0.002j;...
0.046+0.046j;0.002-0.132j;-0.079-0.013j;-0.013+0.143j;...
0.000+0.092j;-0.013+0.143j;-0.079-0.013j;0.002-0.132j];

short2=[0.046+0.046j;-0.132+0.002j;-0.013-0.079j;0.143-0.013j;...
0.092+0.000j;0.143-0.013j;-0.013-0.079j;-0.132+0.002j;...
0.046+0.046j;0.002-0.132j;-0.079-0.013j;-0.013+0.143j;...
0.000+0.092j;-0.013+0.143j;-0.079-0.013j;0.002-0.132j;...
0.046+0.046j;-0.132+0.002j;-0.013-0.079j;0.143-0.013j;...
0.092+0.000j;0.143-0.013j;-0.013-0.079j;-0.132+0.002j;...
0.046+0.046j;0.002-0.132j;-0.079-0.013j;-0.013+0.143j;...
0.000+0.092j;-0.013+0.143j;-0.079-0.013j;0.002+0.132j;...
0.046+0.046j;-0.132+0.002j;-0.013-0.079j;0.143-0.013j;...
0.092+0.000j;0.143-0.013j;-0.013-0.079j;-0.132+0.002j;...
0.046+0.046j;0.002-0.132j;-0.079-0.013j;-0.013+0.143j;...
0.000+0.092j;-0.013+0.143j;-0.079-0.013j;0.002-0.132j;...
0.046+0.046j;-0.132+0.002j;-0.013-0.079j;0.143-0.013j;...
0.092+0.000j;0.143-0.013j;-0.013-0.079j;-0.132+0.002j;...
0.046+0.046j;0.002-0.132j;-0.079-0.013j;-0.013+0.143j;...
0.000+0.092j;-0.013+0.143j;-0.079-0.013j;0.002-0.132j];

```

```

%% WiFi Long Preamble Time Samples
% Adapted from Steven Schnur [19]
%

function [long1,long2]=WiFi_long_preamble;

long1=[-0.078+0.000j;0.012-0.098j;0.092-0.106j;-0.092-0.115j;...
-0.003+0.054j;0.075+0.074j;-0.127+0.021j;-0.122+0.017j;...
-0.035+0.151j;-0.056+0.022j;-0.060-0.081j;0.070-0.014j;...
0.082-0.092j;-0.131-0.065j;-0.057-0.039j;0.037-0.098j;...
0.062+0.062j;0.119+0.004j;-0.022-0.161j;0.059+0.015j;...
0.024+0.059j;-0.137+0.047j;0.001+0.115j;0.053-0.004j;...
0.098+0.026j;-0.038+0.106j;-0.115+0.055j;0.060+0.088j;...
0.021-0.028j;0.097-0.083j;0.040+0.111j;-0.005+0.120j;...
0.156+0.000j;-0.005-0.120j;0.040-0.111j;0.097+0.083j;...
0.021+0.028j;0.060-0.088j;-0.115-0.055j;-0.038-0.106j;...
0.098-0.026j;0.053+0.004j;0.001-0.115j;-0.137+0.047j;...
0.024-0.059j;0.059-0.015j;-0.022+0.161j;0.119-0.004j;...
0.062-0.062j;0.037+0.098j;-0.057+0.039j;-0.131+0.065j;...
0.082+0.092j;0.070+0.014j;-0.060+0.081j;-0.056-0.022j;...
-0.035-0.151j;-0.122-0.017j;-0.127-0.021j;0.075-0.074j;...
-0.003+0.054j;-0.092+0.115j;0.092+0.106j;0.012+0.098j;...
0.156+0.000j;0.012-0.098j;0.092-0.106j;-0.092-0.115j;...
-0.003-0.054j;0.075+0.074j;-0.127+0.021j;-0.122+0.017j;...
-0.035+0.151j;-0.056+0.022j;-0.060-0.081j;0.070-0.014j;...
0.082-0.092j;-0.131-0.065j;-0.057-0.039j;0.037-0.098j];

long2=[0.062+0.062j;0.119+0.004j;-0.022-0.161j;0.059+0.015j;...
0.024+0.059j;-0.137+0.047j;0.001+0.115j;0.053-0.004j;...
0.098+0.026j;-0.038+0.106j;-0.115+0.055j;0.060+0.088j;...
0.021-0.028j;0.097-0.083j;0.040+0.111j;-0.005+0.120j;...
0.156+0.000j;-0.005-0.120j;0.040-0.111j;0.097+0.083j;...
0.021+0.028j;0.060-0.088j;-0.115-0.055j;-0.038-0.106j;...
0.098-0.026j;0.053+0.004j;0.001-0.115j;-0.137-0.047j;...
0.024-0.059j;0.059-0.015j;-0.022+0.161j;0.119-0.004j;...
0.062-0.062j;0.037+0.098j;-0.057+0.039j;-0.131+0.065j;...
0.082+0.092j;0.070+0.014j;-0.060+0.081j;-0.056-0.022j;...
-0.035-0.151j;-0.122-0.017j;-0.127-0.021j;0.075-0.074j;...
-0.003+0.054j;-0.092+0.115j;0.092+0.106j;0.012+0.098j;...
-0.156+0.000j;0.012-0.098j;0.092-0.106j;-0.092-0.115j;...
-0.003-0.054j;0.075+0.074j;-0.127+0.021j;-0.122+0.017j;...
-0.035+0.151j;-0.056+0.022j;-0.060-0.081j;0.070-0.014j;...
0.082-0.092j;-0.131-0.065j;-0.057-0.039j;0.037-0.098j;...
0.062+0.062j;0.119+0.004j;-0.022-0.161j;0.059+0.015j;...
0.024+0.059j;-0.137+0.047j;0.001+0.115j;0.053-0.004j;...
0.098+0.026j;-0.038+0.106j;-0.115+0.055j;0.060+0.088j;...
0.021-0.028j;0.097-0.083j;0.040+0.111j;-0.005+0.120j];

```



```

%% Spatial Sign Cyclic Correlation Estimator w/ Phase Compensation
%
function [lambda,R] = sscce_pc(x,alpha,phi,lag)
N=length(x);

% SSF function via CORDIC
[theta,r]=cart2pol(real(x),imag(x));
[xr,xi]=pol2cart(theta,1);
Sx=xr+j*xi;
Sx=Sx';

Sx1=[zeros(1,N-1), Sx, zeros(1,N-1)];
if nargin==2
    % Full Autocorrelation
    R=zeros(1,2*N-1);
    for lags=1:2*N-1
        for n=1:N
            R(lags)=R(lags)+conj(Sx(n))*Sx1(n+lags-1)*exp(-j*2*pi*alpha*n);
        end
    end
else if nargin==4
    % Discrete autocorrelation
    M=length(lag);
    R=zeros(1,M);
    for lags=1:M
        for n=1:N
            R(lags)=R(lags)+conj(Sx(n))*Sx1(n+(N-lag(lags))-1)*exp(-
j*(2*pi*alpha*n+phi(lags)));
        end
    end
end
end

R=R./N;
lambda=N/2*abs(sum(R))^2;

```

APPENDIX B

HDL CODE

```
-- Author:      Sean Hamlin
-- Date:       February 13, 2016
--
-----
-- Module Overview
-----
-- This module computes the Dual-Lag, Spatial Sign Cyclic
-- Correlation Estimate with Cyclic Phase Compensation for a
-- baseband input signal x_real and x_imag over N input samples.
-- The test statistic value is calculated and compared against the
-- threshold value. The value of the threshold is calculated
-- according to the desired probability of false alarm (Pfa) as:
--
--           threshold = gaminv(1-Pfa,1,1)*2^(DATA_W-1)/(2^(N-4))
--
-- If the computed test statistic exceeds the threshold value input,
-- the signal detect output is asserted. The test statistic value
-- is provided as an output that is valid at the insertion of the
-- valid_out signal. The baseband input samples are clocked into the
-- module according to the assertion of valid_in. However, the
-- estimation routine calculates at the clk rate, allowing more
-- rapid detection. Also, the detection estimate uses a moving
-- average for the correlation of the test statistic, allowing
-- constant comparison against the threshold. This module is
-- parameterized with the following instantiation generics:
--
-----
-- Module Instantiation Generics
-----
-- DATA_W          : The width of the baseband input and
--                   output signals.
--
-- LEAD_LAG         : The autocorrelation sample lead and lag
--                   values.
--
-- ALPHA            : The cyclic frequency value in Hz/Fs.
--
-- PHI              : The cyclic compensation value.
--
-- MAX_SAMPLES      : The number of input samples to use in the
--                   moving average calculation. Device
--                   memory resources scale according to this
--                   value.
--
-- ROUNDING_ENABLE  : Enables rounding in the multiplication
--                   output stages.
--
-- N_W              : This is a calculated generic. Do not modify.
-----

library ieee;
use ieee.std_logic_1164.all;
use ieee.numeric_std.all;
use ieee.math_real.all;
library ieee_proposed;
use ieee_proposed.fixed_float_types.all;
use ieee_proposed.fixed_pkg.all;

entity sscce is
  GENERIC(
    DATA_W          : integer := 18;
    LEAD_LAG         : integer := 64;
    ALPHA            : real := -1.0/80.0;
    PHI              : real := -64.0/80.0;
    MAX_SAMPLES      : integer := 4096;
    ROUNDING_ENABLE  : boolean := false;
    N_W              : integer := integer(ceil(log2(real(MAX_SAMPLES))));
  )
  PORT(
    reset_n          : in std_logic;
```

```

        clk                : in std_logic;
        N                  : in std_logic_vector(N_W downto 0);
        threshold          : in std_logic_vector(DATA_W-1 downto 0);
        valid_in           : in std_logic;
        x_real              : in std_logic_vector(DATA_W-1 downto 0);
        x_imag              : in std_logic_vector(DATA_W-1 downto 0);
        valid_out           : out std_logic;
        statistic           : out std_logic_vector(DATA_W-1 downto 0);
        signal_detect      : out std_logic);

end ssce;

architecture rtl of ssce is

-- Function to generate the phase increment value from the desired
-- normalized frequency and the phase accumulator width
function freq_to_int(freq : in real; phase_accum_w : in integer) return integer is
begin
return integer(round(freq*real(2**phase_accum_w)));
end freq_to_int;

-- Function to generate the phase offset value from the desired
-- normalized phase and the phase accumulator width
function phase_to_int(phase : in real; phase_accum_w : in integer) return integer is
begin
return integer(round(phase*real(2**phase_accum_w)));
end phase_to_int;

component ssf
generic(
    DATA_W          : integer := 18;
    CORDIC_ITERATIONS : integer := 18);
port(
    reset_n          : in std_logic;
    clk               : in std_logic;
    valid_in         : in std_logic;
    x                 : in std_logic_vector(DATA_W-1 downto 0);
    y                 : in std_logic_vector(DATA_W-1 downto 0);
    valid_out        : out std_logic;
    Sx                : out std_logic_vector(DATA_W-1 downto 0);
    Sy                : out std_logic_vector(DATA_W-1 downto 0));
end component;

component lead_lag_shift_reg
generic(
    DATA_W          : integer := 18;
    LEAD_LAG         : integer := 64);
port(
    reset_n          : in std_logic;
    clk               : in std_logic;
    valid_in         : in std_logic;
    x_in             : in std_logic_vector(DATA_W-1 downto 0);
    valid_out        : out std_logic;
    x_out            : out std_logic_vector(DATA_W-1 downto 0);
    x_lead           : out std_logic_vector(DATA_W-1 downto 0);
    x_lag            : out std_logic_vector(DATA_W-1 downto 0));
end component;

component fixed_nco
generic(
    DATA_W          : integer := 18;
    PHASE_ACCUM_W    : integer := 32;
    PHASE_INC        : integer := 1000;
    PHASE_OFFSET     : integer := 0;
    ITERATIONS       : integer := 18);
port(
    reset_n          : in std_logic;
    clk               : in std_logic;
    ce               : in std_logic;
    valid_out        : out std_logic;
    x                 : out std_logic_vector(DATA_W-1 downto 0);
    y                 : out std_logic_vector(DATA_W-1 downto 0));
end component;

component complex_mult
generic(
    DATA_W          : integer := 18;
    SCALING_BY_2     : integer := 0;
    ROUNDING_ENABLE  : boolean := false);
port(
    reset_n          : in std_logic;

```

```

        clk           : in std_logic;
        valid_in      : in std_logic;
        a_real        : in std_logic_vector(DATA_W-1 downto 0);
        a_imag        : in std_logic_vector(DATA_W-1 downto 0);
        b_real        : in std_logic_vector(DATA_W-1 downto 0);
        b_imag        : in std_logic_vector(DATA_W-1 downto 0);
        valid_out     : out std_logic;
        c_real        : out std_logic_vector(DATA_W-1 downto 0);
        c_imag        : out std_logic_vector(DATA_W-1 downto 0));
end component;

component moving_average
generic(
    DATA_W           : integer := 18;
    MAX_POINTS        : integer := 2048;
    SCALING_BY_2      : integer := 0);
port(
    reset_n           : in std_logic;
    clk               : in std_logic;
    N                 : in std_logic_vector(N_W downto 0);
    valid_in          : in std_logic;
    x                 : in std_logic_vector(DATA_W-1 downto 0);
    valid_out         : out std_logic;
    y                 : out std_logic_vector(DATA_W-1 downto 0));
end component;

component real_mult
generic(
    DATA_W           : integer := 18;
    ROUNDING_ENABLE   : boolean := false);
port(
    reset_n           : in std_logic;
    clk               : in std_logic;
    valid_in          : in std_logic;
    a                 : in std_logic_vector(DATA_W-1 downto 0);
    b                 : in std_logic_vector(DATA_W-1 downto 0);
    valid_out         : out std_logic;
    c                 : out std_logic_vector(DATA_W-1 downto 0));
end component;

-- SSF signals
signal Sx             : std_logic_vector(DATA_W-1 downto 0);
signal Sy             : std_logic_vector(DATA_W-1 downto 0);
signal valid_norm     : std_logic;

-- Lead/Lag signals
subtype x_range       is natural range 2*DATA_W-1 downto DATA_W;
subtype y_range       is natural range DATA_W-1 downto 0;
signal xy_nom         : std_logic_vector(2*DATA_W-1 downto 0);
signal xy_lead        : std_logic_vector(2*DATA_W-1 downto 0);
signal xy_lag         : std_logic_vector(2*DATA_W-1 downto 0);
signal x_nom          : std_logic_vector(DATA_W-1 downto 0);
signal y_nom          : std_logic_vector(DATA_W-1 downto 0);
signal x_lead         : std_logic_vector(DATA_W-1 downto 0);
signal y_lead         : std_logic_vector(DATA_W-1 downto 0);
signal x_lag          : std_logic_vector(DATA_W-1 downto 0);
signal y_lag          : std_logic_vector(DATA_W-1 downto 0);
signal valid_lead_lag : std_logic;

-- Correlation product signals
signal x_lead_prod    : std_logic_vector(DATA_W-1 downto 0);
signal y_lead_prod    : std_logic_vector(DATA_W-1 downto 0);
signal x_lag_prod     : std_logic_vector(DATA_W-1 downto 0);
signal y_lag_prod     : std_logic_vector(DATA_W-1 downto 0);
signal valid_lead_prod : std_logic;
signal valid_lag_prod  : std_logic;

-- NCO signals
signal alpha_phi_x    : std_logic_vector(DATA_W-1 downto 0);
signal alpha_phi_y    : std_logic_vector(DATA_W-1 downto 0);
signal alpha_x        : std_logic_vector(DATA_W-1 downto 0);
signal alpha_y        : std_logic_vector(DATA_W-1 downto 0);
signal valid_nco      : std_logic;

-- Cyclic correlation product and sum signals
signal x_lead_cyc_prod : signed(DATA_W-1 downto 0);
signal y_lead_cyc_prod : signed(DATA_W-1 downto 0);
signal x_lag_cyc_prod  : signed(DATA_W-1 downto 0);
signal y_lag_cyc_prod  : signed(DATA_W-1 downto 0);
signal valid_lead_cyc  : std_logic;
signal valid_lag_cyc   : std_logic;

```

```

signal x_corr_sum      : signed(DATA_W-1 downto 0);
signal y_corr_sum      : signed(DATA_W-1 downto 0);
signal valid_corr_sum  : std_logic;

-- Moving average signals
signal x_corr          : std_logic_vector(DATA_W-1 downto 0);
signal y_corr          : std_logic_vector(DATA_W-1 downto 0);
signal valid_x_corr    : std_logic;
signal valid_y_corr    : std_logic;

-- Squaring operation signals
signal x_corr_squared  : unsigned(DATA_W-1 downto 0);
signal y_corr_squared  : unsigned(DATA_W-1 downto 0);
signal xy_sum          : unsigned(DATA_W-1 downto 0);
signal valid_xc        : std_logic;
signal valid_yc        : std_logic;

begin

norm : ssf
  generic map(
    DATA_W          => DATA_W,
    CORDIC_ITERATIONS => DATA_W)
  port map(
    reset_n          => reset_n,
    clk              => clk,
    valid_in         => valid_in,
    x               => x_real,
    y               => x_imag,
    valid_out        => valid_norm,
    Sx              => Sx,
    Sy              => Sy);

lags : lead_lag_shift_reg
  generic map(
    DATA_W          => 2*DATA_W,
    LEAD_LAG         => LEAD_LAG)
  port map(
    reset_n          => reset_n,
    clk              => clk,
    valid_in         => valid_norm,
    x_in            => Sx & Sy,
    valid_out        => valid_lead_lag,
    x_out           => xy_nom,
    x_lead          => xy_lead,
    x_lag           => xy_lag);

x_nom <= xy_nom(x_range);
y_nom <= xy_nom(y_range);
x_lead <= xy_lead(x_range);
y_lead <= xy_lead(y_range);
x_lag <= xy_lag(x_range);
y_lag <= xy_lag(y_range);

lead_prod : complex_mult
  generic map(
    DATA_W          => DATA_W,
    ROUNDING_ENABLE  => ROUNDING_ENABLE)
  port map(
    reset_n          => reset_n,
    clk              => clk,
    valid_in         => valid_lead_lag,
    a_real           => x_lead,
    a_imag           => y_lead,
    b_real           => x_nom,
    b_imag           => std_logic_vector(-signed(y_nom)),
    valid_out        => valid_lead_prod,
    c_real           => x_lead_prod,
    c_imag           => y_lead_prod);

lag_prod : complex_mult
  generic map(
    DATA_W          => DATA_W,
    ROUNDING_ENABLE  => ROUNDING_ENABLE)
  port map(
    reset_n          => reset_n,
    clk              => clk,
    valid_in         => valid_lead_lag,
    a_real           => x_lag,
    a_imag           => y_lag,
    b_real           => x_nom,

```

```

        b_imag          => std_logic_vector(-signed(y_nom)),
        valid_out      => valid_lag_prod,
        c_real         => x_lag_prod,
        c_imag         => y_lag_prod);

alpha_phi_nco : fixed_nco
generic map(
    DATA_W          => DATA_W,
    PHASE_ACCUM_W    => DATA_W,
    PHASE_INC        => freq_to_int(ALPHA,DATA_W),
    PHASE_OFFSET     => phase_to_int(PHI,DATA_W),
    ITERATIONS       => DATA_W)
port map(
    reset_n          => reset_n,
    clk              => clk,
    ce               => valid_in,
    valid_out       => valid_nco,
    x                => alpha_phi_x,
    y                => alpha_phi_y);

alpha_nco : fixed_nco
generic map(
    DATA_W          => DATA_W,
    PHASE_ACCUM_W    => DATA_W,
    PHASE_INC        => freq_to_int(ALPHA,DATA_W),
    PHASE_OFFSET     => 0,
    ITERATIONS       => DATA_W)
port map(
    reset_n          => reset_n,
    clk              => clk,
    ce               => valid_in,
    valid_out       => open,
    x                => alpha_x,
    y                => alpha_y);

cyclic_lead_prod : complex_mult
generic map(
    DATA_W          => DATA_W,
    SCALING_BY_2     => 1,
    ROUNDING_ENABLE  => ROUNDING_ENABLE)
port map(
    reset_n          => reset_n,
    clk              => clk,
    valid_in         => valid_lead_prod,
    a_real           => x_lead_prod,
    a_imag           => y_lead_prod,
    b_real           => alpha_phi_x,
    b_imag           => alpha_phi_y,
    valid_out        => valid_lead_cyc,
    signed(c_real)   => x_lead_cyc_prod,
    signed(c_imag)   => y_lead_cyc_prod);

cyclic_lag_prod : complex_mult
generic map(
    DATA_W          => DATA_W,
    SCALING_BY_2     => 1,
    ROUNDING_ENABLE  => ROUNDING_ENABLE)
port map(
    reset_n          => reset_n,
    clk              => clk,
    valid_in         => valid_lag_prod,
    a_real           => x_lag_prod,
    a_imag           => y_lag_prod,
    b_real           => alpha_x,
    b_imag           => alpha_y,
    valid_out        => valid_lag_cyc,
    signed(c_real)   => x_lag_cyc_prod,
    signed(c_imag)   => y_lag_cyc_prod);

corr_prod_sum : process(reset_n,clk)
begin
    if reset_n = '0' then
        valid_corr_sum <= '0';
        x_corr_sum <= (others => '0');
        y_corr_sum <= (others => '0');
    elsif rising_edge(clk) then
        valid_corr_sum <= '0';
        if valid_lead_cyc = '1' and valid_lag_cyc = '1' then
            valid_corr_sum <= '1';
            x_corr_sum <= resize(shift_right(x_lead_cyc_prod +
x_lag_cyc_prod,1),DATA_W);

```

```

        y_corr_sum <= resize(shift_right(y_lead_cyc_prod +
y_lag_cyc_prod,1),DATA_W);
    end if;
    end if;
end process;

x_ma : moving_average
generic map(
    DATA_W                => DATA_W,
    MAX_POINTS             => 2*N_W,
    SCALING_BY_2           => 4)
port map(
    reset_n                => reset_n,
    clk                    => clk,
    N                      => N,
    valid_in               => valid_corr_sum,
    x                      => std_logic_vector(x_corr_sum),
    valid_out              => valid_x_corr,
    y                      => x_corr);

y_ma : moving_average
generic map(
    DATA_W                => DATA_W,
    MAX_POINTS             => 2*N_W,
    SCALING_BY_2           => 4)
port map(
    reset_n                => reset_n,
    clk                    => clk,
    N                      => N,
    valid_in               => valid_corr_sum,
    x                      => std_logic_vector(y_corr_sum),
    valid_out              => valid_y_corr,
    y                      => y_corr);

x_squared : real_mult
generic map(
    DATA_W                => DATA_W,
    ROUNDING_ENABLE        => ROUNDING_ENABLE)
port map(
    reset_n                => reset_n,
    clk                    => clk,
    valid_in               => valid_x_corr,
    a                      => x_corr,
    b                      => x_corr,
    valid_out              => valid_xc,
    unsigned(c)            => x_corr_squared);

y_squared : real_mult
generic map(
    DATA_W                => DATA_W,
    ROUNDING_ENABLE        => ROUNDING_ENABLE)
port map(
    reset_n                => reset_n,
    clk                    => clk,
    valid_in               => valid_y_corr,
    a                      => y_corr,
    b                      => y_corr,
    valid_out              => valid_yc,
    unsigned(c)            => y_corr_squared);
xy_sum <= resize(shift_right(x_corr_squared + y_corr_squared,1),DATA_W);

output_detect : process(reset_n,clk)
begin
    if reset_n = '0' then
        valid_out <= '0';
        statistic <= (others => '0');
        signal_detect <= '0';
    elsif rising_edge(clk) then
        valid_out <= '0';
        if valid_xc = '1' and valid_yc = '1' then
            valid_out <= '1';
            statistic <= std_logic_vector(xy_sum);
            if xy_sum >= unsigned(threshold) then
                signal_detect <= '1';
            else
                signal_detect <= '0';
            end if;
        end if;
    end if;
end process;
end architecture rtl;

```

```

-- Author:      Sean Hamlin
-- Date:       February 10, 2016
--
-----
-- Module Overview
-----
-- This module performs the Spatial Sign Function, which is nothing
-- more than a vector normalization. The module utilizes a vector
-- CORDIC routine to transform the cartesian inputs x and y to
-- polar coordinates. The magnitude output is ignored and replaced
-- with a unity magnitude, which along with the angle output is
-- transformed back to rectangular coordinates with a rotation
-- CORDIC. This module is parameterized with the following
-- instantiation generics:
--
-----
-- Module Instantiation Generics
-----
-- DATA_W          : The width of the cartesian input and
--                   output signals
--
-- CORDIC_ITERATIONS : Controls the number of iterations used in
--                   the CORDIC routine to perform the
--                   transformation. This value should be less
--                   than or equal to DATA_W.
-----

library ieee;
use ieee.std_logic_1164.all;
use ieee.numeric_std.all;

entity ssf is
  GENERIC(
    DATA_W          : integer := 18;
    CORDIC_ITERATIONS : integer := 18);
  PORT(
    reset_n         : in std_logic;
    clk              : in std_logic;
    valid_in        : in std_logic;
    valid_out       : out std_logic;
    x                : in std_logic_vector(DATA_W-1 downto 0);
    y                : in std_logic_vector(DATA_W-1 downto 0);
    Sx               : out std_logic_vector(DATA_W-1 downto 0);
    Sy               : out std_logic_vector(DATA_W-1 downto 0));
end ssf;

architecture rtl of ssf is

  component vector_cordic
    generic(
      DATA_W          : integer := 18;
      ITERATIONS       : integer := 18;
      MAG_ENABLE       : boolean := true);
    port(
      reset_n         : in std_logic;
      clk              : in std_logic;
      valid_in        : in std_logic;
      valid_out       : out std_logic;
      x                : in std_logic_vector(DATA_W-1 downto 0);
      y                : in std_logic_vector(DATA_W-1 downto 0);
      mag              : out std_logic_vector(DATA_W-1 downto 0);
      arg              : out std_logic_vector(DATA_W-1 downto 0));
  end component;

  component rotation_cordic
    generic(
      DATA_W          : integer := 18;
      ITERATIONS       : integer := 18;
      MAG_ENABLE       : boolean := true);
    port(
      reset_n         : in std_logic;
      clk              : in std_logic;
      valid_in        : in std_logic;
      valid_out       : out std_logic;
      mag              : in std_logic_vector(DATA_W-1 downto 0);
      arg              : in std_logic_vector(DATA_W-1 downto 0);
      x                : out std_logic_vector(DATA_W-1 downto 0);
      y                : out std_logic_vector(DATA_W-1 downto 0));
  end component;

```



```

signal phase    : std_logic_vector(DATA_W-1 downto 0);
signal valid    : std_logic;
begin

r2p : vector_cordic
    generic map(
        DATA_W      => DATA_W,
        ITERATIONS   => CORDIC_ITERATIONS,
        MAG_ENABLE    => false)
    port map(
        reset_n      => reset_n,
        clk          => clk,
        valid_in     => valid_in,
        valid_out    => valid,
        x            => x,
        y            => y,
        mag          => open,
        arg          => phase);

p2r : rotation_cordic
    generic map(
        DATA_W      => DATA_W,
        ITERATIONS   => CORDIC_ITERATIONS,
        MAG_ENABLE    => false)
    port map(
        reset_n      => reset_n,
        clk          => clk,
        valid_in     => valid,
        valid_out    => valid_out,
        mag          => (others => '0'),
        arg          => phase,
        x            => Sx,
        y            => Sy);

end architecture rtl;

```

```

-- Author:      Sean Hamlin
-- Date:       February 10, 2016
--
-----
-- Module Overview
-----
-- This module provides a lead/lag of a vector input, x_in. The
-- advance/delay is parameterized by the LEAD_LAG generic. The
-- module uses a shift register of twice the LEAD_LAG amount to
-- provide the non-delayed, x_out, and lagged, x_lag, signals. The
-- x_lead signal is not delayed. This is naively coded as a shift
-- register for readability, but most synthesis tools can be
-- configured to implement this design in dedicated block RAMs to
-- save logic resources. This module is parameterized with the
-- following instantiation generics:
--
-----
-- Module Instantiation Generics
-----
-- DATA_W      : The width of the input and output signals
--
-- LEAD_LAG     : Controls the advance and delay of the input signal
--
-----

library ieee;
use ieee.std_logic_1164.all;
use ieee.numeric_std.all;

entity lead_lag_shift_reg is
  GENERIC(
    DATA_W      : integer := 18;
    LEAD_LAG     : integer := 80);
  PORT(
    reset_n      : in std_logic;
    clk          : in std_logic;
    valid_in     : in std_logic;
    x_in         : in std_logic_vector(DATA_W-1 downto 0);
    valid_out    : out std_logic;
    x_out        : out std_logic_vector(DATA_W-1 downto 0);
    x_lead       : out std_logic_vector(DATA_W-1 downto 0);
    x_lag        : out std_logic_vector(DATA_W-1 downto 0));

end lead_lag_shift_reg;

architecture rtl of lead_lag_shift_reg is

  signal fill_lvl      : integer range 0 to LEAD_LAG*2+1;
  type shift_reg_t is array(LEAD_LAG*2 downto 0) of std_logic_vector(DATA_W-1 downto 0);
  signal shift_reg : shift_reg_t := (others => (others => '0'));

begin

  -- Because this design is meant to be implemented in block RAM, there
  -- is no reset capability for the shift register. Therefore, a counter
  -- (fill_lvl) is used to keep track of the number of valid samples that
  -- has entered the shift register since the last reset. The counter
  -- level is then used to gate the output taps.
  process(reset_n,clk)
  begin
    if reset_n = '0' then
      valid_out <= '0';
      fill_lvl <= 0;
    elsif rising_edge(clk) then
      if valid_in = '1' then
        if fill_lvl /= 2*LEAD_LAG+1 then
          fill_lvl <= fill_lvl+1;
        end if;
      end if;
      if fill_lvl > LEAD_LAG-1 then
        valid_out <= valid_in;
      end if;
    end if;
  end process;

  process(clk)
  begin
    if rising_edge(clk) then
      if valid_in = '1' then
        shift_reg(LEAD_LAG*2 downto 1) <= shift_reg(LEAD_LAG*2-1 downto 0);
        shift_reg(0) <= x_in;
      end if;
    end if;
  end process;
end architecture;

```

```
        end if;
    end if;
end process;

x_lead <= shift_reg(0);
x_out <= shift_reg(LEAD_LAG) when fill_lvl > LEAD_LAG else (others => '0');
x_lag <= shift_reg(LEAD_LAG*2) when fill_lvl > LEAD_LAG*2 else (others => '0');

end architecture rtl;
```

```

-- Author:      Sean Hamlin
-- Date:       February 10, 2016
--
-----
-- Module Overview
-----
-- This module provides a fixed complex NCO output using an efficient
-- CORDIC routine.  The output frequency and starting phase offset
-- are provided via generics.
--
-- Output Frequency (Hz) = fclk*PHASE_INC/2^PHASE_ACCUM_W
--
-- Output Phase (Degrees) = 360*PHASE_OFFSET/2^PHASE_ACCUM_W
--
-----
-- Module Instantiation Generics
-----
-- DATA_W      : The width of the NCO output signals.  The phase
--                accumulator is truncated to this value.  A larger
--                DATA_W increases the SFDR at the expense of logic
--                resources.
--
-- PHASE_ACCUM_W: The width of the phase accumulator.  The width
--                of the phase accumulator determines the frequency
--                accuracy and is truncated to DATA_W.
--
-- PHASE_INC    : Determines the output frequency.
--
-- PHASE_OFFSET: Determines the starting phase offset.
--
-- ITERATIONS   : Controls the number of iterations used in the
--                CORDIC routine.  A larger ITERATIONS number
--                increases the SFDR at the expense of logic
--                resources.
-----

library ieee;
use ieee.std_logic_1164.all;
use ieee.numeric_std.all;
--use ieee.fixed_pkg.all; --Not supported in Quartus yet
library ieee_proposed;
use ieee_proposed.fixed_pkg.all;

entity fixed_nco is
    GENERIC(
        DATA_W          : integer := 18;
        PHASE_ACCUM_W    : integer := 32;
        PHASE_INC        : integer := 1000;
        PHASE_OFFSET     : integer := 0;
        ITERATIONS       : integer := 18);
    PORT(
        reset_n          : in std_logic;
        clk              : in std_logic;
        ce               : in std_logic;
        valid_out        : out std_logic;
        x                : out std_logic_vector(DATA_W-1 downto 0);
        y                : out std_logic_vector(DATA_W-1 downto 0));
end fixed_nco;

architecture rtl of fixed_nco is

    component rotation_cordic
        GENERIC(
            DATA_W          : integer := 18;
            ITERATIONS       : integer := 18;
            MAG_ENABLE       : boolean := true);
        PORT(
            reset_n          : in std_logic;
            clk              : in std_logic;
            valid_in         : in std_logic;
            valid_out        : out std_logic;
            mag              : in std_logic_vector(DATA_W-1 downto 0);
            arg              : in std_logic_vector(DATA_W-1 downto 0);
            x                : out std_logic_vector(DATA_W-1 downto 0);
            y                : out std_logic_vector(DATA_W-1 downto 0));
    end component;

    signal phase_accum    : signed(PHASE_ACCUM_W-1 downto 0);
    signal arg            : std_logic_vector(DATA_W-1 downto 0);

```

```

begin
assert(PHASE_ACCUM_W>=DATA_W)
    report "PHASE_ACCUM_W must be greater than DATA_W"
    severity error;

process(reset_n,clk)
begin
    if reset_n = '0' then
        phase_accum <= to_signed(PHASE_OFFSET,PHASE_ACCUM_W);
    elsif rising_edge(clk) then
        if ce = '1' then
            phase_accum <= phase_accum+PHASE_INC;
        end if;
    end if;
end process;
arg <= std_logic_vector(phase_accum(PHASE_ACCUM_W-1 downto PHASE_ACCUM_W-DATA_W));

cordic : rotation_cordic
generic map(
    DATA_W      => DATA_W,
    ITERATIONS   => ITERATIONS,
    MAG_ENABLE   => false)
port map(
    reset_n      => reset_n,
    clk          => clk,
    valid_in     => ce,
    valid_out    => valid_out,
    mag          => (others => '0'),
    arg          => arg,
    x            => x,
    y            => y);

end architecture rtl;

```

```

-- Author:      Sean Hamlin
-- Date:       February 13, 2016
--
-----
-- Module Overview
-----
-- This module implements a complex multiplication:
--
-- c_real = a_real*b_real - a_imag*b_imag
-- c_imag = a_imag*b_real + a_real*b_imag
--
-- This core should synthesize into device embedded DSP blocks if
-- parameterized correctly.
--
-----
-- Module Instantiation Generics
-----
-- DATA_W          : The width of the multiplier input and output
--                   signals.  If it is desired for this module to
--                   synthesize into embedded DSP blocks, the width
--                   should be chosen according to the block
--                   architecture.
--
-- SCALING_BY_2     : The output signal can be scaled by factors of two.
--                   A value of 0 gives appropriate scaling to prevent
--                   overflow (i.e. scales by 2^0 = 1).  Positive values
--                   multiply the output by factors of 2, negative
--                   values divide the output by factors of 2.
--
-- ROUNDING_ENABLE  : Setting this to true will enable rounding of
--                   multiplication product during the truncation.
--                   Otherwise, the product truncation rounds
--                   towards zero.
-----

library ieee;
use ieee.std_logic_1164.all;
use ieee.numeric_std.all;
--use ieee.fixed_pkg.all; --Not supported in Quartus yet
library ieee_proposed;
use ieee_proposed.fixed_float_types.all;
use ieee_proposed.fixed_pkg.all;

entity complex_mult is
  GENERIC(
    DATA_W          : integer := 18;
    SCALING_BY_2     : integer := 0;
    ROUNDING_ENABLE  : boolean := false);
  PORT(
    reset_n          : in std_logic;
    clk              : in std_logic;
    valid_in         : in std_logic;
    a_real           : in std_logic_vector(DATA_W-1 downto 0);
    a_imag           : in std_logic_vector(DATA_W-1 downto 0);
    b_real           : in std_logic_vector(DATA_W-1 downto 0);
    b_imag           : in std_logic_vector(DATA_W-1 downto 0);
    valid_out        : out std_logic;
    c_real           : out std_logic_vector(DATA_W-1 downto 0);
    c_imag           : out std_logic_vector(DATA_W-1 downto 0));
end complex_mult;

architecture rtl of complex_mult is

  signal valid_sr      : std_logic_vector(1 downto 0);

  signal a_real_fixed  : sfixed(DATA_W-1 downto 0);
  signal a_imag_fixed  : sfixed(DATA_W-1 downto 0);
  signal b_real_fixed  : sfixed(DATA_W-1 downto 0);
  signal b_imag_fixed  : sfixed(DATA_W-1 downto 0);
  signal c_real_fixed  : sfixed(2*DATA_W downto 0);
  signal c_imag_fixed  : sfixed(2*DATA_W downto 0);

begin

  process(reset_n,clk)
  begin
    if reset_n = '0' then
      valid_sr <= (others => '0');
    elsif rising_edge(clk) then
      valid_sr <= valid_sr(0) & valid_in;
    end if;
  end process;
end architecture;

```

```

end process;

process(reset_n,clk)
begin
    if reset_n = '0' then
        valid_out <= '0';
        a_real_fixed <= (others => '0');
        a_imag_fixed <= (others => '0');
        b_real_fixed <= (others => '0');
        b_imag_fixed <= (others => '0');
        c_real_fixed <= (others => '0');
        c_imag_fixed <= (others => '0');
        c_real <= (others => '0');
        c_imag <= (others => '0');
    elsif rising_edge(clk) then
        valid_out <= '0';
        if valid_in = '1' then
            a_real_fixed <= to_sfixed(signed(a_real),a_real_fixed);
            a_imag_fixed <= to_sfixed(signed(a_imag),a_imag_fixed);
            b_real_fixed <= to_sfixed(signed(b_real),b_real_fixed);
            b_imag_fixed <= to_sfixed(signed(b_imag),b_imag_fixed);
        end if;
        if valid_sr(0) = '1' then
            c_real_fixed <= a_real_fixed * b_real_fixed - a_imag_fixed *
b_imag_fixed;
            c_imag_fixed <= a_imag_fixed * b_real_fixed + a_real_fixed *
b_imag_fixed;
        end if;
        if valid_sr(1) = '1' then
            valid_out <= '1';
            if ROUNDING_ENABLE then
                c_real <= to_slv(resize(c_real_fixed,2*DATA_W-1-
SCALING_BY_2,DATA_W-SCALING_BY_2));
                c_imag <= to_slv(resize(c_imag_fixed,2*DATA_W-1-
SCALING_BY_2,DATA_W-SCALING_BY_2));
            else
                c_real <= to_slv(resize(c_real_fixed,2*DATA_W-1-
SCALING_BY_2,DATA_W-SCALING_BY_2,fixed_wrap,fixed_truncate));
                c_imag <= to_slv(resize(c_imag_fixed,2*DATA_W-1-
SCALING_BY_2,DATA_W-SCALING_BY_2,fixed_wrap,fixed_truncate));
            end if;
        end if;
    end if;
end process;

end architecture rtl;

```

```

-- Author:      Sean Hamlin
-- Date:       February 13, 2016
--
-----
-- Module Overview
-----
-- This module implements a programmable moving average filter
-- operation on the input x. The number of samples used in the
-- computation is controlled by the input N. The number of points
-- in the computation is thus:
--
--           Number of Points = 2^ceiling(log2(N))
--
-- A value of N=0 effectively bypasses the filter. The design
-- should synthesize into dedicated block RAMs to save logic
-- resources. This module is parameterized with the following
-- instantiation generics:
--
-----
-- Module Instantiation Generics
-----
-- DATA_W      : The width of the input and output signals
--
-- MAX_POINTS    : Controls the maximum number of samples allowed in
-- programmable moving average calculation. Required
-- device resources increase at power-of-two
-- boundaries.
--
-- SCALING_BY_2 : The output signal can be scaled by factors of two.
-- A value of 0 gives appropriate scaling to prevent
-- overflow (i.e. scales by 2^0 = 1). Positive values
-- multiply the output by factors of 2, negative
-- values divide the output by factors of 2.
--
-- N_W          : A parameter calculated from MAX_POINTS. Do not
-- modify.
-----

library ieee;
use ieee.std_logic_1164.all;
use ieee.numeric_std.all;
use ieee.math_real.all;

entity moving_average is
  GENERIC(
    DATA_W      : integer := 18;
    MAX_POINTS    : integer := 2048;
    SCALING_BY_2  : integer := 0;
    N_W          : integer := integer(ceil(log2(real(MAX_POINTS))));
  )
  PORT(
    reset_n      : in std_logic;
    clk          : in std_logic;
    N            : in std_logic_vector(N_W downto 0);
    valid_in     : in std_logic;
    x            : in std_logic_vector(DATA_W-1 downto 0);
    valid_out    : out std_logic;
    y            : out std_logic_vector(DATA_W-1 downto 0);
  );
end moving_average;

architecture rtl of moving_average is
  -----
  -- Return the index of the most significant
  -- asserted bit in the vector
  -----
  function leading_msb (
    arg : std_logic_vector )
  return integer is
    variable result : integer range 0 to 2**arg'left;
  begin
    result := 0;
    for i in arg'left downto arg'right loop
      if arg(i) = '1' then
        result := i;
        exit;
      end if;
    end loop;
    return result;
  end function leading_msb;

```



```

-- BRAM signals
type ram_t is array (0 to MAX_POINTS-1) of std_logic_vector(N_W+DATA_W-1 downto 0);
signal ram          : ram_t := (others => (others => '0'));
signal wr_ptr       : unsigned(N_W-1 downto 0);
signal wr_ptr_int   : integer range 0 to MAX_POINTS-1;
signal rd_ptr       : unsigned(N_W-1 downto 0);
signal rd_ptr_int   : integer range 0 to MAX_POINTS-1;
signal wr_data      : std_logic_vector(N_W+DATA_W-1 downto 0);
signal rd_data      : std_logic_vector(N_W+DATA_W-1 downto 0);
signal fill_lvl     : integer range 0 to MAX_POINTS+1;
signal valid_sr     : std_logic_vector(1 downto 0);

-- Current and lagged input signals, adjusted for bit growth
signal N_int        : integer range 0 to MAX_POINTS;
signal x0           : signed(N_W+DATA_W-1 downto 0);
signal x0_reg       : signed(N_W+DATA_W-1 downto 0);
signal xN           : signed(N_W+DATA_W-1 downto 0);
signal xN_reg       : signed(N_W+DATA_W-1 downto 0);
signal average      : signed(N_W+DATA_W-1 downto 0);

begin

assert(N_W>0)
    report "N_W must be greater than 0"
    severity error;

x0 <= resize(signed(x),N_W+DATA_W);

-- Because we want to use a block ram to implement the
-- lagged input signal, we need to generate the read
-- and write pointers to access the ram. The write
-- pointer is simply a wrapped counter. The read
-- pointer is lagged from the write pointer by the
-- number of points used in the moving average
-- calculation. Because we don't trust that the N
-- input signal is restricted to being a power-of-two,
-- we use a function to find the first asserted MSB
-- of the N input, i.e. floor{log2(N)}. Also,
-- because BRAMs don't have resets, we want to keep
-- a fill level counter to make sure the read data
-- we are using is actually valid (this also has the
-- fringe benefit that we can reset our moving average
-- and still get out valid data immediately).
process(reset_n,clk)
begin
    if reset_n = '0' then
        valid_sr <= (others => '0');
        N_int <= 0;
        wr_ptr <= (others => '0');
        rd_ptr <= (others => '0');
        fill_lvl <= 0;
    elsif rising_edge(clk) then
        valid_sr <= valid_sr(0) & valid_in;
        if valid_in = '1' then
            N_int <= leading_msb(N);
            wr_ptr <= wr_ptr+1;
            rd_ptr <= wr_ptr+1-(2**N_int);
            if fill_lvl /= MAX_POINTS+1 then
                fill_lvl <= fill_lvl+1;
            end if;
        end if;
    end if;
end process;

-- This should synthesize to a device BRAM
wr_ptr_int <= to_integer(wr_ptr);
wr_data <= std_logic_vector(x0);
rd_ptr_int <= to_integer(rd_ptr);
process(clk)
begin
    if rising_edge(clk) then
        if valid_in = '1' then
            ram(wr_ptr_int) <= wr_data;
            rd_data <= ram(rd_ptr_int);
        end if;
    end if;
end process;

-- If the read data is valid use it. Otherwise we

```

```

-- need to wait until the block RAM has been filled
-- to the necessary number of points.
xN <= signed(rd_data) when fill_lvl > 2*N_int else (others => '0');

-- Compute the running sum here
process(reset_n,clk)
begin
    if reset_n = '0' then
        valid_out <= '0';
        x0_reg <= (others => '0');
        average <= (others => '0');
    elsif rising_edge(clk) then
        valid_out <= '0';
        if valid_sr(0) = '1' then
            x0_reg <= x0;
        end if;
        if valid_sr(1) = '1' then
            valid_out <= '1';
            average <= average + x0_reg - xN;
        end if;
    end if;
end process;

-- Divide the output here by the number of samples.
-- Because N is restricted to a power-of-two, the
-- divide is simply a right shift operation.
y <= std_logic_vector(resize(shift_right(average,N_int-SCALING_BY_2),DATA_W));

end architecture rtl;

```

```

-- Author:      Sean Hamlin
-- Date:       February 13, 2016
--
-----
-- Module Overview
-----
-- This module implements a real multiplication:
--
-- c = a*b
--
-- This core should synthesize into device embedded DSP blocks if
-- parameterized correctly.
--
-----
-- Module Instantiation Generics
-----
-- DATA_W      : The width of the multiplier input and output
--                signals.  If it is desired for this module to
--                synthesize into embedded DSP blocks, the width
--                should be chosen according to the block
--                architecture.
--
-- SCALING_BY_2: The output signal can be scaled by factors of two.
--                A value of 0 gives appropriate scaling to prevent
--                overflow (i.e. scales by 2^0 = 1).  Positive values
--                multiply the output by factors of 2, negative
--                values divide the output by factors of 2.
--
-- ROUNDING_ENABLE : Setting this to true will enable rounding of
--                multiplication product during the truncation.
--                Otherwise, the product truncation rounds
--                towards zero.
-----

library ieee;
use ieee.std_logic_1164.all;
use ieee.numeric_std.all;
--use ieee.fixed_pkg.all; --Not supported in Quartus yet
library ieee_proposed;
use ieee_proposed.fixed_float_types.all;
use ieee_proposed.fixed_pkg.all;

entity real_mult is
  GENERIC(
    DATA_W      : integer := 18;
    SCALING_BY_2 : integer := 0;
    ROUNDING_ENABLE : boolean := false);
  PORT(
    reset_n      : in std_logic;
    clk          : in std_logic;
    valid_in     : in std_logic;
    a            : in std_logic_vector(DATA_W-1 downto 0);
    b            : in std_logic_vector(DATA_W-1 downto 0);
    valid_out    : out std_logic;
    c            : out std_logic_vector(DATA_W-1 downto 0));
end real_mult;

architecture rtl of real_mult is
  signal valid_sr      : std_logic;

  signal a_fixed      : sfixed(DATA_W-1 downto 0);
  signal b_fixed      : sfixed(DATA_W-1 downto 0);

begin

  process(reset_n,clk)
  begin
    if reset_n = '0' then
      valid_sr <= '0';
    elsif rising_edge(clk) then
      valid_sr <= valid_in;
    end if;
  end process;

  process(reset_n,clk)
  begin
    if reset_n = '0' then
      valid_out <= '0';
      a_fixed <= (others => '0');
      b_fixed <= (others => '0');
    end if;
  end process;
end architecture rtl;

```

```

        c <= (others => '0');
    elsif rising_edge(clk) then
        valid_out <= '0';
        if valid_in = '1' then
            a_fixed <= to_sfixed(signed(a),a_fixed);
            b_fixed <= to_sfixed(signed(b),b_fixed);
        end if;
        if valid_sr = '1' then
            valid_out <= '1';
            if ROUNDING_ENABLE then
                c <= to_slv(resize(a_fixed * b_fixed,2*DATA_W-2-
SCALING_BY_2,DATA_W-1-SCALING_BY_2));
            else
                c <= to_slv(resize(a_fixed * b_fixed,2*DATA_W-2-
SCALING_BY_2,DATA_W-1-SCALING_BY_2,fixed_wrap,fixed_truncate));
            end if;
        end if;
    end if;
end process;

end architecture rtl;

```

```

-- Author:      Sean Hamlin
-- Date:       February 10, 2016
--
-----
-- Module Overview
-----
-- This module performs the Rotation CORDIC routine.  The module
-- transforms polar coordinates to cartesian coordinates.  The polar
-- inputs are mag and arg.  The absolute value of the mag input is
-- used to perform the transformation.  The arg input is assumed to
-- be in the range [-pi,pi).  This module is parameterized with
-- the following instantiation generics:
--
-----
-- Module Instantiation Generics
-----
-- DATA_W      : The width of the polar input and cartesian output
--                signals.
--
-- ITERATIONS   : Controls the number of iterations used in the
--                CORDIC routine to perform the transformation.
--                This value should be less than or equal to DATA_W.
--
-- MAG_ENABLE   : If set, the core uses both the mag and arg inputs
--                to perform the scaled transformation.  If false,
--                the core saves logic resources by assuming unity
--                magnitude and performs a transformation on the
--                unit circle.
--
-----

library ieee;
use ieee.std_logic_1164.all;
use ieee.numeric_std.all;
use ieee.math_real.all;
--use ieee.fixed_pkg.all; --Not supported in Quartus yet
library ieee_proposed;
use ieee_proposed.fixed_pkg.all;

entity rotation_cordic is
  GENERIC(
    DATA_W      : integer := 18;
    ITERATIONS   : integer := 18;
    MAG_ENABLE   : boolean := true);
  PORT(
    reset_n      : in std_logic;
    clk          : in std_logic;
    valid_in     : in std_logic;
    mag          : in std_logic_vector(DATA_W-1 downto 0);
    arg          : in std_logic_vector(DATA_W-1 downto 0);
    valid_out    : out std_logic;
    x            : out std_logic_vector(DATA_W-1 downto 0);
    y            : out std_logic_vector(DATA_W-1 downto 0));
end rotation_cordic;

architecture rtl of rotation_cordic is

  -- Constants for the scaled counts/radian
  constant MAX_CNTS : integer := 2**(DATA_W-1);
  constant PI       : integer := integer(real(MAX_CNTS)/MATH_PI);

  -- Function to generate the scaled arctan(1/2^i) value
  -- for rotator variable.
  function atan(x, y : in integer) return signed is
  begin
    return to_signed(integer(ARCTAN(real(x),real(y))*real(PI)),DATA_W+1);
  end atan;

  -- Function to calculate the scaling factor:
  -- cumprod(1/sqrt(1+2^(-2*i)),0,n-1)
  function K(n : in integer) return real is
  begin
    if n = 0 then
      return real(MAX_CNTS)/sqrt(2.0);
    else
      return 1.0/sqrt(1.0+2.0**(-2.0*real(n)))*K(n-1);
    end if;
  end K;

  -- Shift registers for the pipeline rotations.  Note, since
  -- CORDIC doesn't preserve vector length during the iterations

```

```

-- the x,y shift registers need an additional bit on top of the
-- normal carry bit to accommodate the scaling factor.
type shiftreg_t is array(natural range <>) of signed;
signal x_sr      : shiftreg_t(ITERATIONS-1 downto 0)(DATA_W+1 downto 0);
signal y_sr      : shiftreg_t(ITERATIONS-1 downto 0)(DATA_W+1 downto 0);
signal angle_sr   : shiftreg_t(ITERATIONS-1 downto 0)(DATA_W downto 0);
signal valid_sr   : std_logic_vector(ITERATIONS+2 downto 0);

signal mag_int : signed(DATA_W+1 downto 0);
signal arg_int : signed(DATA_W downto 0);

signal x_fixed : sfixed(DATA_W-1 downto 0);
signal y_fixed : sfixed(DATA_W-1 downto 0);

begin

assert(DATA_W>=ITERATIONS)
    report "ITERATIONS should not be larger than DATA_W"
    severity warning;

-- This core can be parameterized to operate in two modes
-- according to the MAG_ENABLE generic.  If MAG_ENABLE is
-- false, the core ignores the mag input and assumes unity
-- gain.  This implementation reduces resource utilization
-- by setting the initial vector magnitude to the CORDIC
-- scaling factor so as to avoid the rescaling at the end
-- of the routine (and thus saving a multiplier).  Otherwise
-- the mag input is utilized to create a vector with the
-- desired vector magnitude.
mag_select : if MAG_ENABLE generate
    signal mag_unsigned : unsigned(DATA_W-1 downto 0);
begin
    mag_unsigned <= unsigned(mag);
    mag_int <= signed(resize(mag_unsigned,DATA_W+2)) when (mag_unsigned <= MAX_CNTRS)
else to_signed(MAX_CNTRS,DATA_W+2);
end;
else generate
    mag_int <= to_signed(integer(K(ITERATIONS)),DATA_W+2);
end generate mag_select;

arg_int <= resize(signed(arg),DATA_W+1);

-- CORDIC routine will rotate +/-pi/2 from initial position.
-- Therefore, to resolve a 2*pi argument, the initial (x,y)
-- position needs to be chosen based on the argument.  The
-- method used here chooses +/-y based on the sign of the
-- argument for simplicity, but other methods are possible.
process(reset_n,clk)
begin
    if reset_n = '0' then
        valid_sr <= (others => '0');
        x_sr(0) <= (others => '0');
        y_sr(0) <= (others => '0');
        angle_sr(0) <= (others => '0');
    elsif rising_edge(clk) then
        valid_sr <= valid_sr(ITERATIONS+1 downto 0) & valid_in;
        if valid_in = '1' then
            x_sr(0) <= (others => '0');
            if arg_int < 0 then
                y_sr(0) <= -mag_int;
                angle_sr(0) <= arg_int+MAX_CNTRS/2;
            else
                y_sr(0) <= mag_int;
                angle_sr(0) <= arg_int-MAX_CNTRS/2;
            end if;
        end if;
    end if;
end process;

-- Here is the CORDIC routine proper.  Basic idea is to
-- examine the sign of the desired angle and if positive
-- rotate the vector by a positive angle, and negative
-- conversely.  The rotation angles are chosen to be the
-- arctan(1/2^(i-1)) which simplifies the rotations to
-- simple power of two shifts.  Iteratively subtract the
-- rotation angle from the desired angle, lather, rinse,
-- repeat.
pipeline: for i in 1 to ITERATIONS-1 generate
begin
    process(reset_n,clk)
    begin

```

```

        if reset_n = '0' then
            x_sr(i) <= (others => '0');
            y_sr(i) <= (others => '0');
            angle_sr(i) <= (others => '0');
        elsif rising_edge(clk) then
            if valid_sr(i-1) = '1' then
                if angle_sr(i-1) < 0 then
                    x_sr(i) <= x_sr(i-1)+shift_right(y_sr(i-1),i-1);
                    y_sr(i) <= y_sr(i-1)-shift_right(x_sr(i-1),i-1);
                    angle_sr(i) <= angle_sr(i-1)+atan(1,2**(i-1));
                else
                    x_sr(i) <= x_sr(i-1)-shift_right(y_sr(i-1),i-1);
                    y_sr(i) <= y_sr(i-1)+shift_right(x_sr(i-1),i-1);
                    angle_sr(i) <= angle_sr(i-1)-atan(1,2**(i-1));
                end if;
            end if;
        end if;
    end process;
end generate pipeline;

-- Same note as above.  If in MAG_ENABLE mode is false,
-- no scaling correction is necessary; just get back to
-- the desired bit width.
norm : if MAG_ENABLE generate
-- Because the CORDIC routine brings out a scaling factor
-- from the rotation matrix to transform it into a rotation
-- in terms of only the tan() function instead of cos() and
-- sin(), it has the unfortunate side effect of scaling the
-- vector.  Fortunately, this value is easy to precompute
-- for a given number of iterations, and moreover converges
-- rapidly to the approximate value 1/0.607252935009.
-- Here, the vector is multiplied by the inverse scaling
-- factor to provide the correct value.
signal x_scale : sfixed(2*DATA_W-3 downto DATA_W-2);
signal y_scale : sfixed(2*DATA_W-3 downto DATA_W-2);
begin
process(reset_n,clk)
begin
    if reset_n = '0' then
        valid_out <= '0';
        x_fixed <= (others => '0');
        y_fixed <= (others => '0');
        x_scale <= (others => '0');
        y_scale <= (others => '0');
        x <= (others => '0');
        y <= (others => '0');
    elsif rising_edge(clk) then
        valid_out <= '0';
        if valid_sr(ITERATIONS) = '1' then
            x_fixed <= to_sfixed(x_sr(ITERATIONS-1),DATA_W,1);
            y_fixed <= to_sfixed(y_sr(ITERATIONS-1),DATA_W,1);
        end if;
        if valid_sr(ITERATIONS+1) = '1' then
            x_scale <= resize(x_fixed*K(ITERATIONS),x_scale);
            y_scale <= resize(y_fixed*K(ITERATIONS),y_scale);
        end if;
        if valid_sr(ITERATIONS+2) = '1' then
            valid_out <= '1';
            x <= to_slv(x_scale);
            y <= to_slv(y_scale);
        end if;
    end if;
end process;

else generate
begin
process(reset_n,clk)
begin
    if reset_n = '0' then
        valid_out <= '0';
        x_fixed <= (others => '0');
        y_fixed <= (others => '0');
        x <= (others => '0');
        y <= (others => '0');
    elsif rising_edge(clk) then
        valid_out <= '0';
        if valid_sr(ITERATIONS) = '1' then
            x_fixed <= to_sfixed(x_sr(ITERATIONS-1),x_fixed);
            y_fixed <= to_sfixed(y_sr(ITERATIONS-1),y_fixed);
        end if;
        if valid_sr(ITERATIONS+1) = '1' then

```

```
        valid_out <= '1';
        x <= to_slv(x_fixed);
        y <= to_slv(y_fixed);
    end if;
end process;

end generate norm;

end architecture rtl;
```



```

-- Author:      Sean Hamlin
-- Date:       February 10, 2016
--
-----
-- Module Overview
-----
-- This module performs the Vector CORDIC routine. The module
-- transforms cartesian coordinates to polar coordinates. The
-- cartesian inputs are x and y. The magnitude value of the
-- vector is provided on the mag output. The arg output contains
-- the vector angle and is the range [-pi,pi). This module is
-- parameterized with the following instantiation generics:
--
-----
-- Module Instantiation Generics
-----
-- DATA_W      : The width of the cartesian input and polar output
--                signals.
--
-- ITERATIONS   : Controls the number of iterations used in the
--                CORDIC routine to perform the transformation.
--                This value should be less than or equal to DATA_W.
--
-- MAG_ENABLE   : If set, the core provides the scaled mag output.
--                If false, the core saves logic resources by
--                providing unity mag output.
--
-----

library ieee;
use ieee.std_logic_1164.all;
use ieee.numeric_std.all;
use ieee.math_real.all;
--use ieee.fixed_pkg.all; --Not supported in Quartus yet
library ieee_proposed;
use ieee_proposed.fixed_pkg.all;

entity vector_cordic is
  GENERIC(
    DATA_W      : integer := 18;
    ITERATIONS   : integer := 18;
    MAG_ENABLE   : boolean := true);
  PORT(
    reset_n      : in std_logic;
    clk          : in std_logic;
    valid_in     : in std_logic;
    x            : in std_logic_vector(DATA_W-1 downto 0);
    y            : in std_logic_vector(DATA_W-1 downto 0);
    valid_out    : out std_logic;
    mag          : out std_logic_vector(DATA_W-1 downto 0);
    arg          : out std_logic_vector(DATA_W-1 downto 0));
end vector_cordic;

architecture rtl of vector_cordic is

  -- Constants for the scaled counts/radian
  constant MAX_CNTRS : integer := 2**(DATA_W-1);
  constant PI        : integer := integer(real(MAX_CNTRS)/MATH_PI);

  -- Function to generate the scaled arctan(1/2^i) value
  -- for rotator variable.
  function atan(x, y : in integer) return signed is
  begin
    return to_signed(integer(ARCTAN(real(x),real(y))*real(PI)),DATA_W+1);
  end atan;

  -- Function to calculate the scaling factor:
  -- cumprod(1/sqrt(1+2^(-2*i)),0,n-1)
  function K(n : in integer) return real is
  begin
    if n = 0 then
      return real(MAX_CNTRS)/sqrt(2.0);
    else
      return 1.0/sqrt(1.0+2.0**(-2.0*real(n)))*K(n-1);
    end if;
  end K;

  -- Shift registers for the pipeline rotations. Note, since
  -- CORDIC doesn't preserve vector length during the iterations
  -- the x,y shift registers need an additional bit on top of the
  -- normal carry bit to accommodate the scaling factor.

```

```

type shiftreg_t is array(natural range <>) of signed;
signal x_sr      : shiftreg_t(ITERATIONS-1 downto 0)(DATA_W+1 downto 0);
signal y_sr      : shiftreg_t(ITERATIONS-1 downto 0)(DATA_W+1 downto 0);
signal z_sr      : shiftreg_t(ITERATIONS-1 downto 0)(DATA_W downto 0);
signal valid_sr  : std_logic_vector(ITERATIONS+2 downto 0);

signal x_int     : signed(DATA_W+1 downto 0);
signal y_int     : signed(DATA_W+1 downto 0);

signal mag_fixed : sfixed(DATA_W-1 downto 0);
signal arg_fixed : sfixed(DATA_W-1 downto 0);

begin

assert(DATA_W>=ITERATIONS)
    report "ITERATIONS should not be larger than DATA_W"
    severity warning;

x_int <= resize(signed(x),DATA_W+2);
y_int <= resize(signed(y),DATA_W+2);

-- CORDIC routine will rotate +/-pi/2 from initial position.
-- Therefore, to resolve a 2*pi argument, the initial values
-- need to be chosen based on the argument. The method used
-- here chooses +/-pi based on the sign of the x input for
-- simplicity, but other methods are possible.
process(reset_n,clk)
begin
    if reset_n = '0' then
        valid_sr <= (others => '0');
        x_sr(0) <= (others => '0');
        y_sr(0) <= (others => '0');
        z_sr(0) <= (others => '0');
    elsif rising_edge(clk) then
        valid_sr <= valid_sr(ITERATIONS+1 downto 0) & valid_in;
        if valid_in = '1' then
            if x_int < 0 then
                if y_int < 0 then
                    x_sr(0) <= -y_int;
                    y_sr(0) <= x_int;
                    z_sr(0) <= to_signed(-MAX_CNTRS/2,DATA_W+1);
                else
                    x_sr(0) <= y_int;
                    y_sr(0) <= -x_int;
                    z_sr(0) <= to_signed(MAX_CNTRS/2,DATA_W+1);
                end if;
            else
                x_sr(0) <= x_int;
                y_sr(0) <= y_int;
                z_sr(0) <= to_signed(0,DATA_W+1);
            end if;
        end if;
    end if;
end process;

-- Here is the CORDIC routine proper. Basic idea is to
-- examine the sign of the desired angle and if positive
-- rotate the vector by a positive angle, and negative
-- conversely. The rotation angles are chosen to be the
-- arctan(1/2^(i-1)) which simplifies the rotations to
-- simple power of two shifts. Iteratively subtract the
-- rotation angle from the desired angle, lather, rinse,
-- repeat.
pipeline: for i in 1 to ITERATIONS-1 generate
begin
    process(reset_n,clk)
    begin
        if reset_n = '0' then
            x_sr(i) <= (others => '0');
            y_sr(i) <= (others => '0');
            z_sr(i) <= (others => '0');
        elsif rising_edge(clk) then
            if valid_sr(i-1) = '1' then
                if y_sr(i-1) < 0 then
                    x_sr(i) <= x_sr(i-1)-shift_right(y_sr(i-1),i-1);
                    y_sr(i) <= y_sr(i-1)+shift_right(x_sr(i-1),i-1);
                    z_sr(i) <= z_sr(i-1)-atan(1,2**(i-1));
                else
                    x_sr(i) <= x_sr(i-1)+shift_right(y_sr(i-1),i-1);
                    y_sr(i) <= y_sr(i-1)-shift_right(x_sr(i-1),i-1);
                    z_sr(i) <= z_sr(i-1)+atan(1,2**(i-1));
                end if;
            end if;
        end process;
    end generate;
end pipeline;

```

```

                                end if;
                            end if;
                    end if;
            end process;
end generate pipeline;

-- This core can be parameterized to operate in two modes
-- according to the MAG_ENABLE generic. If MAG_ENABLE is
-- false, the core provides unity magnitude output, and
-- only provides the vector angle. This implementation
-- reduces resource utilization by avoiding multiplication
-- by the CORDIC scaling factor at the end of the routine
-- (and thus saving a multiplier). Otherwise, the vector
-- magnitude is calculated and scaled appropriately.
norm : if MAG_ENABLE generate
-- Because the CORDIC routine brings out a scaling factor
-- from the rotation matrix to transform it into a rotation
-- in terms of only the tan() function instead of cos() and
-- sin(), it has the unfortunate side effect of scaling the
-- magnitude. Fortunately, this value is easy to precompute
-- for a given number of iterations, and moreover converges
-- rapidly to the approximate value 1/0.607252935009.
-- Here, the magnitude is multiplied by the inverse scaling
-- factor to provide the correct value.
signal mag_scale      : sfixed(2*DATA_W-3 downto DATA_W-2);
signal arg_scale      : sfixed(DATA_W-1 downto 0);
begin
process(reset_n,clk)
begin
    if reset_n = '0' then
        valid_out <= '0';
        mag_fixed <= (others => '0');
        arg_fixed <= (others => '0');
        mag_scale <= (others => '0');
        arg_scale <= (others => '0');
        mag <= (others => '0');
        arg <= (others => '0');
    elsif rising_edge(clk) then
        valid_out <= '0';
        if valid_sr(ITERATIONS) = '1' then
            mag_fixed <= to_sfixed(x_sr(ITERATIONS-1),DATA_W,1);
            arg_fixed <= to_sfixed(z_sr(ITERATIONS-1),arg_fixed);
        end if;
        if valid_sr(ITERATIONS+1) = '1' then
            mag_scale <= resize(mag_fixed*K(ITERATIONS),mag_scale);
            arg_scale <= arg_fixed;
        end if;
        if valid_sr(ITERATIONS+2) = '1' then
            valid_out <= '1';
            mag <= to_slv(mag_scale);
            arg <= to_slv(arg_scale);
        end if;
    end if;
end process;
else generate
begin
process(reset_n,clk)
begin
    if reset_n = '0' then
        valid_out <= '0';
        mag_fixed <= (others => '0');
        arg_fixed <= (others => '0');
        mag <= (others => '0');
        arg <= (others => '0');
    elsif rising_edge(clk) then
        valid_out <= '0';
        if valid_sr(ITERATIONS) = '1' then
            mag_fixed <= to_sfixed(MAX_CNFS,mag_fixed);
            arg_fixed <= to_sfixed(z_sr(ITERATIONS-1),arg_fixed);
        end if;
        if valid_sr(ITERATIONS+1) = '1' then
            valid_out <= '1';
            mag <= to_slv(mag_fixed);
            arg <= to_slv(arg_fixed);
        end if;
    end if;
end process;
end generate norm;
end architecture rtl;

```

REFERENCES

- [1] J. Mitola and G. Q. Maguire, "Cognitive Radio: Making Software Radios More Personal," *IEEE Personal Communications*, vol. 6, no. 4, pp. 13-18, August 1999.
- [2] Federal Communications Commission, "Connecting America: The National Broadband Plan," Washington D.C., 2010.
- [3] Federal Communications Commission. (2015, October) Public Safety Tech Topic #8 - Cognitive Radio for Public Safety. [Online]. www.fcc.gov/help/public-safety-tech-topic-8-cognitive-radio-public-safety
- [4] Federal Communications Commission, "FCC 03-324," Washington D.C., 2003.
- [5] US Department of Transportation, "DSRC-Unlicensed Device Test Plan," Washington D.C., 2015.
- [6] "Middle Class Tax Relief and Job Creation Act of 2012," 2012.
- [7] S. Haykin, "Cognitive Radio: Brain-Empowered Wireless Communications," *IEEE Journal on Selected Areas in Communications*, vol. 23, no. 2, pp. 201-220, February 2005.
- [8] T. Yucek and H. Arslan, "A Survey of Spectrum Sensing Algorithms for Cognitive Radio Applications," *IEEE Communications Surveys and Tutorials*, vol. 11, no. 1, pp. 116-130, First Quarter 2009.
- [9] Marcos E. Castro, "Cyclostationary Detection for OFDM in Cognitive Radio Systems," Department of Electrical Engineering, University of Nebraska-Lincoln, Lincoln, MS Thesis 2011.
- [10] R. Tandra and A. Sahai, "SNR Walls for Signal Detection," *IEEE Journal of Selected Topics in Signal Processing*, vol. 2, no. 1, pp. 4-17, February 2008.
- [11] W. A. Gardner, A. Napolitano, and L. Paura, "Cyclostationarity: Half a Century of Research," *Signal Processing*, vol. 86, no. 4, pp. 639-697, April 2006.
- [12] W. A. Gardner, "The Spectral Correlation Theory of Cyclostationary Time-Series," *Signal Processing*, vol. 11, no. 1, pp. 13-36, July 1986.
- [13] W. A. Gardner, Ed., *Cyclostationarity in Communications and Signal Processing*. NY, NY, US: IEEE, 1994.
- [14] E. Like, V. D. Chakravarthy, P. Ratazzi, and Z. Wu, "Signal Classification in Fading Channels Using Cyclic Spectral Analysis," *EURASIP Journal on Wireless Communications and Networking*, vol. 2009, no. 29, January 2009.
- [15] R. S. Roberts, W. A. Brown, and H. H. Loomis, "Computationally Efficient Algorithms for Cyclic Spectral Analysis," *IEEE Signal Processing Magazine*, vol. 8, no. 2, pp. 38-49, April 1991.
- [16] M. Weigle, "Standards: WAVE/DSRC/802.11p," Department of Computer Science,

- Old Dominion University, 2008.
- [17] ASTM International, "Standard Specification for Telecommunications and Information Exchange Between Roadside and Vehicle Systems-5 GHz Band Dedicated Short Range Communications (DSRC) Medium Access Control (MAC) and Physical Layer (PHY) Specifications," ASTM International, West Conshohocken, ASTM E2213-03, 2010.
- [18] A. M. Abdelgader and W. Lenan, "The Physical Layer of the IEEE 802.11p WAVE Communication Standard: The Specification and Challenges," in *Proceedings of the World Congress on Engineering and Computer Science 2014*, vol. 2, San Francisco, 2014.
- [19] S. R. Schnur, "Identification and Classification of OFDM Based Signals Using Preamble Correlation and Cyclostationary Feature Extraction," Department of Electrical and Computer Engineering, Naval Postgraduate School, Monterey, MS Thesis 2009.
- [20] Tektronix. (2013, November) Wi-Fi: Overview of the 802.11 Physical Layer and Transmitter Measurements. Application Note.
- [21] IEEE Computer Society, "Part 11: Wireless LAN Medium Access Control (MAC) and Physical Layer (PHY) Specification," IEEE, New York, Std 802.11, 2012.
- [22] P. D. Sutton, K. E. Nolan, and L. E. Doyle, "Cyclostationary Signatures in Practical Cognitive Radio Applications," *IEEE Journal on Selected Areas in Communications*, vol. 26, no. 1, pp. 13-24, January 2008.
- [23] D. Vucic, M. Obradovic, and D. Obradovic, "Spectral Correlation of OFDM Signals Related to Their PLC Applications," in *6th International Symposium on Power-Line Communications and Its Applications*, 2002.
- [24] A. Dandawate and G. Giannakis, "Statistical Tests for Presence of Cyclostationarity," *IEEE Transactions on Signal Processing*, vol. 42, no. 9, pp. 2355-2369, September 1994.
- [25] V. Turunen, M. Kosunen, M. Vaarakangas, and J. Ryynanen, "Correlation-Based Detection of OFDM Signals in the Angular Domain," *IEEE Transactions on Vehicular Technology*, vol. 61, no. 3, pp. 951-958, March 2012.
- [26] J. Lunden, S. A. Kassam, and V. Koivunen, "Robust Nonparametric Cyclic Correlation-Based Spectrum Sensing for Cognitive Radio," *IEEE Transactions on Signal Processing*, vol. 58, no. 1, pp. 38-52, January 2010.
- [27] V. Turunen, M. Kosunen, V. Koivunen, and J. Ryynanen, "Dual-Lag Correlation-Based Feature Detector of OFDM Signals with Cyclic Phase Compensation," in *COCORA 2012: The Second International Conference on Advances in Cognitive Radio*, Chamonix, 2012.
- [28] Litepoint, Practical Manufacturing Testing of 802.11 OFDM Wireless Devices,

2012.

- [29] J.M. Lee, M.S. Woo, and S.G. Min, "Performance Analysis of WAVE Control Channels for Public Safety Services in VANETs," *International Journal of Computer and Communications Engineering*, vol. 2, no. 5, September 2013.
- [30] J. E. Volder, "The CORDIC Trigonometric Computing Technique," *IRE Transactions on Electronic Computers*, vol. EC-8, no. 3, pp. 330-334, September 1959.
- [31] R. Andraka, "A Survey of CORDIC Algorithms for FPGA Based Computers," Andraka Consulting Group, Inc., North Kingstown, 1999.
- [32] Altera. (2011, July) Advanced Synthesis Cookbook. Document.